Deltares

Enabling Delta Life

Setup of an effect-chain model for the Eems-Dollard

Results 2010

Deltares

Setup of an effect-chain model for the Eems-Dollard

Results 2010

Jasper Dijkstra
Thijs van Kessel
Bas van Maren
Claudette Spiteri
Willem Stolte

1202298-000

Deltares

Title
Setup of an effect-chain model for the Eems-Dollard

Client	Project	Reference	Pages
Rijkswaterstaat Waterdienst	1202298-000	1202298-000-ZKS-0002	88

Keywords
Place keywords here

Summary
Place summary here

References
Place references here

Version	Date	Author	Initials	Review	Initials	Approval	Initials
	May 2011	Jasper Dijkstra		Hans Los		Tom Schilperoort	
		Thijs van Kessel					
		Bas van Maren					
		Claudette Spiteri					
		Willem Stolte					

State
final

Contents

1 Introduction

The Ems-Dollard estuary, located at the eastern side of the Dutch Wadden Sea, is influenced by conflicting human demands ranging from flood protection, shipping, ports and dredging activities, nature preservation, energy demands, fisheries, tourism and recreational activities. This combination of pressures jeopardizes the water quality and ecological functioning and demands for an integrated sustainable development plan.

As part of the strategic management plan for the area, Deltares is developing an “effect chain modeling” framework, a process-based approach that combines biotic and abiotic processes, the main ecological components and the relevant anthropogenic demands. The integrated modelling framework is implemented in Delft3D and is composed of separate building blocks for hydrodynamics (Delft3D-FLOW) and sediment transport (Delft3D-sedonline or Delft3D WAQ), water quality (Delft3D-WAQ/BLOOM) and ecological interactions with higher trophic levels using a GIS-based spatial analysis tool (HABITAT).

The management questions, policies and scenarios relevant for the Ems-Dollard were collected in 2008 by Jager et al. (2009). In 2009, a system analysis was done through literature reviews and models were setup for each of the separate building blocks (see Van Maren (2010), Spiteri (2010), and Dijkstra (2010)). Model results were presented for the sediment part. The current report describes model results of sediment transport, water quality and habitats from the year 2010.

2 Sediment Transport modelling in the Eems-Dollard

2.1 Introduction

In 2009, sediment transport was modelled with sediment online, in which sediment transport is computed simultaneously with the flow (Van Maren, 2010). An advantage of this approach is that it allows a coupling between sediment concentration and damping of turbulence mixing, which was concluded to contribute to the trapping of sediment in the Ems River. The model results of 2009 produced a reasonable agreement with observations in the Ems Estuary and qualitatively reproduced the trapping of sediment in the Ems River. However, this model had two important shortcomings. First of all, the model is relatively slow and does not allow simulations of full or multiple years. Secondly, in terms of physics, the sedimentation on the mudflats was underestimated, also resulting in an underestimation of sediment concentrations in the Dollard. Additionally, the 2009 model did not include waves. Therefore the aims of 2009 were to:

1) Extend the simulation time to determine whether the low sediment concentrations and sedimentation rates result from a model that is not yet in dynamic equilibrium;
2) Model buffering of fines in the sand bed, which will be released only during high-energetic conditions;
3) Adding waves and locally generated wind-driven currents.

The implementation and results of these model improvements will be discussed in this chapter.

2.2 Model set-up

2.2.1 Introduction

As stated in the previous section, the computational speed needed to be increased, mudflat sedimentation improved, and waves added. All these requirements can be implemented in a flexible way in Delft3D-WAQ. WAQ simulations use pre-computed hydrodynamics, which therefore do not have to be simulated for each sediment computation (as in Sediment online used in 2009). As result, computations are much faster. Computations can be speed up even further through aggregation: hydrodynamic grid points can be clustered to become one grid cell in the WAQ computation. This may be important in areas were (1) the grid resolution is high due to grid design issues (hydrodynamic grids need to maintain a certain orthogonality and smoothness) whereas processes are not spatially variable, or (2) the hydrodynamic processes are complex but sediment transport processes are not.

In terms of processes, WAQ offers two possibilities which are not implemented in sed-online. The most important one is the ‘buffer model’, developed in the framework of Maasvlakte-2 studies, which is an extension of the standard Krone-Partheniades (KP) formulations. The second is that relatively simple formulations are available in WAQ to compute waves (in sed-online, only the computationally expensive SWAN model is available). This is an important advantage in areas where detailed hindcast of the wave height distribution is not very important, but a long simulation periods are needed, such as in the Eems-Dollard.

An important drawback of this model is that is does not account for the interaction with turbulence; the implications of this will be evaluated in the end of this chapter. Additionally, no detailed sand-transport formulations (such as the van Rijn 2004 formulations) are available.

The grid, bathymetry, roughness, and hydrodynamic forcing of the model (except for wave and wind effects) have not changed compared to the model reported in 2009 (see van Maren, 2009). For a description of these and a validation of the hydrodynamics, the reader is referred to this report. Here we focus on a description of the buffer model.

2.2.2 The buffer model

For a detailed description of WAQ, the reader is referred to the user manual. A detailed description of the buffer model is found in Van Kessel et al. (2010). In essence, the buffer model is a two-layer bed module in which most vertical exchange occurs between the water column and bed layer 1. Erosion from bed layer 2 only occurs during storm conditions. Most sediment is stored (buffered) in bed layer 2; bed layer 1 represent the typically thin fluff layer on top of the solid bed: see Figure 2.1 for a schematic presentation.

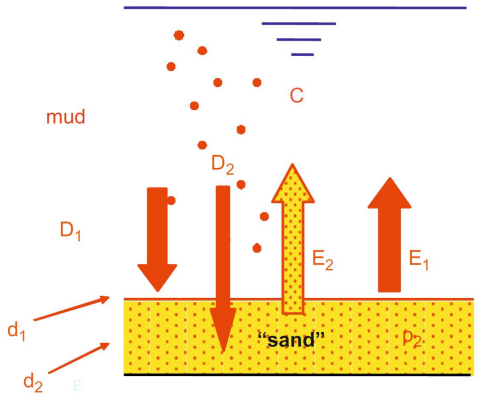

Figure 2.1 Schematic representation of the two-layer model. Layer 1 = thin fluff layer; layer 2 = sandy seabed infiltrated with fines. d_i = thickness of layer i, D_i = deposition flux towards layer i, E_i = erosion flux from layer i (i = 1,2) and C = SPM concentration.

In the buffer model, the erosion rate depends linearly on the amount of available sediment below a user-defined threshold. This has the important consequence that also in dynamic environments the equilibrium sediment mass is non-zero, contrary to standard Krone-Partheniades (KP) models. Typically, this results is smoother and more realistic model behaviour in mixed sand-mud environments, such as the Ems-Dollard. For completely muddy areas, the buffer model switches to standard KP formulations for erosion of bed layer 1.

An additional difference between the buffer model and the standard KP formulations is the deposition efficiency *f*. Deposition *D* is defined as $D = fw_sC$, where w_s is the settling velocity. With *f* = 1, most sediment that settles from suspension around slack tide is deposited on the bed, resulting in low near-bed sediment concentrations. However, observations frequently show that the near-bed sediment concentrations are higher around slack tide. Using a lower value for *f* reduced the sediment deposition rate and increases the near-bed sediment concentration. In estuarine environments where residual transport of fine sediment is strongly influenced by estuarine circulation (with net surface outflow and net near-bed

inflow), a reduction of the deposition efficiency therefore increases landward transport of fine sediments.

The buffer model parameter setting has not been specifically calibrated for the Ems-Dollard area, but we use the settings form the existing Wadden Sea and North Sea model .Two sediment fraction have been applied with settling velocity 0.125 and 1 mm/s. The first value is representative for small primary (weakly flocculated) mud particles, the second value for mud flocs. The critical shear stress for erosion is set at the same value (0.05 Pa) as in the 2009 FLOW model. The erosion rate is low (10^{-4} kg/m^2/s); at a sediment mass per unit area less than 43.2 kg/m^2 (approx. 0.1 m) first order erosion applies. To avoid excessive deposition at the North Sea, the critical shear stress for erosion of bed layer has been reduced to τ_{crit2} = 1 Pa. The reason for this change is the different approach for wave forcing. Wave forcing is applied with a simple fetch-approach within WAQ. The fetch length is set at 25 km at the North Sea, 10 km at the Wadden Sea and Ems-Dollard Estuary and 1 km in the Ems River. This results in an underestimation of the wave climate at the North Sea, but this area is not the point of attention for the present study. An overview of all parameter settings is shown in Table 1.

Three simulations are presented here to illustrate the effect of the buffer model and the deposition efficiency:

I. With suspended sediment only (without erosion and deposition, but with settling in the water column);
II. As I, but now including erosion and deposition and two bed layers according to the buffer model formulations;
III. As II, but assuming a deposition efficiency of 0.1 instead of 1. Parameters M_1, M_2 and α are also changed to maintain a similar typical fluff layer thickness and equilibrium mud content as for II.

The reasons for three different simulations are:

- Comparison between simulations I and II makes it possible to analyse to what extent the suspended sediment distribution is steered by processes in the water column or by exchanges processes with or within the bed.
- Comparison between simulations II and III makes it possible to analyse the importance of estuarine circulation. A lower deposition efficiency results in a higher near-bed concentration, notably around slack water. The stronger the estuarine circulation, the higher the sensitivity on deposition efficiency.

Table 2.1 Overview of parameter settings. Note that settings for both fractions are equal apart from their settling velocity.

parameter	I	II	III	units
w_s	1.0 / 0.125	1.0 / 0.125	1.0 / 0.125	mm/s
α	–	0.05	0.1	–
τ_{crit1}	–	0.05	0.05	Pa
M_0	–	1.0×10^{-4}	1.0×10^{-4}	kg/m^2/s
M_1	–	2.3×10^{-6}	4.6×10^{-7}	s^{-1}
d_2	–	0.01	0.01	m
τ_{crit2}	–	1.0	1.0	Pa
M_2	–	$1.75\ 10^{-7}$	$7.0\ 10^{-8}$	kg/m^2/s
p_{dep}	–	1	0.1	–

2.2.3 Model settings and boundary conditions

We use the hydrodynamics computed for the period of May 2001 (from 2001/04/29 16:00 to 2001/05/29 04:00), with a constant Ems discharge of 80 m^3/s and a variable wind speed measured at Lauwersoog (average of 6.4 m/s, see Figure 2.2). The hydrodynamic results of this period are continuously repeated.

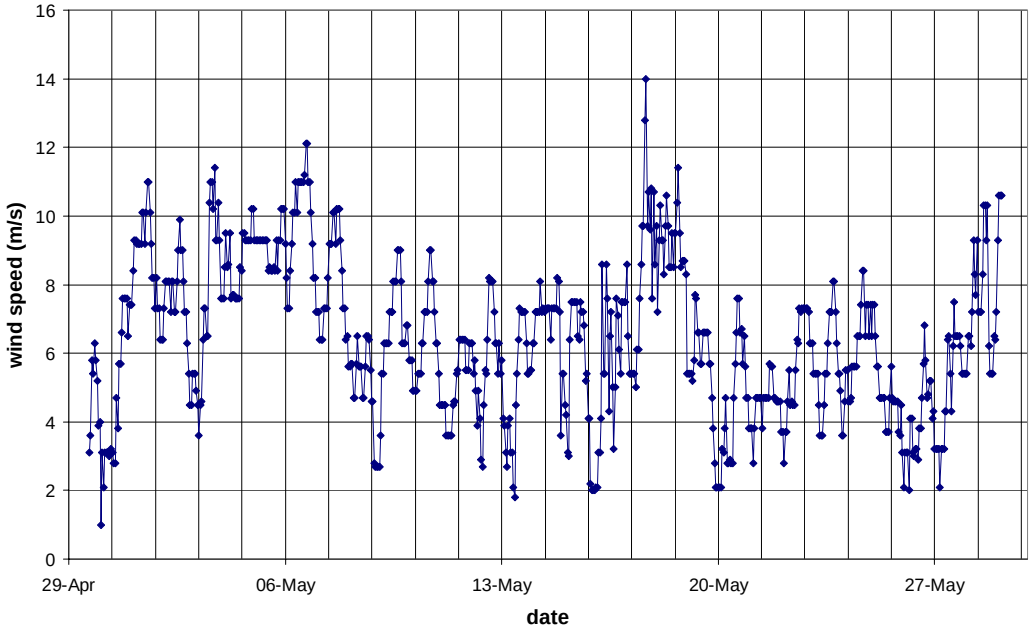

Figure 2.2 Measured hourly wind speed (m/s) at Lauwersoog in the period May 2001.

Representative sediment concentrations are prescribed at the boundaries, based on expert judgement (see Table 2.2). The applied values for total concentration are consistent with estimates on time-average concentrations based on long-term observations Loads are water and sediment fluxes entering the model domain other than boundary conditions: usually being (small) rivers or dumped sediment. The applied loads are shown in Table 2.3. These loads are identical to the loads applied in the 2009 flow model. A large number of numerical schemes are available in WAQ. Here we use a horizontal flux corrected transport scheme, vertically implicit centrally discretized in time (scheme 12). The time step is 60 s. The computation time of a single period of 1 month is about 12 hours on a single node of Deltares' computation cluster. A one-year period therefore requires one week of computation, which is generally sufficient to reach dynamic equilibrium.

Table 2.2 Applied sediment concentration boundary conditions (both fractions, in mg/l)

Boundary Section	Fraction 1	Fraction 2
North Sea	5	5
Wadden Sea	10	10
Ems	50	50

Table 2.3 Applied loads (in mg/l)

Load	Discharge (m^3/s)	Total Load (kton/year)	C fraction 1 (mg/l)	C fraction 2 (mg/l)
Leda	2	6.3	50	50
Nieuw Statenzijl	6.85	21.6	50	50
Delfzijl	10.7	33.7	50	50
Lauwersmeer	45	141.9	50	50

2.3 Results

All results presented here are results of simulations that are in complete dynamic equilibrium. Dynamic equilibrium is defined here as two consecutive computations (of a one month period) which change less than 1%. This implies that the results are independent from the applied (uniform) initial conditions, but result form the process formulations and boundary conditions only. As discussed previously, these settings have not yet been optimised to minimize the difference between model results and observations (i.e. not calibrated). This will be done in 2011 based on a full year of hydrodynamic forcing.

The required time-scale to reach equilibrium is about one year (i.e. 12 one-month cycles at present). Note that the thickness of the buffer layer in simulations 2 and 3 have been set at a small value (0.01 m). This setting hardly affects equilibrium concentrations and equilibrium bed composition, but reduces spin-up time considerably. With more realistic settings (order 0.1 m) the spin-up (and response) time would be substantially longer. The present spin-up time is therefore no reliable indication of the actual response Eems-Dollard system time with regard to fine sediment dynamics.

In the remainder of this chapter results are presented and discussed in terms of suspended sediment concentration, bed composition and mud balances.

2.3.1 Concentration

Figure 2.3 shows the yearly-averaged near-surface (left) and near-bed (right) suspended sediment concentration for simulations I (top), II (middle) and III (bottom). Concentrations for simulation I (without water-bed exchange) are highest and for simulation II lowest. Concentrations for simulation III are between those for I and II, but much closer to II than to I.

Apparently, the Eems-Dollard estuary is a very efficient sediment trap. The concentration gradient between the North Sea and the estuary is very high in simulation I, resulting from a combination of estuarine circulation and tidal asymmetry. The relative importance of these mechanisms can be determined by carrying out a simulation without freshwater discharge – this is part of future work.

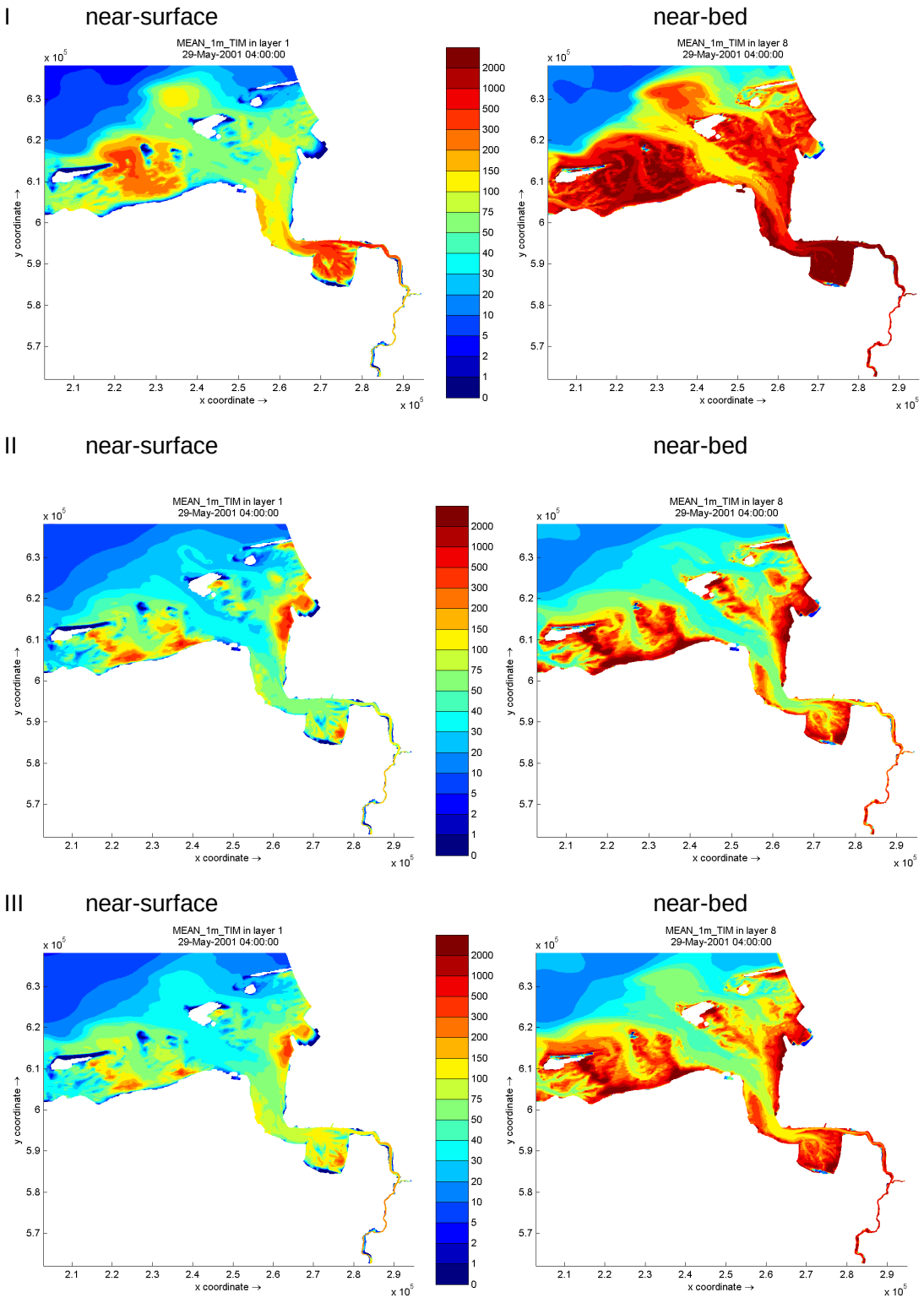

Figure 2.3 time-averaged near-surface (left) and near-bed (right) suspended sediment concentration for simulations I (top), II (middle) and III (bottom).

Figure 2.4 shows time series of the computed near-surface SPM concentration at Groote Gat Noord and Bocht van Watum. MWTL-observations are also shown, but because of their low temporal resolution, the number of observations is limited. Based on this comparison, it appears that computed SPM levels for simulation I are too high. Table 2.4 shows the time-average SPM concentration at a number of MWTL-locations, both computed and observed. It confirms the conclusion that SPM levels of simulation I are too high (with about a factor of 2). Simulation II underestimates the SPM-levels, whereas the computed levels in simulation III are within 30% of the observed levels. Note that the absolute overall concentration level can be easily adapted by changing the boundary conditions, but that the longitudinal concentration gradient is modified by changing settings for settling speed and deposition efficiency.

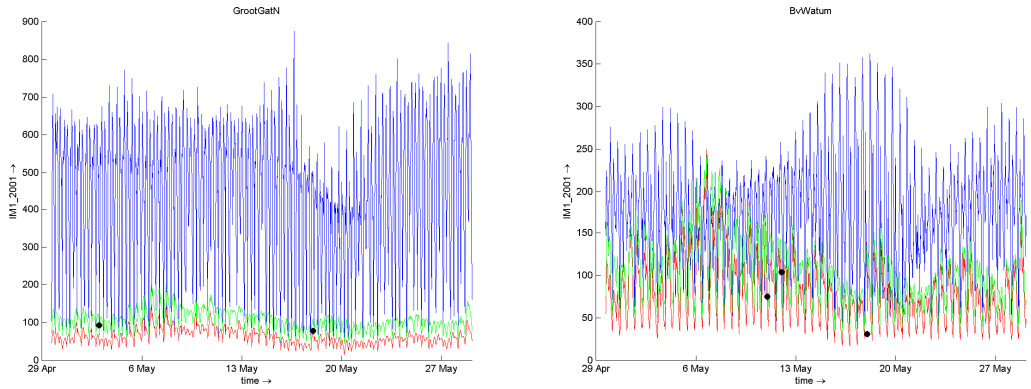

Figure 2.4 Computed and observed near-surface SPM-levels at Groote Gat Noord (left) and Bocht van Watum (right). I: blue; II: red; III: green; black dots: MWTL observations.

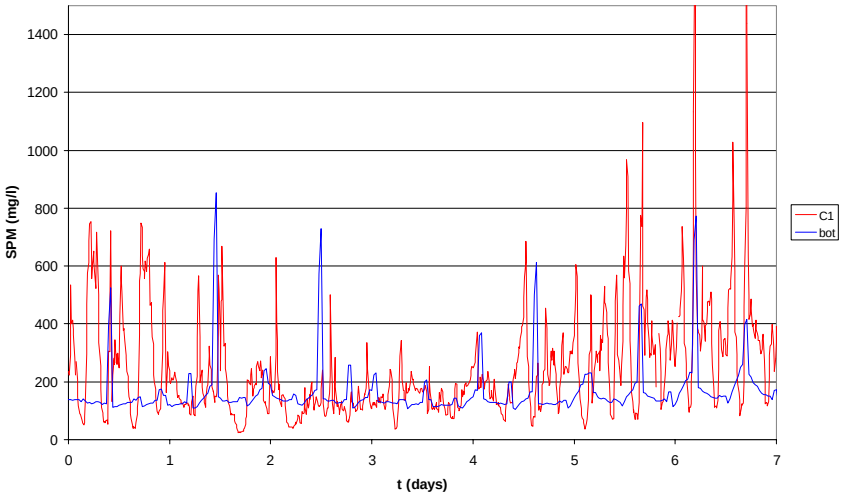

Figure 2.5 Comparison between computed (simulation III, 'bot') and observed ('C1') SPM concentration 0.15 m above the bed at Groote Gat Noord. Observation period 15 – 22/10/1991. Simulation period 29/4 – 5/5/2001.

Table 2.4 Computed and observed mean SPM concentration levels (mg/l).

Location/simulation	I	II	III	observed	sdev	n obs
Huibertgat	69	33	37	29	38	726
Doekegat	93	41	55	64	47	278
Bocht van Watum	161	80	103	79	64	324
Groote Gat Noord	254	63	107	127	105	801

Figure 2.5 shows the computed and observed concentration at Groote Gat Noord for a one-week period. A direct comparison is not possible, as the conditions during these periods differ. Base levels and peak values of SPM have the same order of magnitude, but the variability of the observations is much larger than that of the simulation. It is recommended to carry out such comparison for the same period, as it is unclear which part of the difference between computations and observations may be attributed to different forcing (tide, wind, freshwater discharge, history of sediment supply) and which part to model deficiencies. This would require a hydrodynamic simulation for the year 1996.

Compared to the 2009 mud model based on Delft3D-FLOW, the reproduction of typical concentration levels in the Dollard estuary has significantly been improved. For example, typical SPM levels at BOA bridge (Figure 2.6) agree well with observations (Figure 2.7). However, a direct comparison is not possible, as simulation and observation period differ.

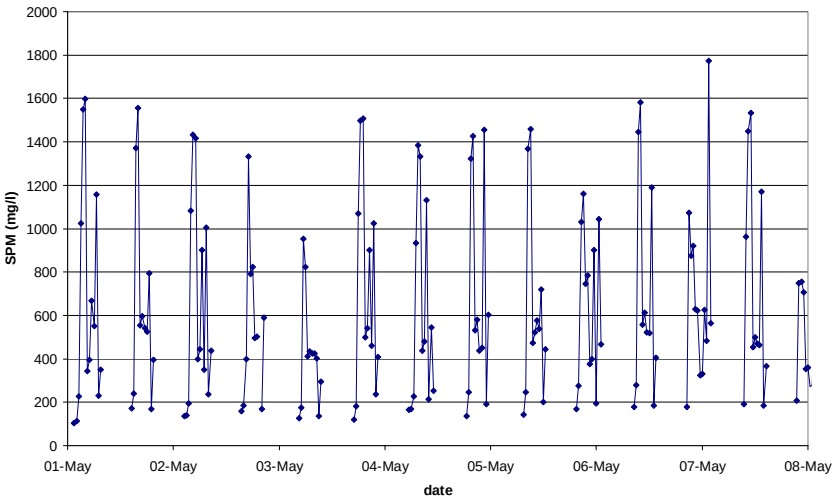

Figure 2.6 Computed near-bed SPM concentration at BOA bridge(simulation III). Simulation period 1/5 – 8/5/2001. Results do not cover a complete tidal cycle as the BOA bridge falls dry.

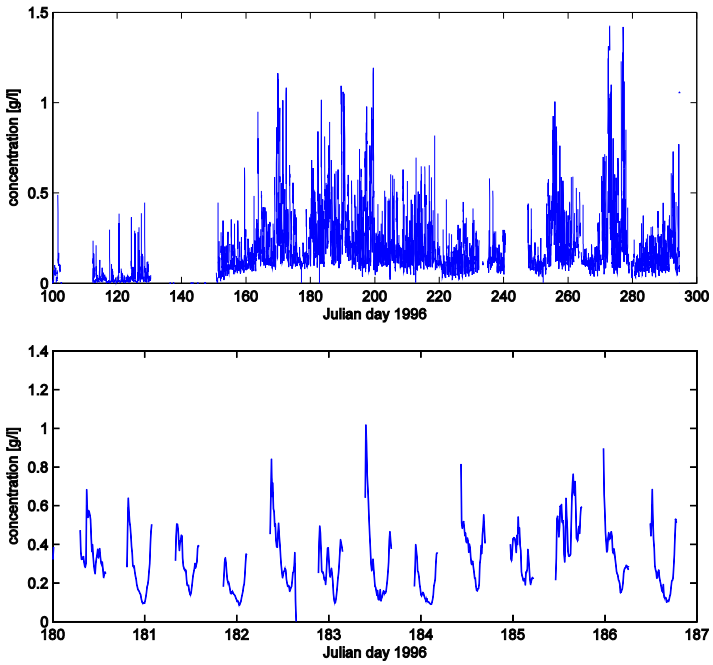

Figure 2.7 Observed sediment concentration at the Boa bridge, 1996: full data series (top) and detail (bottom).

2.3.2 Bed composition and accretion

Two types of areas occur in the simulations:

1. intermediate to high-dynamic areas in which the bed composition is in dynamic equilibrium with the local bed shear stress climate and sediment supply;
2. low-dynamic areas in which net sediment accumulation occurs.

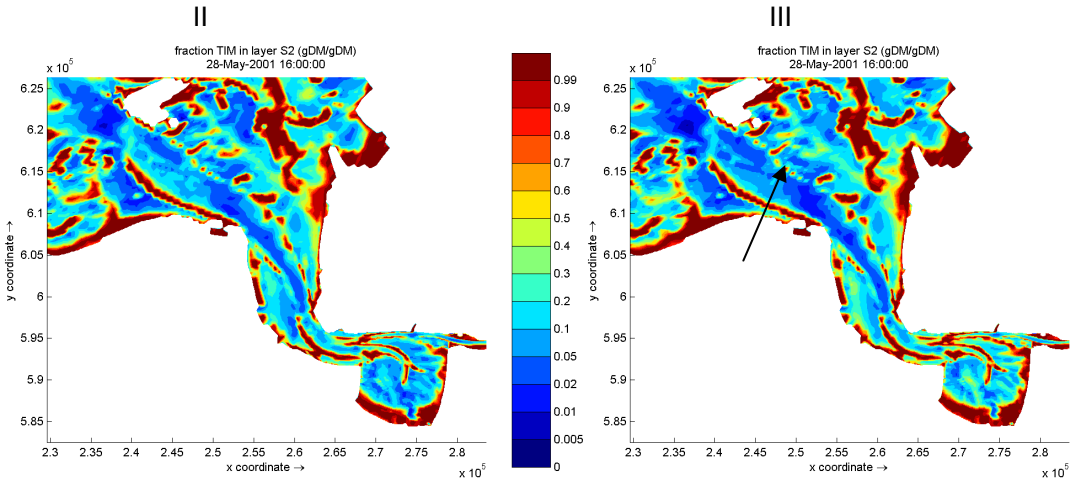

Figure 2.8 Computed equilibrium mud fraction (–) for simulations II and III.

Figure 2.8 shows the computed equilibrium bed composition of simulations II and III. Note that simulation I does not include water-bed exchange, so no bed composition is computed. The computed equilibrium bed composition is independent from the initial conditions. Different zones can be discerned, notably the tidal channels with a low mud content (typically only a

few percent or less) and the channel edges (where the mud supply is high) and higher tidal flats (where the hydrodynamic forcing is very mild), exhibiting a mud percentage up to 100. The lower tidal flats typically show a mud percentage between 5 and 50, probably caused by wave forcing. The agreement may be improved by increasing the critical shear stress for erosion in the model.

Some instabilities in mud content appear to occur along the channel edges (indicated with black arrow). However, these variations are caused by similar variations in bed shear stress and bathymetry in the hydrodynamic simulation. Along the channel edges, strong bed level gradients may result in staircase boundaries on coarse grids. A higher grid resolution would reduce such artefacts.

Figure 2.9 shows a comparison with observed data (De Jonge, 2000). Most and least dynamic areas are similar with respect to mud content (low and high, respectively), but also substantial differences are observed. According to observations, the Dollard is on average muddier than according to computations.

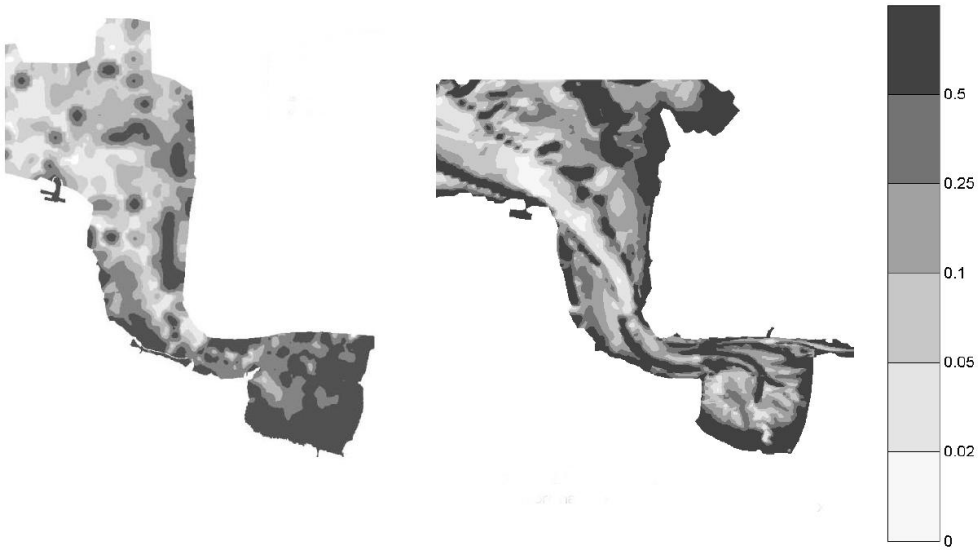

Figure 2.9 Observed (left, De Jonge, 2000) and modelled (right, sim. III) mud fraction.

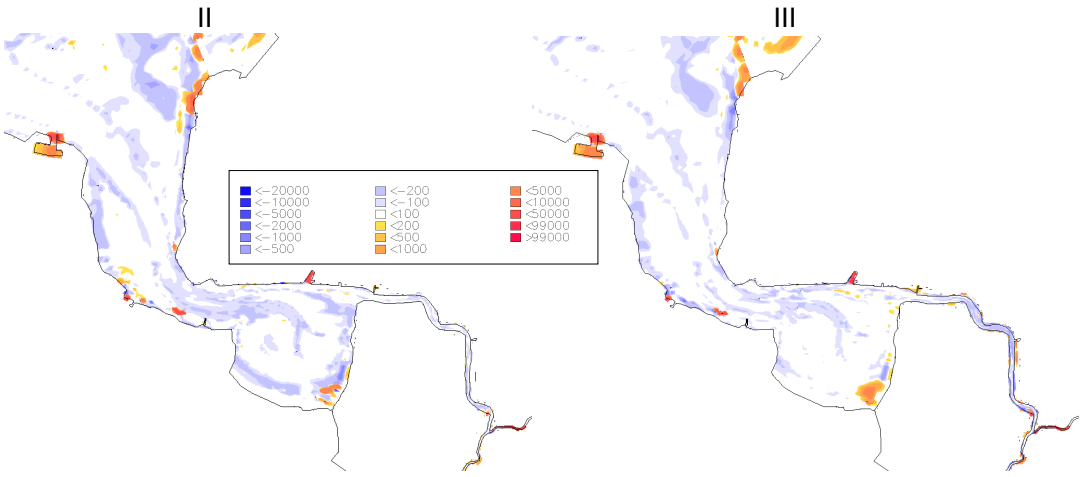

Figure 2.10 Computed net erosion and deposition (g/m2/y) for simulations II and III.

Figure 2.10 shows the computed net erosion and deposition patterns. Severe deposition (> 99 kg/m^2/y does occur in the harbours and harbour entrances of Eemshaven, Emden and Delfzijl and locally in some low-dynamic sections in the lower Ems. Moderate deposition (range 0.5 – 5 kg/m^2/year) does occur at some high mud flats in the south-eastern part of the Dollard and in Leybucht.

As remarked earlier, severe net erosion is impossible at equilibrium in the present model set-up. Some light net erosion (less than 1 kg/m^2/year) does occur at a number of places, as full equilibrium has been closely approached, but not yet completely attained because of required computation time.

No net deposition is computed for 'Bocht van Watum', whereas such deposition is observed in the field. If observed deposits are predominantly muddy, a better agreement may be attained by increasing the critical shear stress for erosion. If observed deposits are mostly sandy, they are by definition beyond the predictive capabilities of the present model, which does not include sand transport.

2.3.3 Mud balance

Figure 2.11 defines the areas for which a water and mud balance has been made for simulations I, II and III. The water balance is equal for all simulations, as they are based on the same hydrodynamic simulation. From the water balance (Figure 2.12) the magnitude of the freshwater discharges and tidal volumes can be quantified.

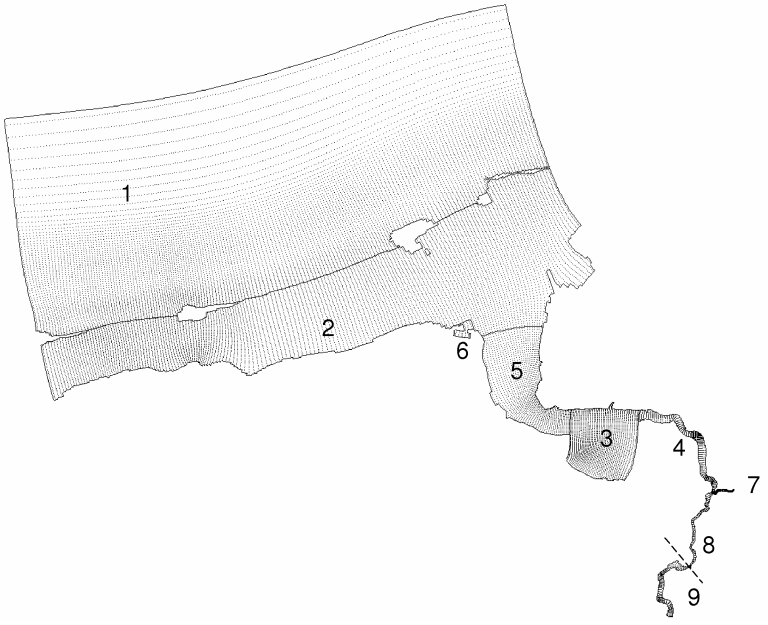

Figure 2.11 Definition of balance areas

The net mud balance of simulation I (Figure 2.13) is straightforward, as water-bed exchange is disabled. At full equilibrium, the residual seaward sediment flux equals the fluvial sediment load. For areas 7, 8, 9 this is indeed exactly the case, notably for area 5 a full equilibrium has not yet completely been reached. The (orange) storage term implies that still 280 kton/year accumulates in area 5 over a year. TSM-levels are therefore still further increasing in this area.

For simulations II and III, the net accumulation per area is added to the net flux balance. This implies that at full equilibrium, the residual seaward sediment flux equals the fluvial sediment load minus the net deposition in the estuary. As the net deposition term is quite sensitive to parameters settings such as the critical shear stress for erosion, this term is in fact steered by modeller. If the net estuarine deposition D exceeds the fluvial load L, a net import of marine sediments must occur. However, it can be demonstrated that for a well-mixed estuary the fraction of marine sediment $f_{mar} = T_{sea} / (T_{sea} + L)$ with T_{sea} the gross sediment flux from sea and L the fluvial load. Typically, gross terms of the mud balance are much larger than net terms. As often $T_{sea} >> L$, an estuary typically imports marine sediment at a rate $f_{mar}D$ close to D, even if $L > D$. Based on these basic principles and the gross mud balances presented (Figure 2.14 and Figure 2.15), a significant fluvial sediment fraction is only expected in areas 7, 8 and 9. Area 4 is expected to be a transition zone between fluvial and marine domination.

An important observation in both model simulations approximately 0.3 Mt/y is deposited in the Ems river (areas 4, 7 8 and 9), which is less than the applied fluvial load. As a result, the net seaward transport dominates as far downstream as the outer Ems Estuary. The implications hereof will be discussed in the next section.

2.4 Conclusions and recommendations

It is concluded that the Delft3D-WAQ mud model reproduces the main features of fine sediment dynamics in the Ems-Dollard estuary. The typical levels and the typical gradients in sediment concentration are well reproduced. This suggests that the governing physical processes are adequately simulated. This is further supported by the good agreement between observed and modelled mud fraction in the Ems Dollard estuary. Both the good spatial variation in the sediment concentration and the mud fraction is an important improvement compared to the sediment transport simulations in 2009 (Van Maren, 2010), when the typical concentrations in the Ems Estuary and the Ems River were well reproduced, but the sediment deposition in the Dollard (and resulting high sediment concentrations) were underestimated. Further improving the modelled sediment concentration against measured concentration data requires the use of representative hydrodynamic and meteo forcing (i.e. tide, wind, freshwater discharge). The most accurate sediment concentration measurements in the Ems-Dollard estuary are from 1990-1991 (see Van Maren, 2010). Simulating the hydrodynamics and sediment transport during this period is part of future work.

It should be realized that the model forcing applied in this study is of May 2001, which can be considered a relatively low energy period. Fine sediment is transported towards mudflats by tidal currents through a combination of asymmetries or variations in the current field and bed level and of sediment characteristics, giving rise to settling, scour, and mixing lags. This onshore transport generates a pronounced sediment concentration gradient from the muddy intertidal area to the relatively clear seawater which, in combination with the oscillating tidal currents, produces a seaward directed sediment flux. The sediment concentration gradient is substantially higher during storms due to increased bed shear stress due to waves (especially in the shallow areas), water level setup (making the generally fine-grained supra-tidal deposits available for erosion) and wind-driven currents. This often results in a net offshore directed transport during storms, compensated by net onshore transport during calm weather. Since we have only simulated low-energy conditions, and extrapolated this to yearly fluxes, the net landward flux is overestimated in the model. This effect will be analysed in more detail in 2011, when a full year of hydrodynamics will be available for reference.

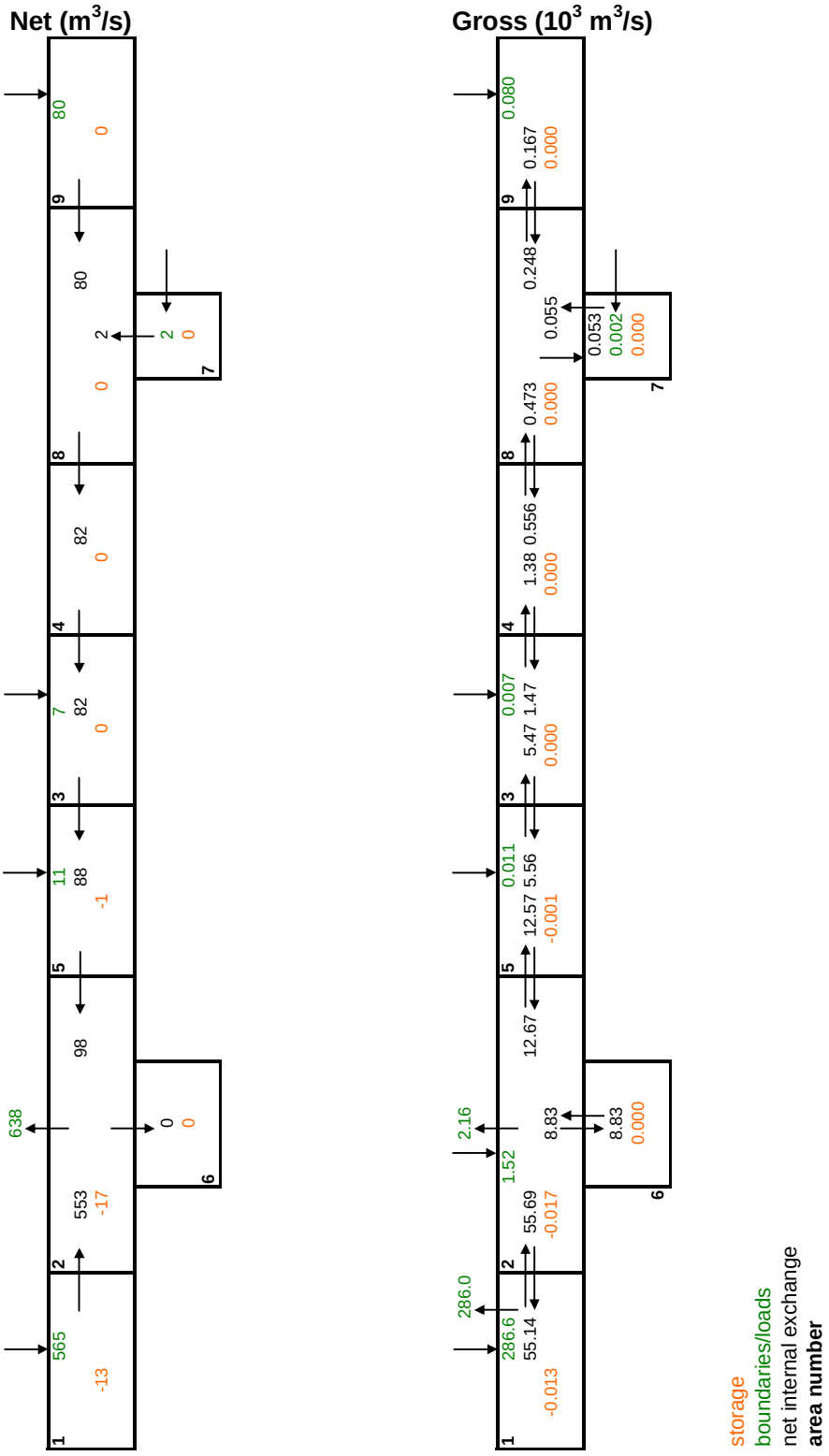

Figure 2.12 Water balance

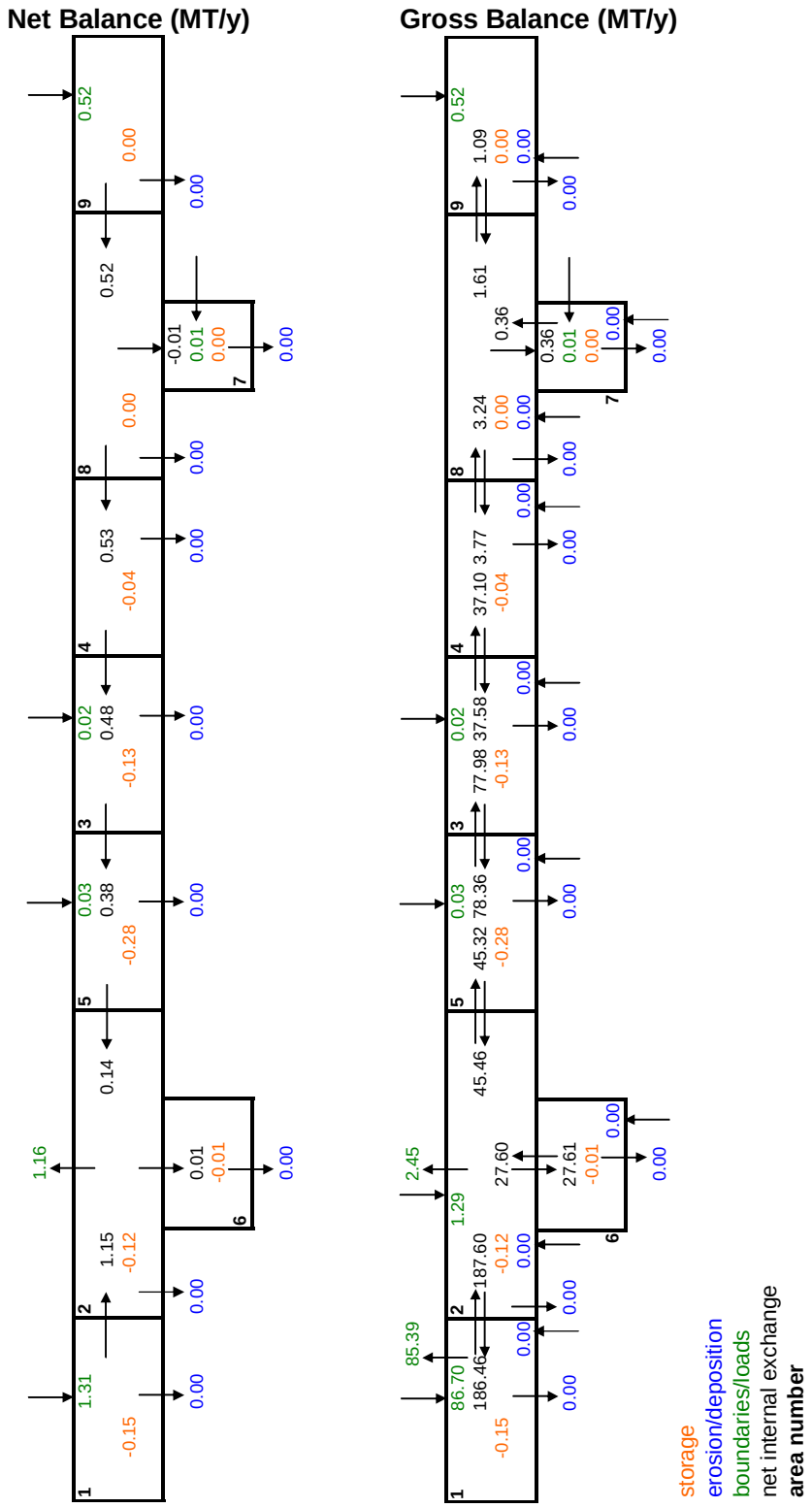

Figure 2.13 Sediment balance simulation I.

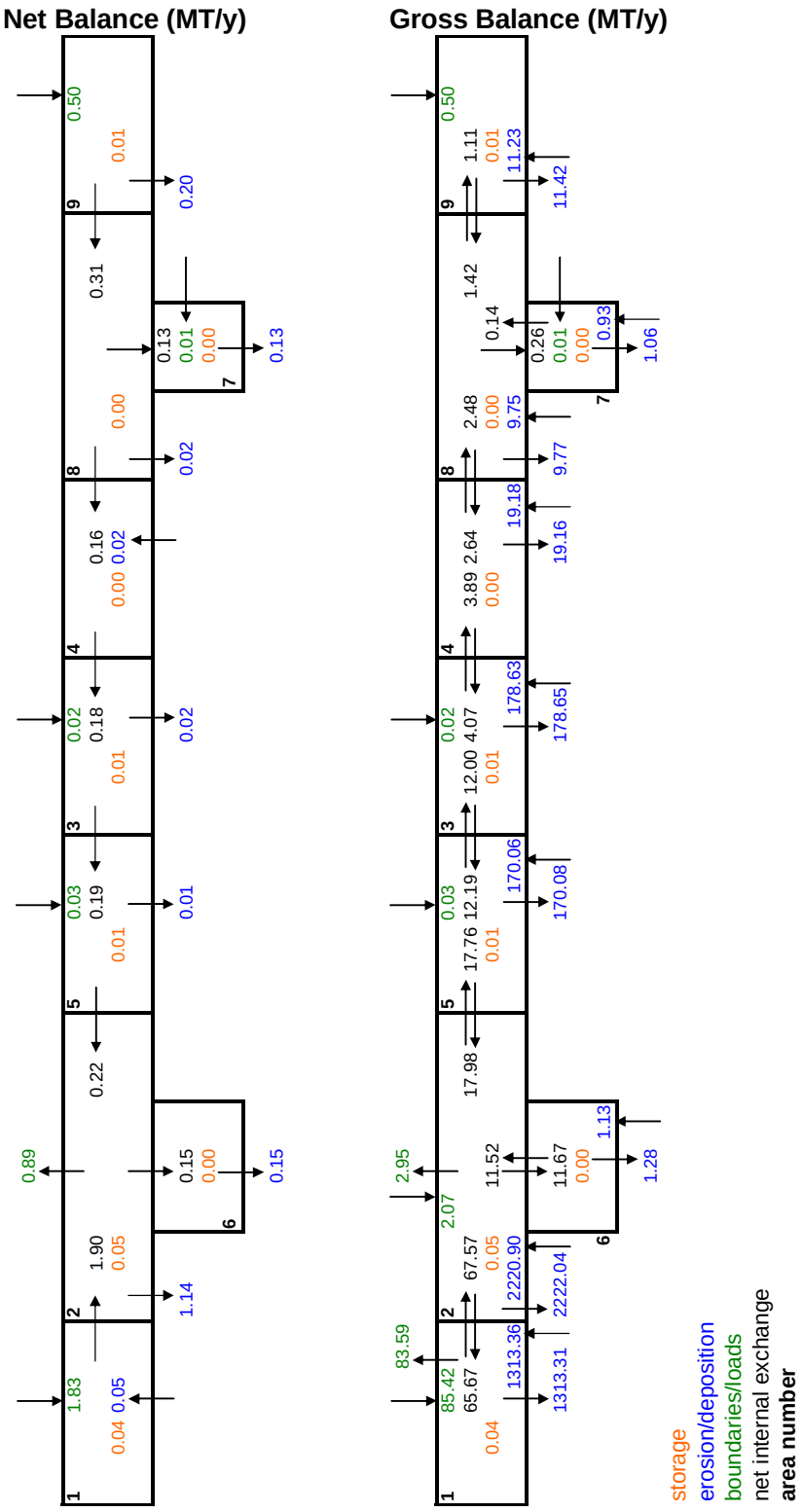

Figure 2.14 Sediment balance simulation iI.

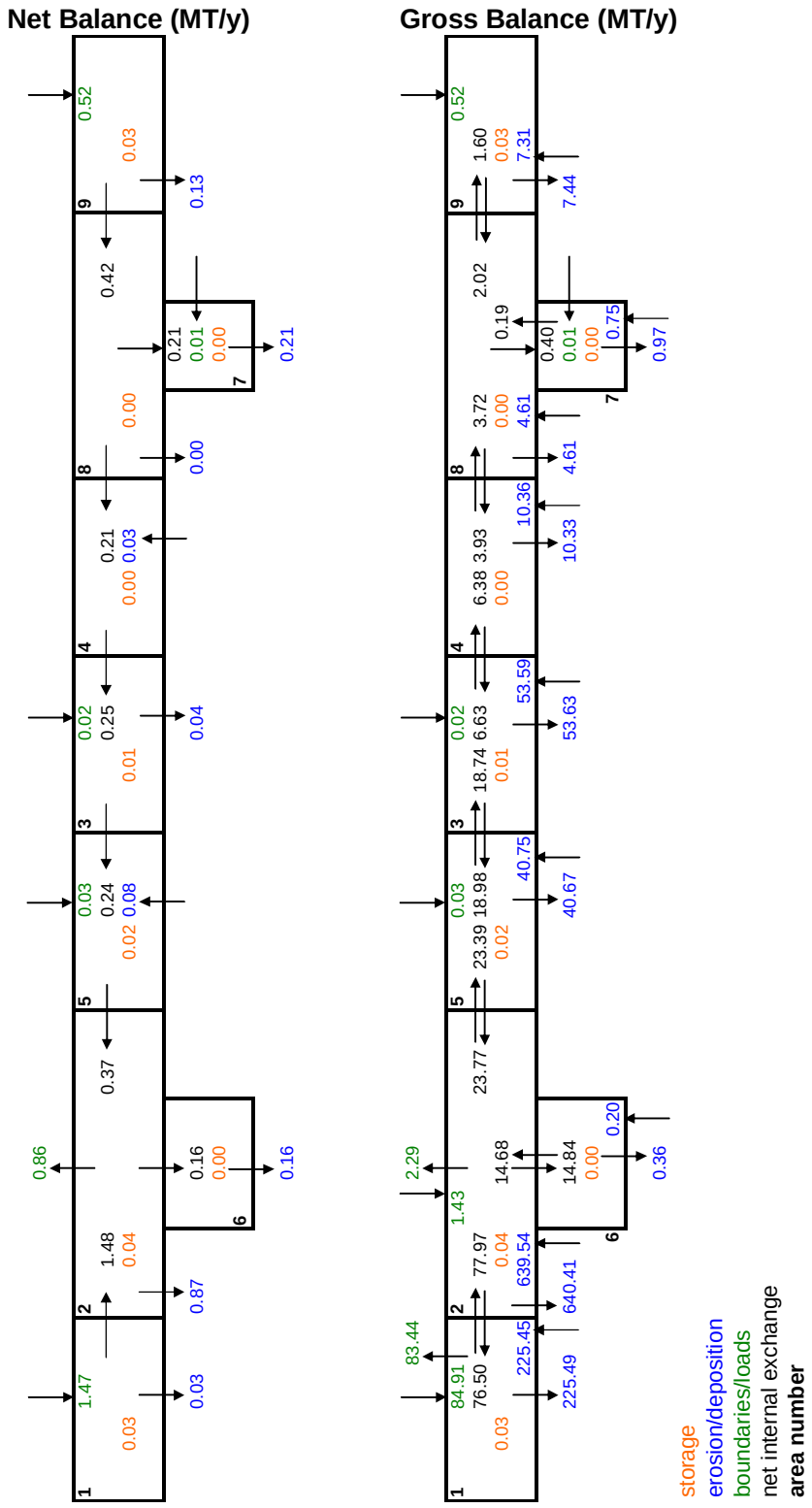

Figure 2.15 Sediment balance simulation III.

Although the sediment dynamics in the Ems Estuary and the Dollard Estuary are well reproduced, the WAQ model underestimated transport into the Ems River. The model predicts deposition of 0.3 Mt/y, which is less than the (imposed) discharge from the Ems River. With a typical slurry density of 250 kg/m^3, 0.3 Mt/y is equal to 1.2 million m^3/year. Approximately 2 million m^3/year is annually dredged from the Ems River, which therefore suggests the model only underestimates deposition with 50%. However, the organic content of the mud deposits suggest that most of the sediment in the Ems River (up to Herbrum) is of marine origin (pers. comm. A. Schoel). Hence, the fluvial input is overestimated while the marine input into the Ems River is underestimated. The overestimation of the fluvial input is probably the result of the imposed sediment concentration from the lower Ems River: 100 mg/l is probably too high. The underestimation of the trapping of marine sediments may have two explanations. Van Maren (2010) concluded that (1) primarily sediment with a settling velocity of 1 mm/s or higher is transported in the upstream direction (whereas here fractions of 0.125 and 1 mm/s are used), and (2) damping of turbulence mixing by sediment-induced density gradients are important for net import of sediment. This damping of turbulence mixing was the main reason to model sediment within sediment-online in 2009.

Conclusively, there are now two sediment transport models available for sediment transport in the Ems-Dollard estuary. The 2009 model better reproduces sediment import into the Ems River, but the 2010 WAQ model better reproduces sediment dynamics in the Ems and Dollard estuaries. Both models can be improved by a more detailed comparison against observation data. Preferably, the strong points of both model concepts should be combined into one model. For example, the effect of turbulence damping may be included in parameterised form in the WAQ model or some of the buffer functionality may be included in the sediment-online model. This will be investigated in 2011.

3 Eems-Dollard Water Quality Modelling

3.1 Introduction

This part of the report deals with the setting-up and validation of the water quality/primary production model. This building block in the “effect chain” framework is coupled to the output of the hydrodynamic/sediment transport models and provides input to the ecological assessment by HABITAT. The ultimate aim of the modelling framework is to develop a robust and quantitative assessment tool to support management decision related to site-specific issues, such as the relation between high turbidity and oxygen-depleted zones or the effect of nutrient inputs and dredging activities on water quality and habitat suitability. This will enhance the understanding of cause-effect relationships between the physical, natural environment and system stressors.

3.2 System description

The Ems-Dollard estuary, located on the border of the Netherlands and Germany, is a semi-enclosed body of water stretching from the Island of Borkum to the weir in Herbrum, the end of the range of tidal influence. Three main subareas can be identified in the Ems-Dollard estuary: the Lower, Middle and Dollard reaches. The Ems-Dollard estuary is forced by semidiurnal tides with tidal ranges increasing from 2.3 m at the inlet to ~3.5 m in the river. The other dominant physical processes that affect the estuary are wind (both waves and shear) and freshwater inflow from the Ems River and Westerwoldse Aa. Approximately 90 % of the freshwater input comes from the Ems River which drains a basin of ~ 12,600 km^2, discharging an average of ~ 80 m^3/s. Westerwoldse Aa discharges around 12.5 m^3/s. Although small, this river had a huge impact in the 60s and 70s because it carried a very high organic load originating from potato waste effluents. The average freshwater discharge to the estuary varies from 10 to 40 m^3/s during the summer months to a maximum of ~600 m^3/s during wet winter periods (yearly average is 80–110 m^3/s). Water temperature varies from 0°C to 25°C between winter and summer.

3.3 Model setup

3.3.1 Introduction

The primary objective of the water quality/ecological model is to get a better understanding of those factors that determine the biogeochemical and ecological dynamics in the Ems-Dollard estuary. More specifically, the model provides insight in the factors controlling primary production to determine whether primary production is nutrient-limited or light-limited. Considering the high nutrient concentrations and the reduced light climate due to suspended sediments in an estuary, primary production is expected to be predominantly controlled by light availability. The availability of light to primary producers is determined by: (a) the amount of incident light, (b) the bathymetry, (c) vertical mixing, and (d) the presence of inorganic particles. Consequently, the ecological model should accurately describe these factors. The sections below detail how this is achieved. The second major issue concerns oxygen levels and the occurrence of oxygen-depleted zones. Oxygen can be considered as a key variable, meaning that its concentration is determined by the complex interaction of physical (advection and diffusion, governed by hydrodynamic circulation), chemical (re-oxidation of reduced

species) and biological (primary production vs organic matter degradation) processes. The interaction of these processes forms the basis of the water quality/primary production model described in the following sections.

3.3.2 Model description

3.3.2.1 Coupling to hydrodynamic model

The water quality model, set up in Delft3D-WAQ, is coupled to the results of the flow model (implemented in Delft3D-FLOW) used to simulate hydrodynamic circulation, water velocities and salinity (see Van Maren, 2010). These results are the basis for the further modelling activities related to suspended matter, nutrients and phytoplankton productivity and hence also to the ecosystem. The hydrodynamic simulation, which only considers a period of one month (29th April - 29th May 2001), is rewound 12 times to obtain a full year water quality simulation. In this way, the seasonal variations in water quality can be accounted for. This provides a first approximation since the boundary conditions in the hydrodynamic model are only representative for the simulated time period during which the discharge of the Ems River is also kept constant at the average "baseline" value of 80 m^3/s (Figure 3.1). The validation of baseline water quality model is based on field measurements (meterological conditions,

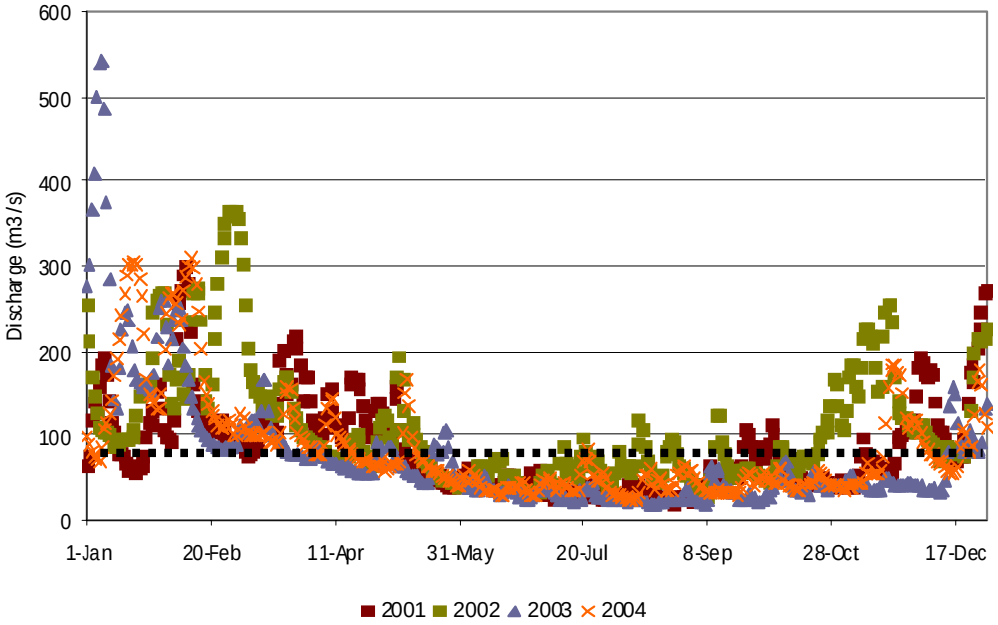

substance concentrations, polder discharges etc.) for the year 2001.

Figure 3.1 Daily Ems discharge (m^3/s) for different years between 2001 - 2004

3.3.2.2 Water quality/primary production modules

As described in more detail in Spiteri (2010), the setting up of the water quality/primary production model will take place in steps. As a first step, the water quality model includes the main processes of the Generic Ecological Model (GEM) in combination with the phytoplankton module BLOOM (Los et al. 2008, Blauw et al. 2008). This allows for the simulation of nutrient dynamics, including the effect of light availability and primary production

(Figure 3.2). BLOOM models the competition between species and the adaptation by species to limiting factors such as nutrients and light. Table 3.1 gives an overview of the processes that are currently implemented in GEM and BLOOM. Phosphorus sorption/desorption, microphytobenthos and grazing are not yet part of the current model setup but will be included in the next steps of model extension to refine the simulation of primary production. Sediment diagenesis in DELWAQ-G that simulates explicitly the diagenetic processes in the sediment compartment might be considered at a later stage, depending on the amount and quality of the sediment data available to validate this module.

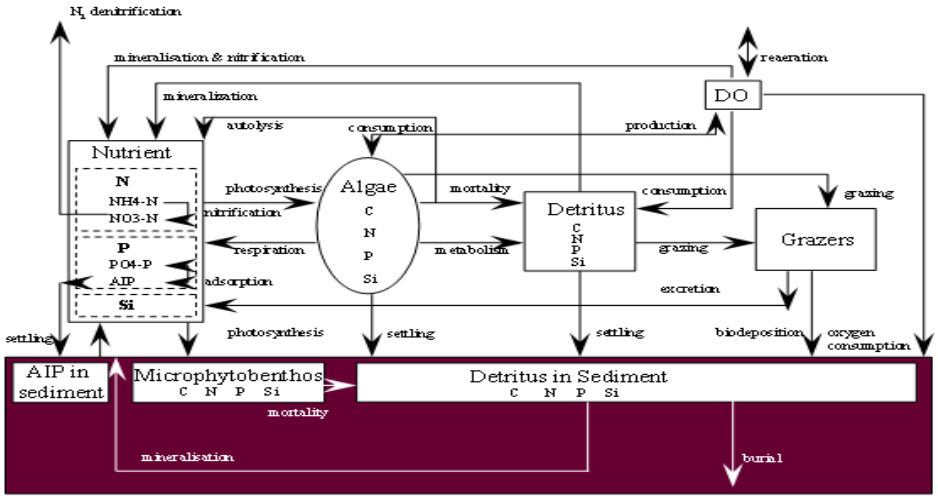

Figure 3.2 Schematic overview of the main DELWAQ processes and variables

Table 3.1 An overview of the main processes in the model. The list of processes and process parameters, primarily derived from the ZUNO model, is given in Appendix A. Grey processes are not yet active in the current set-up.

Process	**GEM**	**BLOOM**	**CONSBL**	**S1/S2**	**DELWAQ-G**
sedimentation and resuspension	**x**			x	x
Re-aeration of oxygen	**x**				
aerobic decomposition of organic substances	**x**				x
denitrification	**x**				x
nitrification	**x**				x
phosphorus sorption/desorption	x				x
light extinction	**x**				
phytoplankton		**x**			
growth/respiration/mortality					
atmospheric deposition	**x**				
microphytobenthos		x			
grazing			x		
sediment diagenesis					x

Table 3.2 An overview of the state variables in the model. The list of processes and process parameters, primarily derived from the ZUNO model is given in Appendix A

State variable	Name used in the model
Water column	
Salinity	Salinity (FrCon, FrFlow, SalBnd) [1]
Pelagic phytoplankton community	4 species/12 types [2] (DINOFLAG, MDIATOMS, MFLAGELA, PHAEOCYS)
detritus fraction of organic carbon, nitrogen, silica and phosphorus	DetC, DetN, DetSi, DetP
inorganic nitrogen (ammonia, nitrate) inorganic dissolved silica inorganic phosphorus (dissolved ortho-phosphate)	NH4, NO3 Si PO4
dissolved oxygen	OXY
Sediment	
organic fraction of organic carbon, nitrogen, silica and phosphorus	DetCS1, DetNS1, DetSiS1, DetPS1

[1] Used to recompute *Salinity* based on variable freshwater discharge from the Ems River through the process *VarSal*

[2] Each phytoplankton species is composed of 3 types: N-type representing the ecophysiological condition of a species under nitrogen limitation, a P-type for phosphorus limitation and an E-type representing the state of a species under low light

The salinity obtained from the hydrodynamic model is based on the assumption that the Ems discharge is constant over the one month simulation period. Rewinding the hydrodynamic simulation by 12 times to reconstruct the full year will therefore result in an unrealistic salinity field. For this reason the process VarSal is implemented in the water quality model to recompute Salinity based on the “real” intra-annual variation in the Ems discharge rates reflecting the seasonal variations measured in the field. Using the variable fresh water flows, the effect of temporal variations on salinity can be taken into account. Dissolved oxygen saturation is a function of salinity. Next to temperature-dependent mortality, algal mortality is increased by salinity stress, implying that freshwater algae start dying when salinity increases whereas marine algae die off when salinity drops. Since algal lysis increases the concentration of detritus, also light extinction is affected by this process (see below).

Technically VarSal is implemented as follows:

1) The discharge at the average flow rate is defined (e.g. 80 m^3/s) with a concentration of 1 (m^3/m^3).
2) The computed concentration patterns show the fraction of fresh water in the water column (FrCon).
3) The local salinity now equals (1-FrCon) * SalBnd, where SalBnd = the salinity without the contribution of the river.

4) Next, a discharge proportional to the river flow (FrFlow) is defined which has a value of, for instance 1.1 when the flow rate is 110 percent of the average flow.
5) The time variable salinity concentration can now be approximated according to the term (1-FrCon)/(1-FrFlow)* SalBnd.
6) SalBnd is corrected with the term obtained in step 5. This means that if the actual riverine discharge rate is higher than the average flow and FrFlow is > 1 (e.g. 1.1), the term computed in step 5 is negative, and therefore the computed salinity is lower than SalBnd due to the relative diluting effect. The opposite also applies when the discharge rate is lower than the average flow and therefore FrFlow < 1.
7) This results in time variable salinity concentrations in proportion to the actual (fluctuating) flow.

Light availibility is tightly coupled to the water turbidity determined by the total light extinction in the water column. This is the sum of background extinction (water itself and non-modelled substances) and extinction due to phytoplankton, detritus and inorganic matter.

$$K_d = 0.067 + 0.081\left(19.4 - \frac{S}{1.8}\right) + 0.03POC + 0.036SS_1 + 0.005SS_2$$

where S is the salinity, POC is the particulate organic carbon concentration (mg C/l) and SS_1 and SS_2 are the concentration of small and large suspended sediment particles respectively. In this case, Salinity is used as a proxy for land-derived dissolved organic matter (humic material). Phytoplankton growth/mortality is simulated by BLOOM and is coupled to the detritus in GEM. The distribution of Inorganic matter is obtained directly from the results of the sediment transport modelling (Section 2) and implemented as a segment function (variable in time and space).

3.3.2.3 Nutrient sources

Point sources

Four main discharge sources are considered in the model. These are Eems/Leda tributary, NW-Statenzijl (Westerwoldse Aa), Delfzijl (Eemskanaal) and Lauwersmeer (Lauwersoog) (Figure 3.3). In the hydrodynamic model, as well as in the water quality model, the discharge rates are assumed constant in time (Table 3.3). Although the discharge rates of the point sources are lower than the Ems river discharge, it is possible that their impact is locally significant. Field measurements for 2001 are obtained for three of the four identified sources (NW-Statenzijl, Delfzijl and Lauwersmeer) but data should still be retrieved for the Eems/Leda tributary draining in the German side of the estuary.

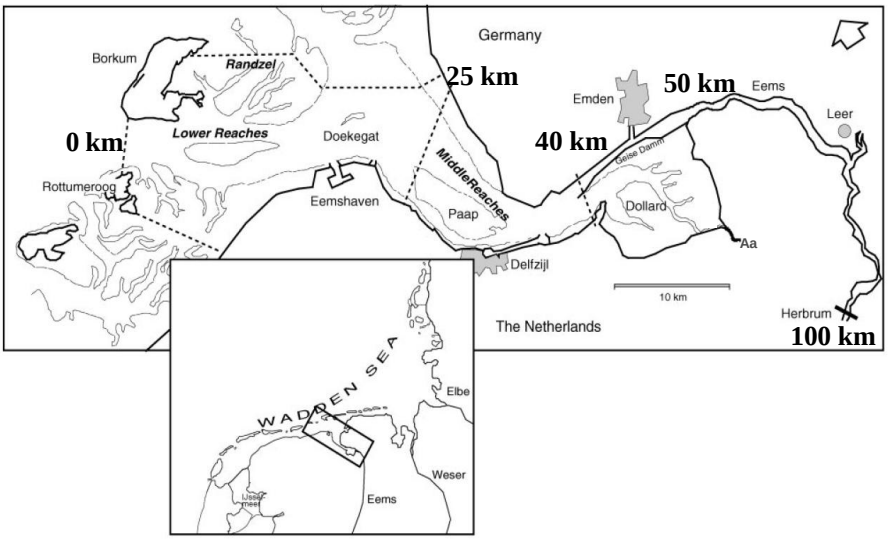

Figure 3.3 Map of the Ems-Dollard estuary showing the location of Westerwoldse Aa, draining into the Dollard, Delftzijl in the Middle Reach and Eemshaven in the Lower Reach (Source: De Jonge et al., 2000).

Table 3.3 List of main discharge sources into the Ems-Dollard estuary and their respective discharge rates

Discharge source	Discharge rate (m^3/s)
Eems/Leda	2
NW-Stratenzijl	6.85
Delfzijl	10.7
Lauwersmeer	15 *3

The field measurements include Total nitrogen (TotN), nitrate (NO3), ammonia (NH4), Total phosphorus (TotP) and ortho-phosphate (PO4). The time series measurements included in the model are shown in Figure 3.4. As a first approximation, detritus nitrogen (DetN) is assumed to be the difference between TotN and DIN (where DIN is the sum of NO3 and NH4). Similarly detritus phosphorus (DetP) is approximated as the difference between TotP and PO4. The consequence of this assumption is that the model most likely overestimates the fraction of nitrogen available for primary production, because no refractory portion of nitrogen is considered in the model. Likewise, the availability of phosphorus is overestimated, because no irreversibly bound phosphorus is considered yet. This may lead to overestimated production rates, and therefore chlorophyll concentrations.

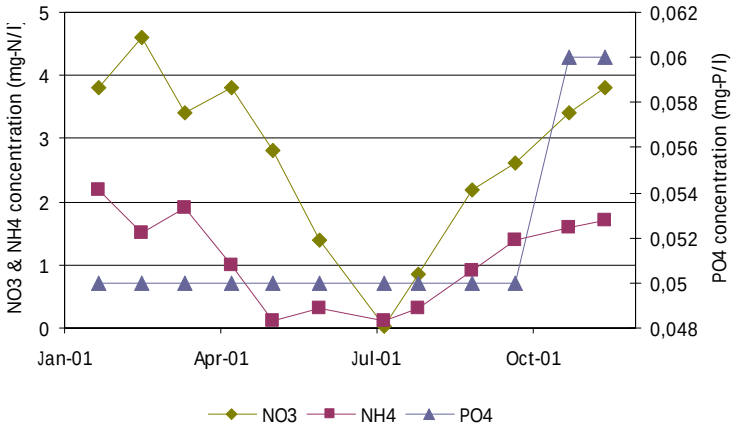	Westerwoldse Aa (NW-Statenzijl)
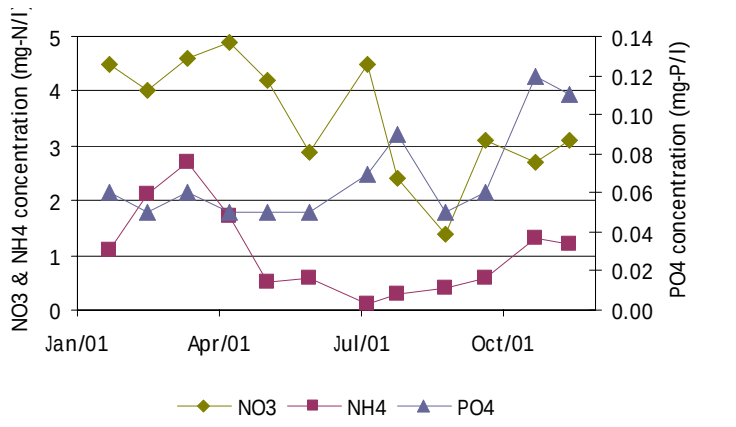	Eemskanaal (Delfzijl)
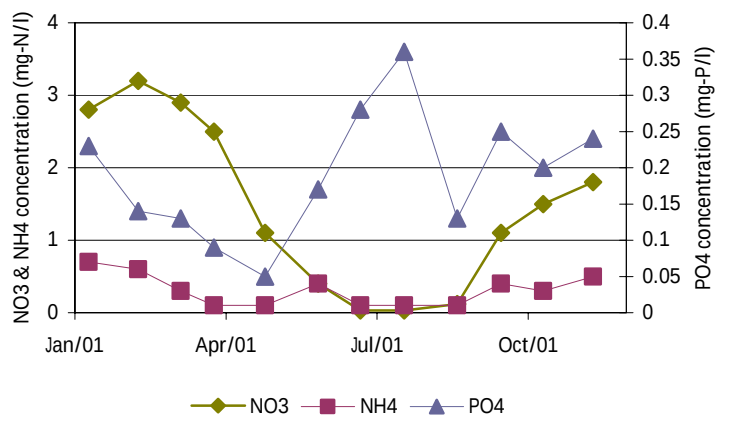	Lauwersoog (Lauwersmeer)

Figure 3.4 Nutrient concentration in the main polder loads into the Ems-Dollard estuary for the year 2001. Data from Waterschap Noorderzijlvest and Waterschap Hunze en Aa's.

Atmospheric deposition

As a first approach, a constant deposition of oxidized and reduced nitrogen in time and space is assumed. Modelled data for atmospheric deposition in the Eems-Dollard area were obtained from EMEP through the Baltic Nest interface (nest.su.se). Spatial variation in the area is visualized by interpolated EMEP modelling results (Figure 3.5, origin: Baltic Nest). There is a gradient where lowest deposition is at the North Sea side of the estuary, and higher values towards the Ems outlet. As a first approximation, values are chosen so that they correspond with the values close to the North Sea boundary (light blue part of the figures), which are 600 mg/m^2/yr and 900 mg/m^2/yr for oxidized and reduced nitrogen respectively. This will underestimate the atmospheric deposition at the estuary part of the system, where loadings from land are highest, and overestimate slightly the atmospheric deposition close to the North Sea boundary.

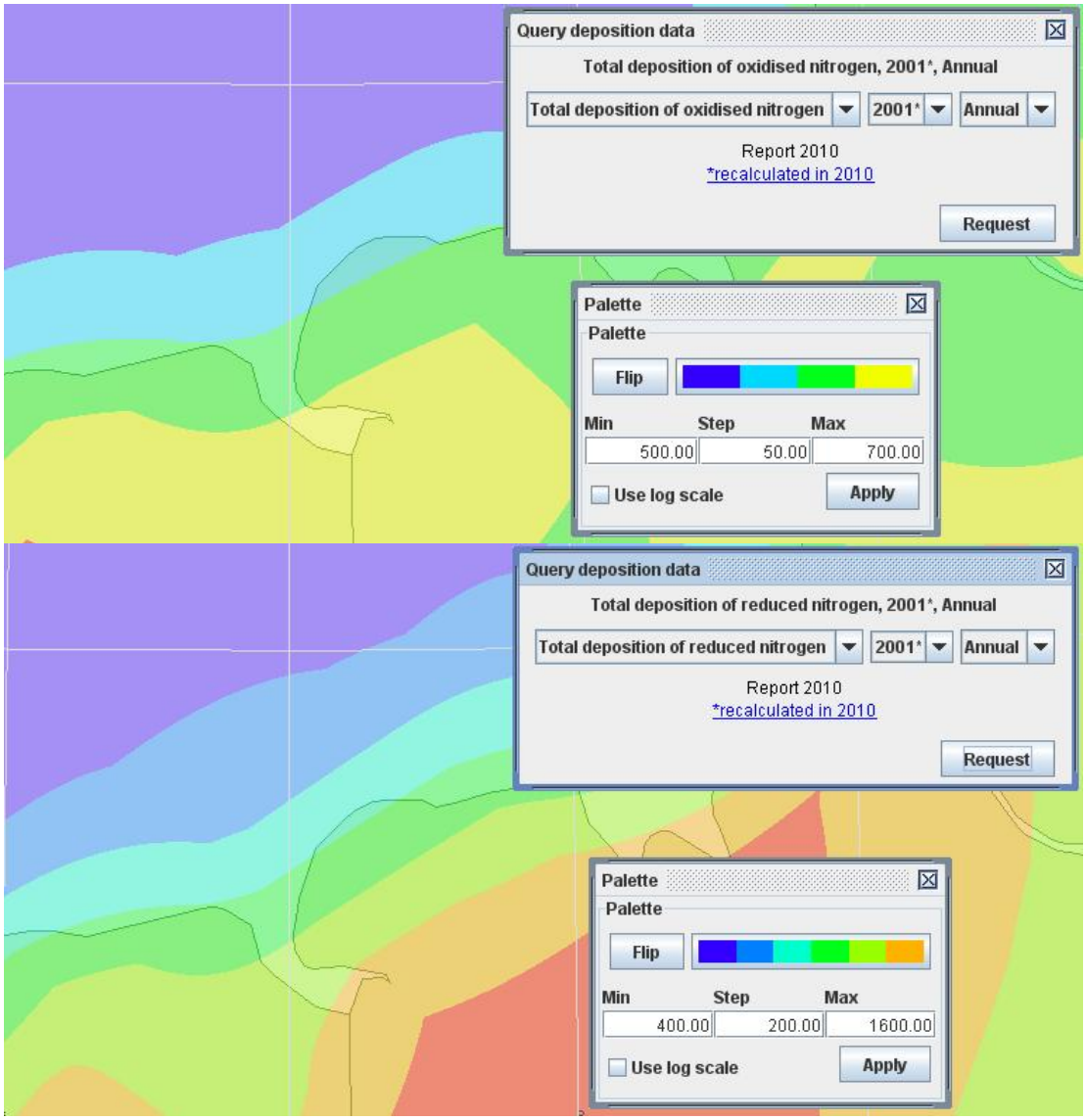

Figure 3.5 Maps of the area around the estuary showing the spatial distribution of total deposition of oxidized (top) and reduced (bottom) nitrogen. Data shown by the screenshots are modelled values from EMEP through the Baltic Nest interface (nest.su.se)

The monthly variation within the year 2001 is not available from this source, but can be shown by measured data of wet deposition at a monitoring station, Kollumerwaard, closest to the area of interest (Figure 3.6). As expected, wet nitrogen deposition varies with precipitation. Variation of wet nitrogen deposition within a year is mostly noticed in the first two months, where values were lower than in the rest of the year. Therefore, the choice for a constant atmospheric deposition might give an underestimation of nitrogen load only in January and February. This underestimation is clearer in 2001 as compared to an average year (Figure 3.7). Note that dry deposition is not included here, which may alter this situation. An average deposition is finally used in the model set-up (Table 3.4).

Figure 3.6 Measurement station for wet deposition closest to the estuary

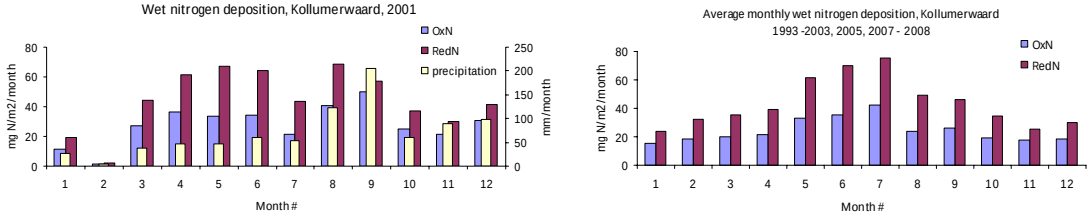

Figure 3.7 Monthly wet nitrogen deposition for 2001 (left panel) and averaged over the years 1993-2003, 2005, 2007-2008). Data from EMEP (www.emep.int).

Table 3.4 Atmospheric deposition values used for the current model set-up.

	DELWAQ variable		mg N/m^2/year	g N/m^2/day
oxN		NO_3	600	0.0016438
redN		NH_4	900	0.0024658

Contribution of Atmospheric deposition to model results

Including atmospheric deposition for nitrogen results in a small increase of dissolved inorganic nitrogen DIN (<3 %) for the landward stations Groote Gat noord and Bocht van Watum. This is due to the relatively large effect of land loadings on nitrogen concentration close to the load outlets. However, there is a noticeable increase of DIN (max 15 %) at the seaward station Huibertgat noordoost.

Atmospheric nitrogen is likely to be readily available for phytoplankton growth. At least the wet deposition of nitrogen, when considering a number of years, is highest during summer, when also the potential for primary production is likely to be highest. Therefore, it is concluded that atmospheric deposition should be included in the model for a correct

description of water quality. Furthermore, it should be considered to include a higher level of temporal resolution, due to the fact that deposition is highest during summer. It can be discussed whether it is needed to include a higher level of detail in spatial resolution at the moment.

3.3.2.4 Boundary Conditions

As already mentioned in Spiteri (2010), two alternatives were considered for setting up the downstream boundary conditions (Figure 3.8**Error! Reference source not found.**: all boundaries except Top-bottom 5): a) including substances loads via nesting from the North Sea model (ZUNO model, Los et al., 2008) using Delft3D-NESTWQ and b) assignment of boundary concentrations based on field concentrations. After several test runs, it was decided to use field measurements (Table 3.5) since the performance of the ZUNO model in the eastern Wadden Sea is still questionable, implying that the nested values do not corrrespond to the conditions in the field. The location of the monitoring locations considered for the different boundaries is shown in Figure 3.8. The field measurements from these stations include salinity, OXY, TotN, NO3, NH4, TotP and PO4 concentration. Figure 3.9 and **Error! Reference source not found.** show the 2001 time series for salinity and nutrients at the three monitoring locations used to contrain the downstream boundaries. As a first approximation, DetN is assumed to be the difference between TotN and DIN, whereas DetP is approximated as the difference between TotP and PO4.

Table 3.5 Used stations for boundary conditions

Boundary name	**Monitoring station used as boundary conditions**
Left-right 1	Rottum3
Top-bottom 1	Rottum3
Top-bottom 2	Rottum3
Top-bottom 3	NZR9TS010 (Terschelling 10)
Top-bottom 4	WZ480 (Zoutkamperlaag)
Top-bottom 5	Upstream Ems concentrations from input ZUNO model (OSPAR values)

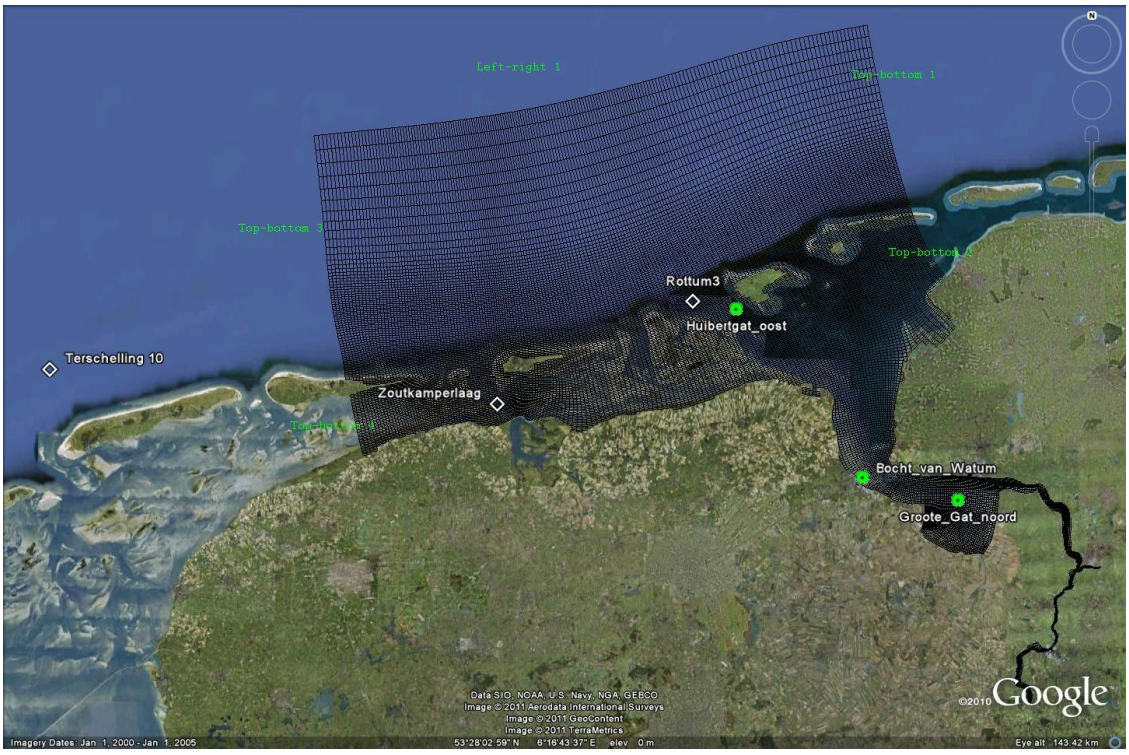

Figure 3.8 Location of boundaries, measurement stations for boundary conditions (squares) and monitoring stations for validation (green circles)

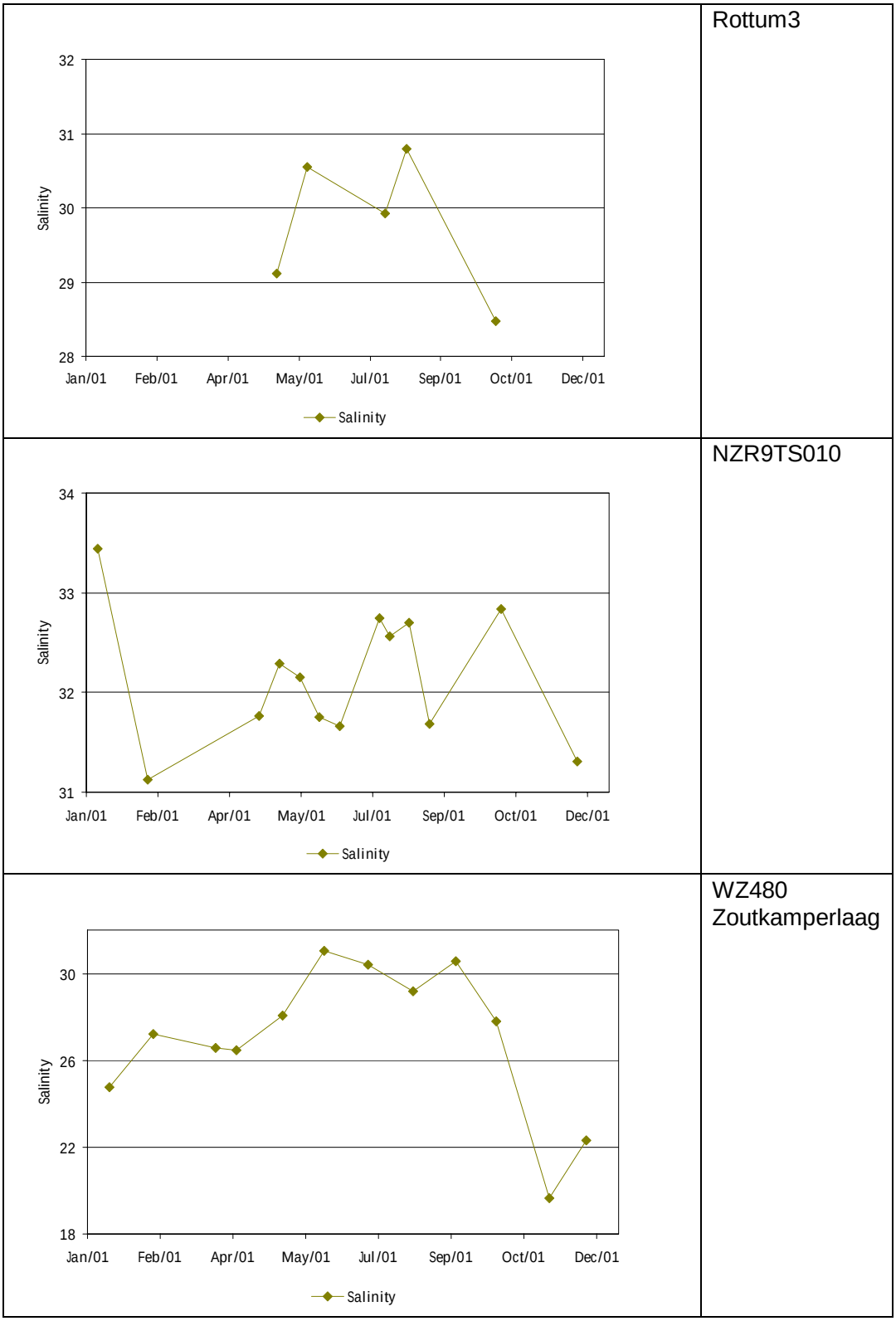

Figure 3.9 Measured salinity at the stations used for boundary conditions

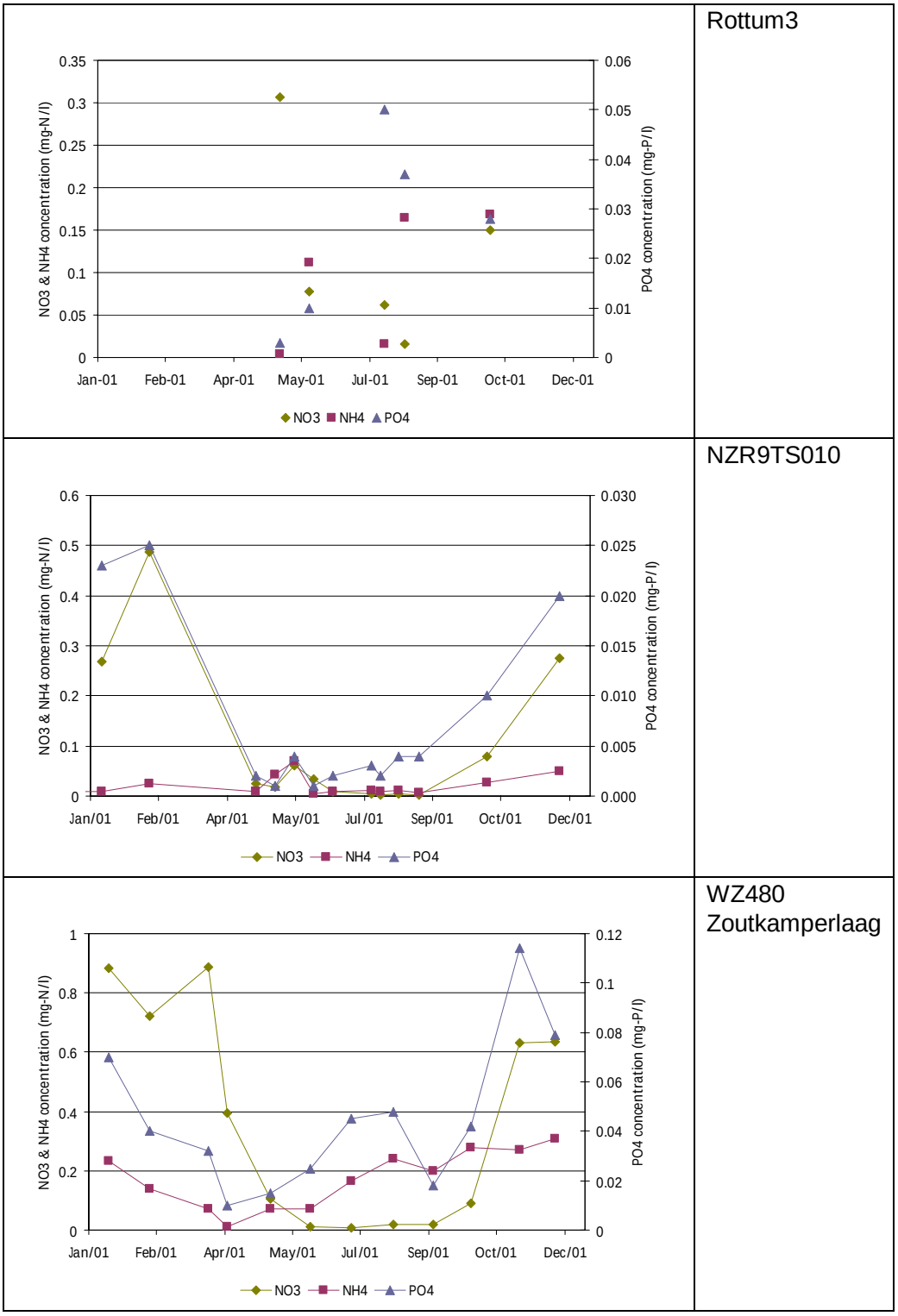

Figure 3.10 Measured nutrient concentrations at the stations used for boundary conditions

Values for the upstream boundary condition (Top-bottom 5, Figure 3.8) corresponding to the Ems River, are obtained from the OSPAR compilation based on field measurements, also used as an input in the ZUNO model. Field measuerements for NO3, NH4, PO4 (Figure 3.11) Si and OXY concentrations for 2001 are considered in the model.

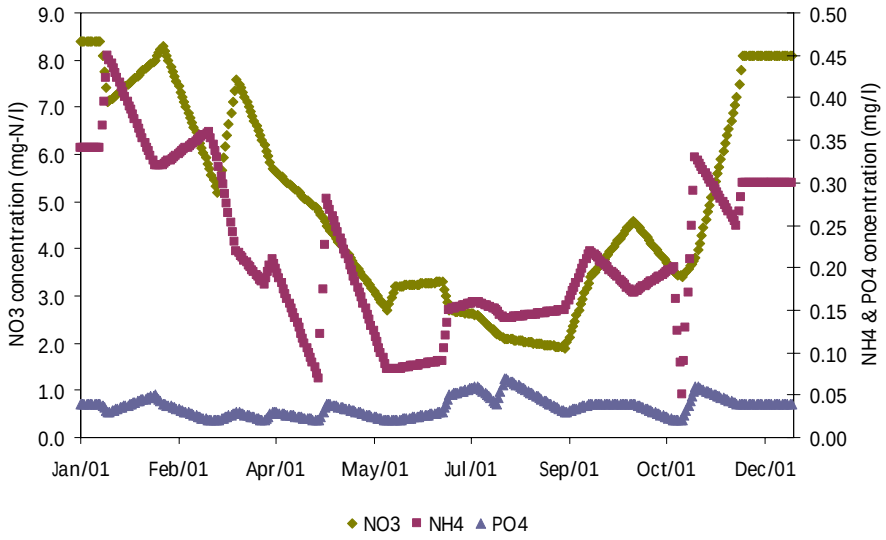

Figure 3.11 Measured nutrient concentrations at the Ems River, used as boundary condition.

3.3.2.5 *Forcing of the model*

SPM - Variations in inorganic suspended matter, and hence in the underwater light regime, are considerable both in time and space. Starting from the suspended sediment distribution from the sediment model output (section 2), an average spatial distribution over the time period 29/04/2001 and 29/05/2001 is derived per model layer. Seasonal variations over one year are then simulated by means of a cosine function around the computed average sediment field, with relatively high values in winter and low values in summer (Los et al. 2008). Its amplitude is based upon the level of variation in the measurements. Figure 3.12 shows a comparison of the sediment function composed of two sediment fractions (IM1 and IM2) and the measured sediment concentrations in the three reference monitoring locations (surface concentrations).

The segment function derived at the landward stations Groote Gat Noord and Bocht van Watum captures the magnitude and seasonal variation reasonably well. In the seaward station Huibertgat Oost the cosine function based on the modelled average suspended sediment concentration overestimates the measured sediment concentrations throughout the whole year, even though the typical sediment concentrations found in the Lower Reach are significantly lower than in the Dollard and Middle Reach. This implies that the results of the sediment model in the seaward region need to be further improved. Moreover, the effect of wind speed, which could play a role in the dispersion of suspended sediment, is not taken into account when extrapolating the average concentration field to the seasonally variable concentrations. This effect could be included to adjust the cosine function and hence improve the fit to the measured values. The most significant improvements in the sediment fit will result from the overall improvement of the sediment model, by coupling to, for instance, a full year hydrodynamic simulations when it becomes available.

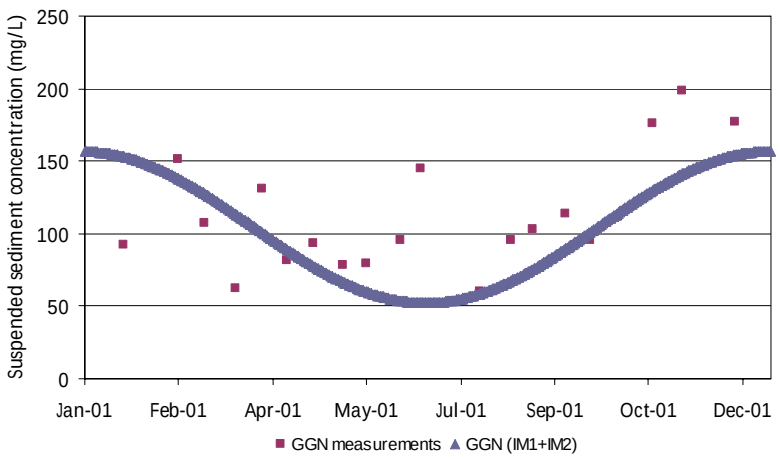	Groote Gat Noord (GGN)
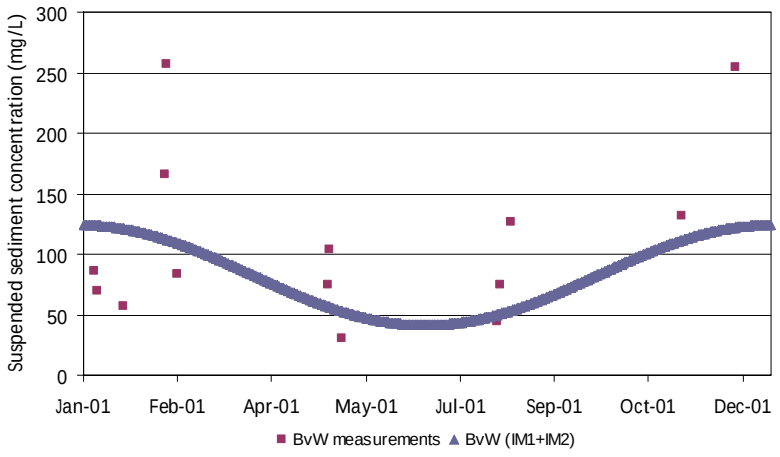	Bocht van Watum (BvW)
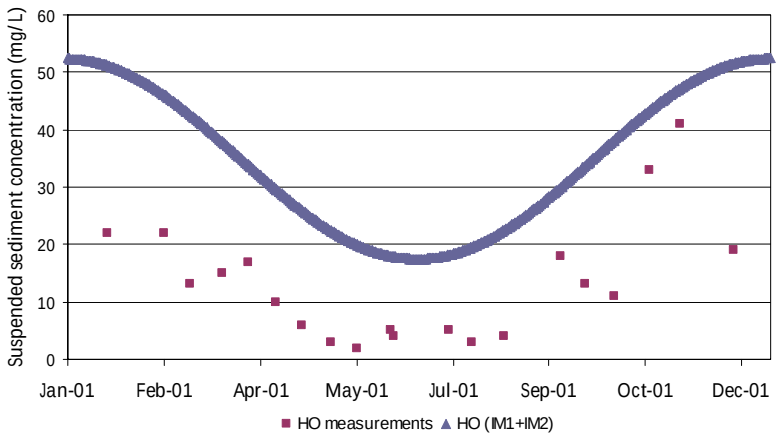	Huibertgat Oost (HO)

Figure 3.12 Measured surface suspended sediment concentration and segment function composed of IM1 and IM2. The cosine distribution is derived from the modelled sediment concentration.

Water temperature - The water temperature is derived from 2001 field measurements in the three reference monitoring locations: Groote Gat Noord (GGN) in the Dollard basin, Bocht van Watum (BvW) in the Middle Reach and Huibertgat Oost (HO) in the Lower Reach (Figure 3.3). Temperature is assumed to be spatially constant but varies temporally as shown in Figure 3.13.

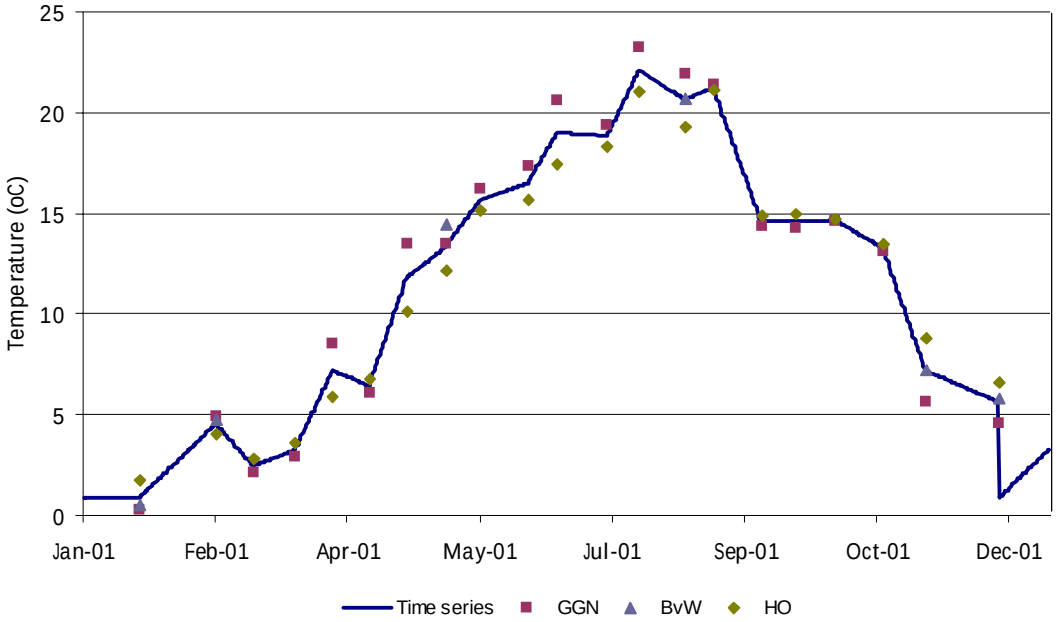

Figure 3.13 Water temperature at the three reference monitoring stations.

Surface irradiance - Surface radiation values (J/m^2/d) obtained from the KNMI station "Nieuw Beerta" are converted to daily averaged fluxes W/m^2 (Figure 3.14). It is assumed that the surface radiation varies in time but is spatially constant.

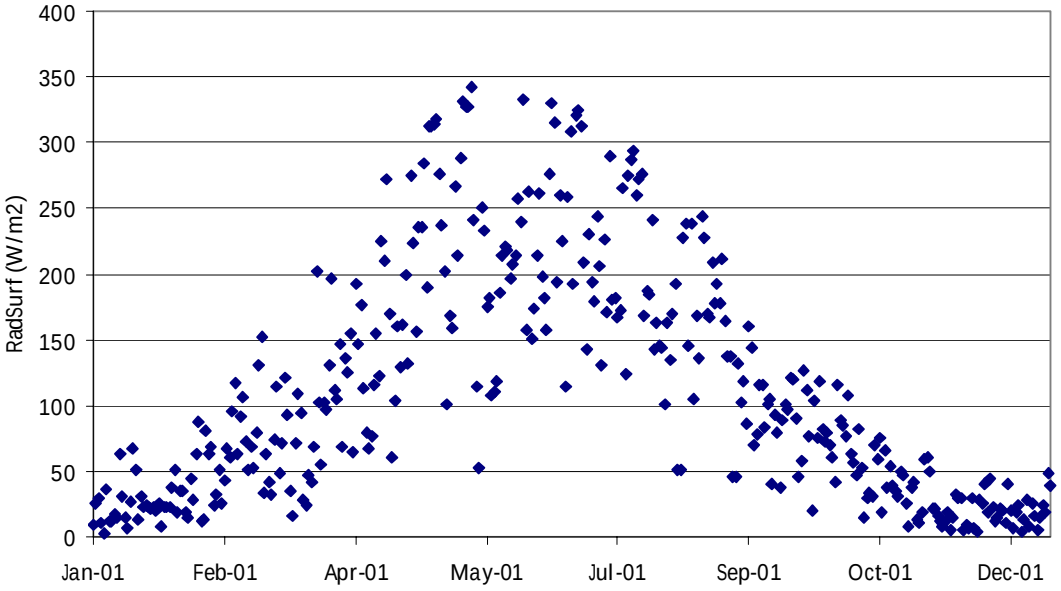

Figure 3.14 Measured daily averaged irradiance, calculated from surface irradiance at station "Nieuw Beerta".

Wind velocity - Daily measurements of wind speeds for year 2001 at "Nieuw Beerta" are obtained from KNMI database. As for surface irradiance, wind velocity is assumed to be spatially constant but temporally variable specified as time series measurements. Wind velocity is included in the water quality model since it is used to determine oxygen re-aeration between the water surface and the overlying atmosphere and vice-versa.

3.3.3 Schematization and numerical aspects

Grid schematization

The schematization of the water quality model is based on the grid used in the hydrodynamics and sediment model. The hydrodynamic model uses a grid consisting of approximately 500,000 active cells in 8 layers. For the water quality model, the aim is to lower substantially the amount of active cells, in order to obtain a simulation time which allows sensitivity analyses and validation runs within a reasonable amount of time.

The 2x2 aggregation of the grid schematization reduces the number of active cells to ~54,000 and to ~24,000 in case of 3x3 aggregation. The number of layers in the water quality model is kept at eight, since no aggregation is performed in the vertical direction. At this stage, only regular (structured) aggregation in the horizontal direction is considered. Further model developments would require irregular (unstructured) aggregation that can allow for the local refinement in areas of interest, example in and around mudflat areas.

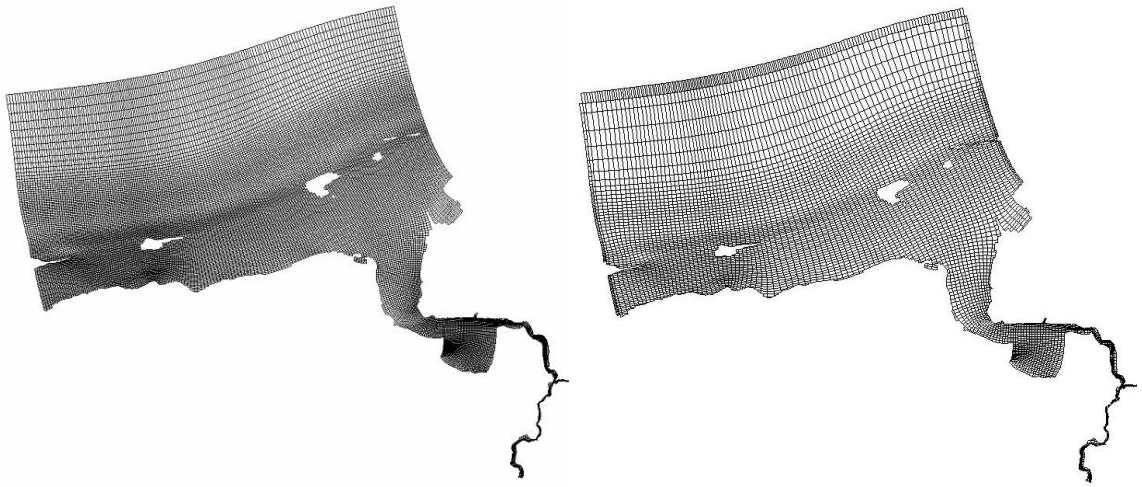

Figure 3.15 Grid aggregations of 2x2 (left) and 3x3 (right) as compared to the hydrodynamical grid.

Multiple runs are performed to test and compare the effect of different grid aggregations, i.e. non-aggregated, 2x2 and 3x3 grid aggregation. Table 3.6 summarizes the average absolute deviation in the accuracy of the simulated salinity at the three reference locations, as compared to the non-aggregated grid scenario. In these tests, the time stepis set at 10 minutes and the numerical scheme is 21 (see next section).

Table 3.6 Salinity output dependency of the grid aggregation

Location	**Average absolute salinity difference**	
	Aggregation 2x2	Aggregation 3x3
Groote Gat Noord	1.3	3.1
Bocht van Watum	1.5	4.0
Huibertogat Oost	0.4	0.9

Numerical Scheme

A comparison of the performance in terms of speed and accuracy using different computation schemes is carried out for a simple water quality model setup. The model includes two state variable “Continuity” and Salinity”, temporally constant boundary concentrations for salinity and constant freshwater discharge from the Ems river (80 m^3/s). Three different numerical schemes are considered:

Scheme 12: horizontally, flux-corrected, vertically implicit central scheme
Scheme 15: iterative solver, backward difference
Scheme 21: local flux-corrected transport

In general, Scheme 12 is more accurate than Schemes 15 and 16 but it can only be applied with a small time step. Scheme 15 smoothens gradients whereas Scheme 21 tends to maintain concentration gradients, and is therefore most suitable for estuarine applications.

The simulations are performed on the non-aggregated grid for an arbitrary simulation time period (29th April - 29th Dec 2001). This requires the “rewinding” of the one-month hydrodynamic simulation (29th April - 29th May 2001). The evaluation of the “simulation speed” considers the CPU time for the water quality simulation period. “Accuracy” is expressed as the average absolute difference between the salinity in the water quality simulation (Salinity) and the salinity computed in the hydrodynamic simulation (Salflow) over the last 3 months (29th Sep - 29th Dec 2001) at the three reference monitoring locations.

Different time steps are considered for each set of simulations with the three numerical schemes. An overview of the results in given in Table 3.7 and Figure 3.16.

Table 3.7 Salinity output dependency of numerical scheme and time step

Run	Numerical Scheme	Time step (mins)	CPU time (hrs)	Average absolute salinity difference		
				GGN	BvW	HO
a.	12	0.5	53.0	7.8	8.1	2.7
b.	15	0.5	224.0	2.7	2.7	1.1
c.	15	5	35.2	1.5	1.4	0.9
d.	21	5	37.7	6.3	6.5	2.8
e.	15	10	21.6	1.1	1.6	0.7
f.	**21**	**10**	**22.9**	**4.0**	**3.8**	**2.5**
g.	15	30	13.7	2.5	4.0	0.4
h.	21	30	12.3	2.8	2.8	1.1

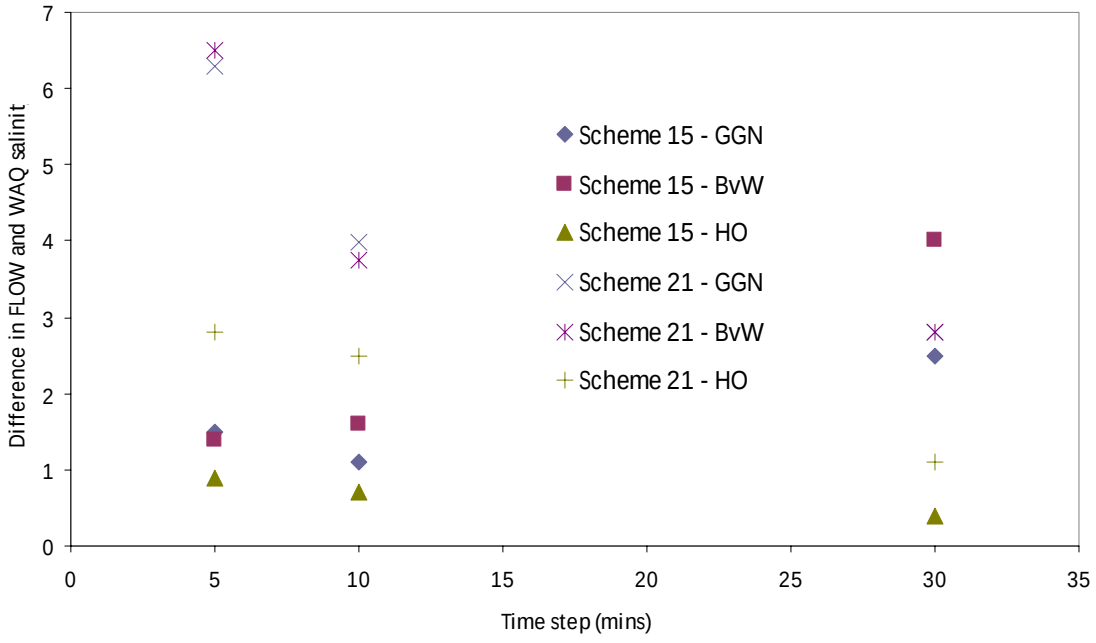

Figure 3.16 Difference in output salinity from the hydrodynamic model (FLOW) and the water quality model (WAQ) as a function of time step

The simulation using Scheme 12 (Run a) is not included in the analysis since this scheme is limited by a small time step. The parallel run with Scheme 15 and a time step of 0.5 mins (Run b) is computationally long (224 hours) and is therefore also excluded from the comparison. Runs c, e and g (Scheme 15 and increasing time step) do not yield a linear trend in salinity differences at the discrete monitoring locations. The corresponding runs with Scheme 21 (Runs d, f and g) generally show decreasing differences between the FLOW and

WAQ salinities with increasing time step. This results from the characteristic feature of Scheme 21 to maintain salinity gradients. In this respect, the higher the average absolute salinity difference, the bigger is deviation from the FLOW salinities but the closer the WAQ salinities are to the measured salinities. Therefore, run d gives a better fit to the measurements than run f, which is in turn better than run h, in particular in the landward stations GGN and BvW. Based on the above test runs, it was decided to use a 2x2 aggregated grid, Scheme 21 and a time step of 10 minutes (run f) in the reference water quality simulations. This combination of settings presented the most reasonable trade-off between accuracy, maintainance of salinity gradients, limiting the computational time to around 3 days for one year simulation.

3.3.4 Initial conditions

Initialization of such a complex model with a high number of variables can not be done by interpolation or extrapolation of measurements. The model is initialized by running it for one year before the target period (2001). Initial conditions for the test run were taken from the output at the last day of this initialization run. This way too large deviations from an “equilibrium” values are prevented, and the behavior of the model immediately after initialization is less variable. In the presented runs, the initialization was done with the same meteorological and boundary conditions as the test run.

3.4 Results

3.4.1 Consistency checks

Conservation of mass

A conservative state variable called “continuity” has been simulated. This variable is initialised at a value of 1.0 and is given boundary conditions equal to 1.0. If the hydrodynamical forcing (water volumes and water fluxes) are consistent, the resulting concentration consistently should be 1.0 in space and time. Deviations from these results could indicate errors due to differences in numerical schemes for the hydrodynamic model and the water quality model, or inconsistent boundary conditions. This demonstrates the conservation of water in the hydrodynamic forcing, which ensures conservation of mass in the water quality model. Figure 3.17 illustrates that the model is consistent in this respect.

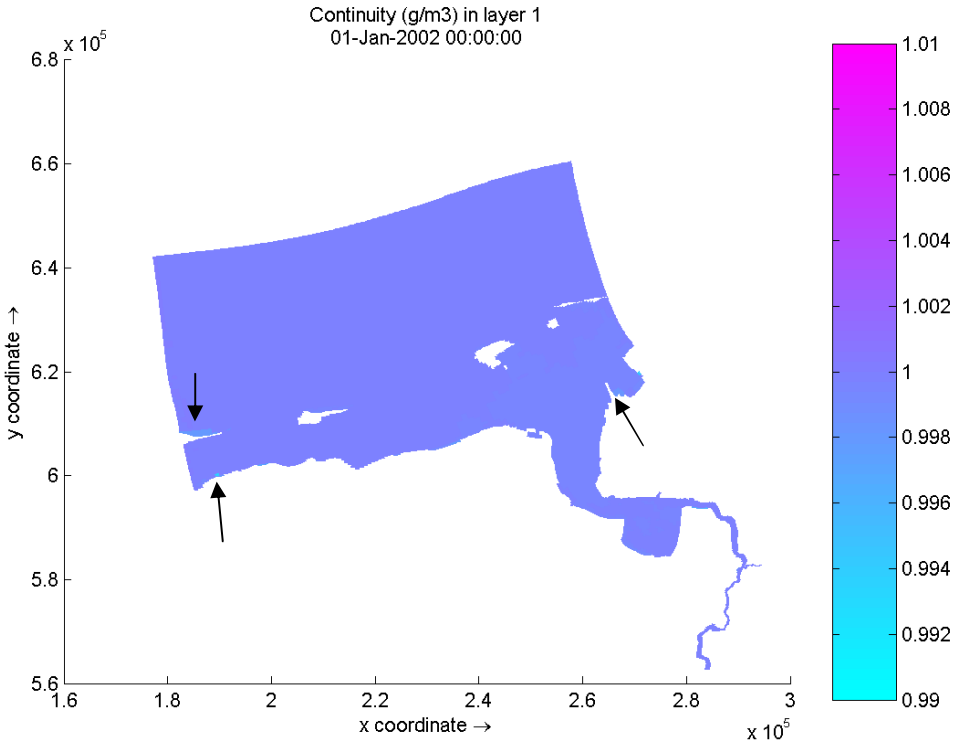

Figure 3.17 Distribution of continuity at the end of a one year simulation. Only at some intertidal areas, the value deviates from 1 (indicated with arrows).

3.4.2 Model validation

In the model validation, three parallel scenarios are considered:
a) **Reference/baseline scenario** in which the discharge of the Ems River is assumed to be 80 m^3/s representative of the annual average discharge rate
b) **Scenario 1** with a discharge rate of 120 m^3/s
c) **Scenario 2** with a discharge rate of 40 m^3/s

In the three cases, the discharge rate is assumed constant during the one month hydrodynamic simulation. In the following comparison, results from the three runs are plotted together to show the effect of variable riverine loadings at different times of the year.

The following main water quality parameters are included in the model validation:

1. Salinity
2. Oxygen
3. Chlorophyll-a
4. Nutrients:
    a. Total nitrogen, NH4, NO3
    b. Total Phosphorus, PO4
5. Light extinction
    – this parameter could only be compared to measurements for other years, since no extinction measurements for 2001 were available.

For each substance, time series model results and field measurements (when available) are shown for the three reference locations, Groote Gat Noord, Bocht van Watum and Huibertgat Oost (Figure 3.18 - Figure 3.27).

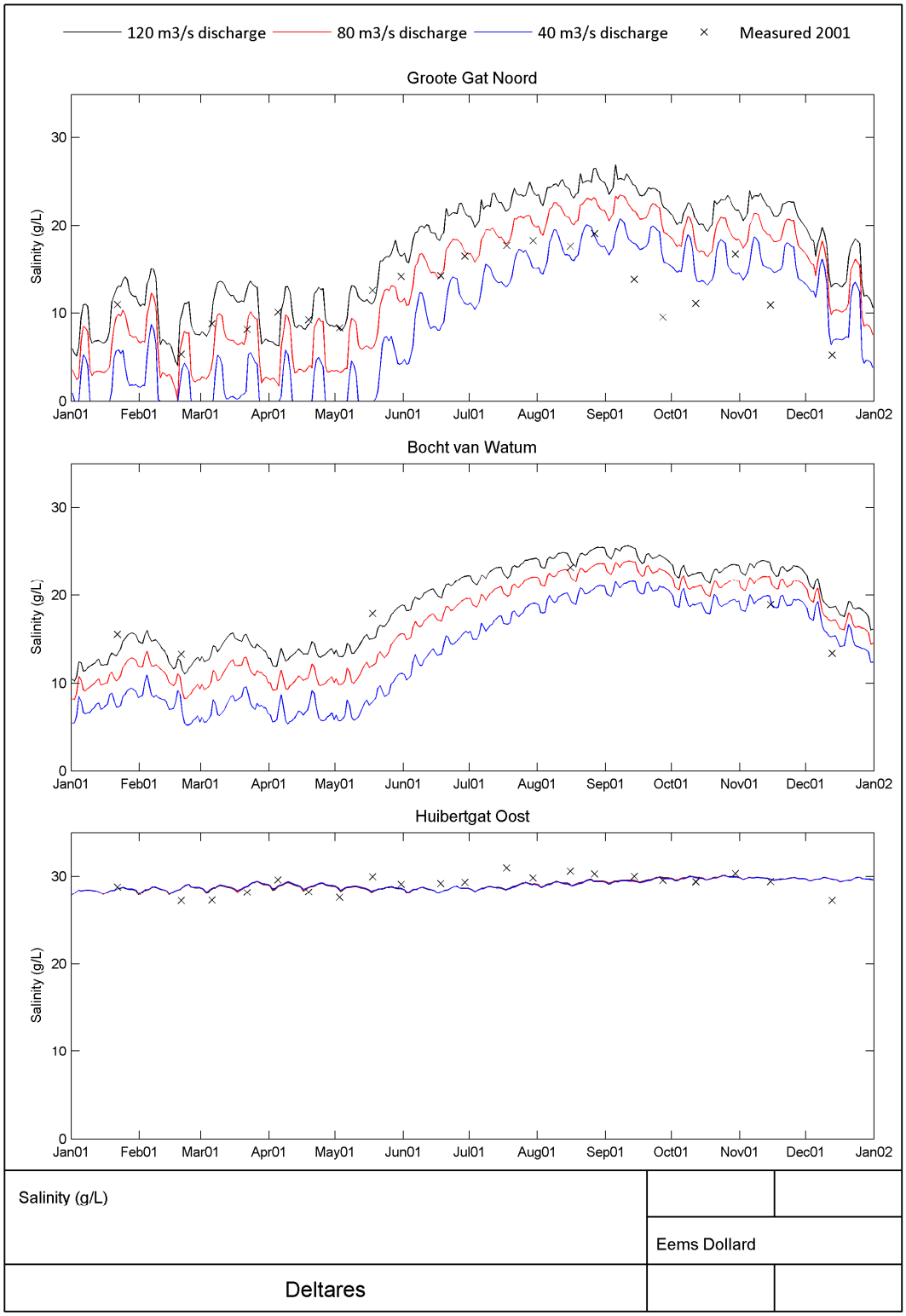

Figure 3.18 Measured and modelled salinity at the reference stations

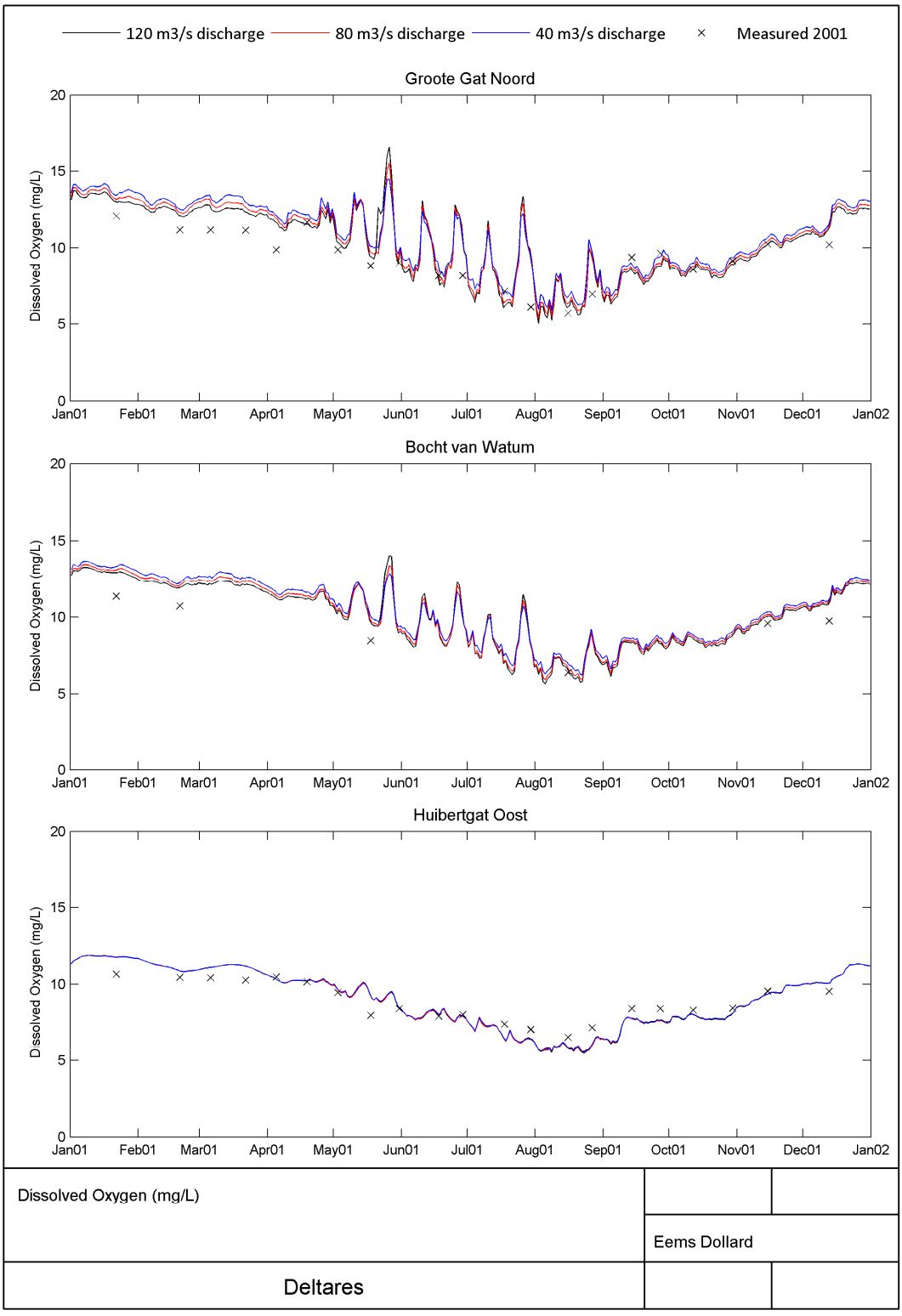

Figure 3.19 Measured and modelled dissolved oxygen concentration at the reference stations

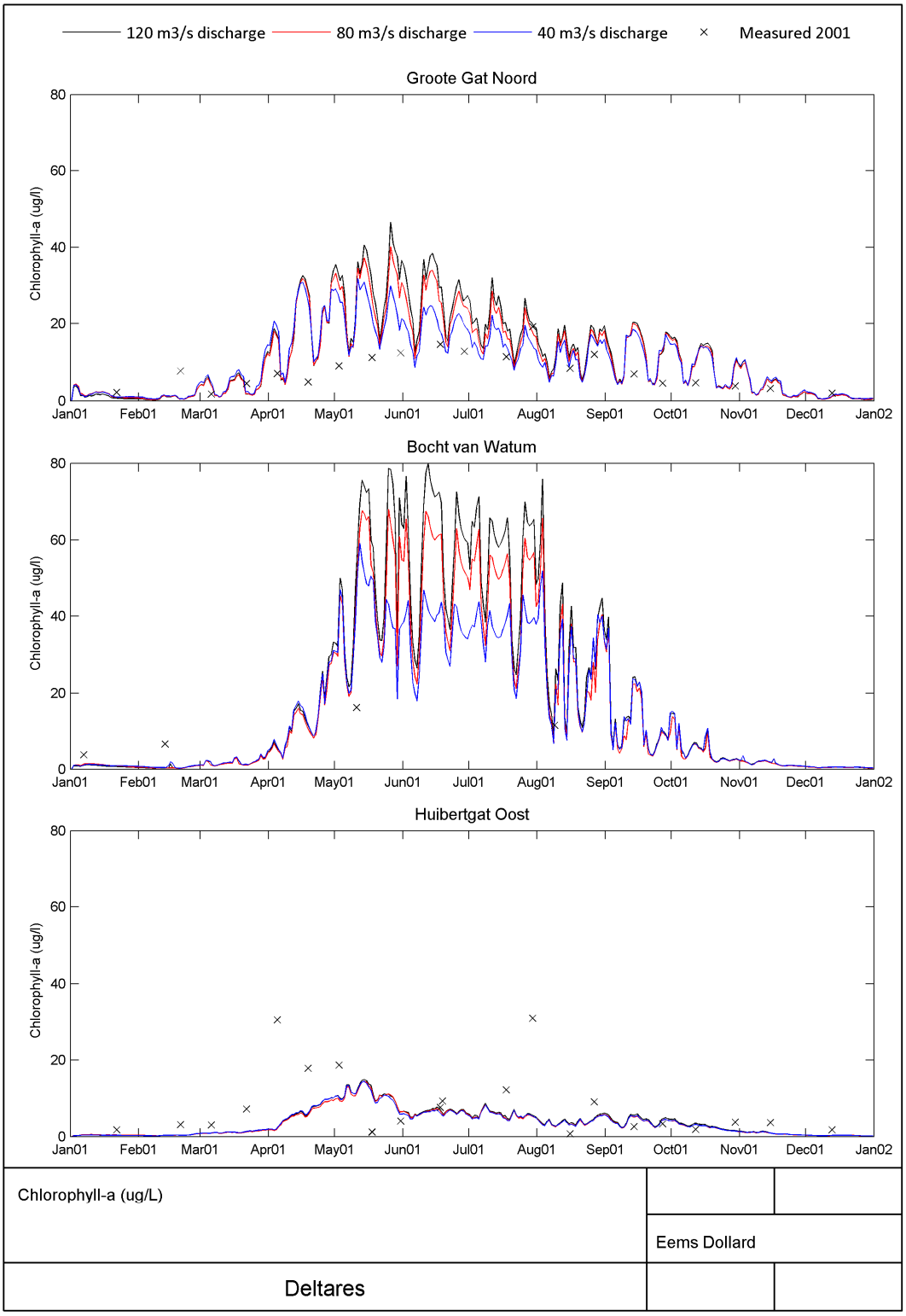

Figure 3.20 Measured and modelled chlorophyll-a concentration at the reference stations

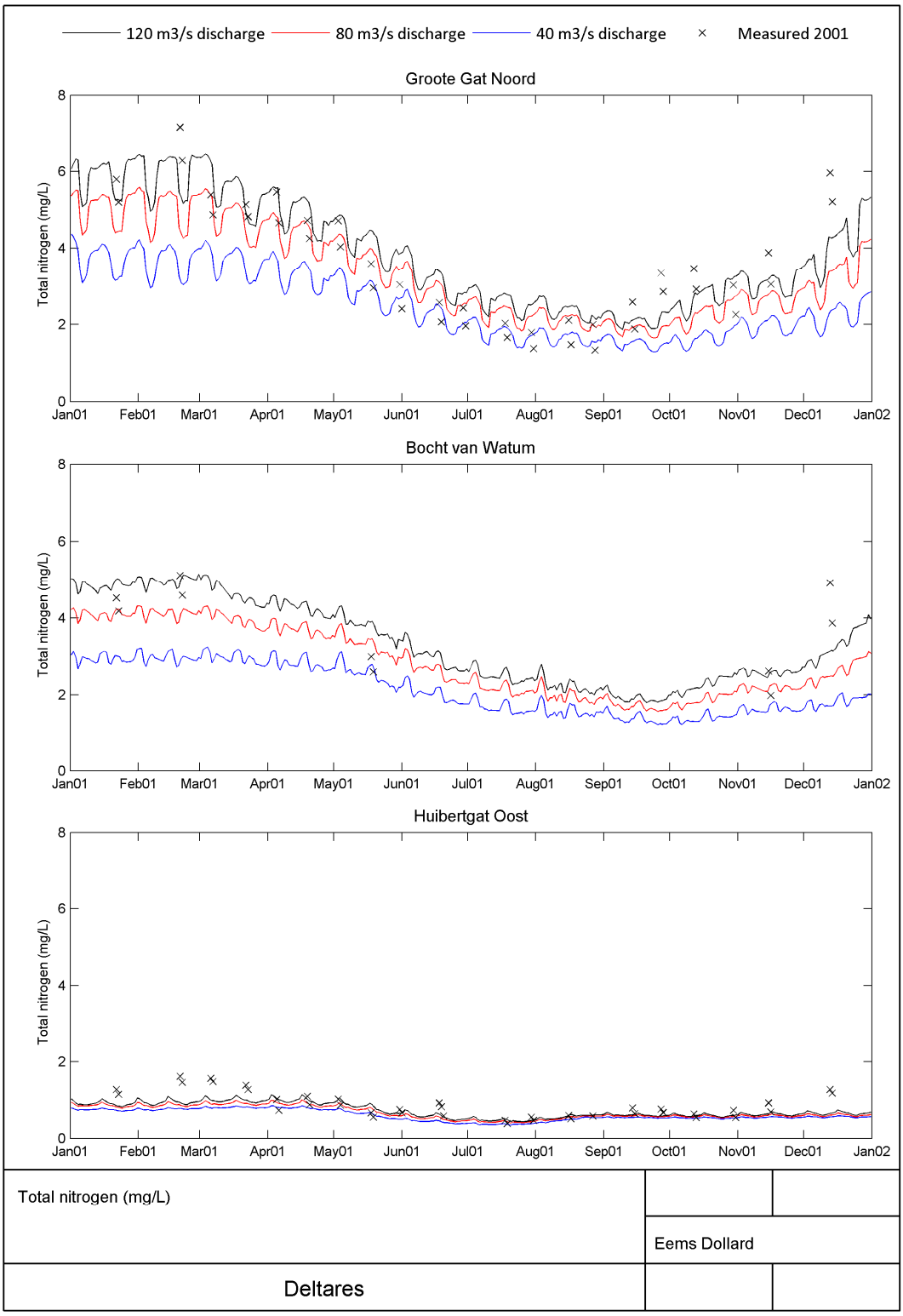

Figure 3.21 Measured and modelled total nitrogen concentration at the reference stations

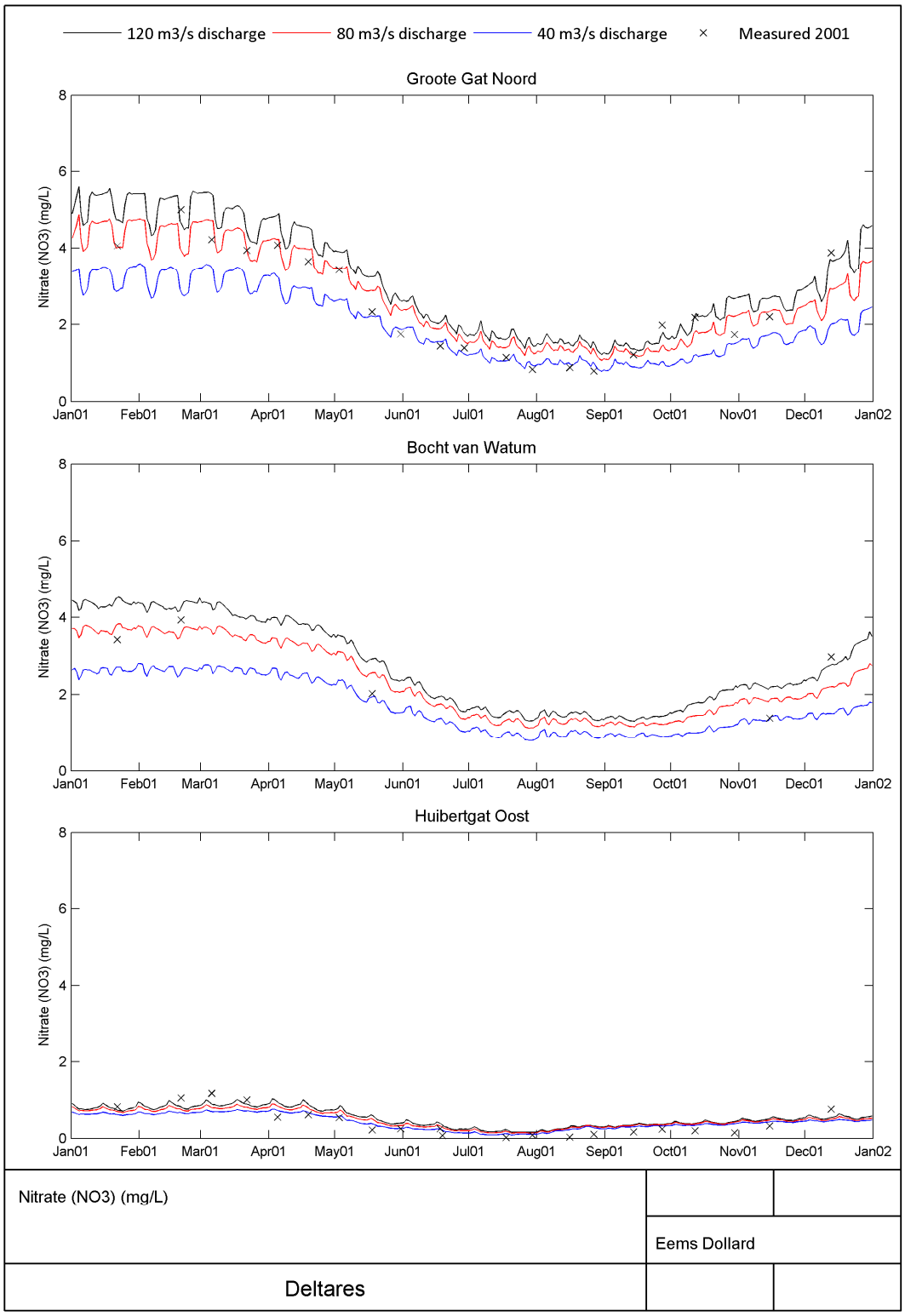

Figure 3.22 Measured and modelled nitrate concentration at the reference stations

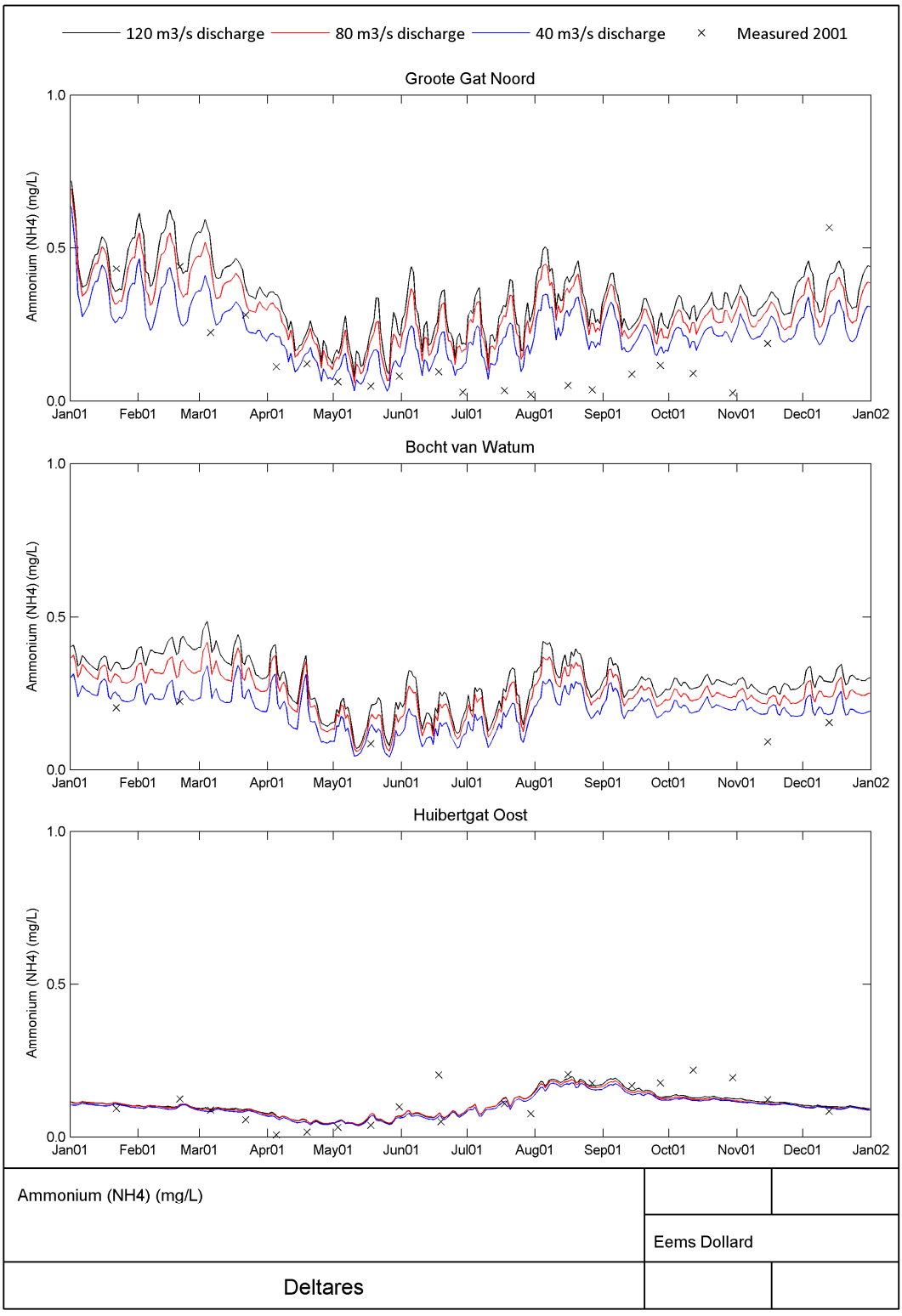

Figure 3.23 Measured and modelled ammonium concentration at the reference stations

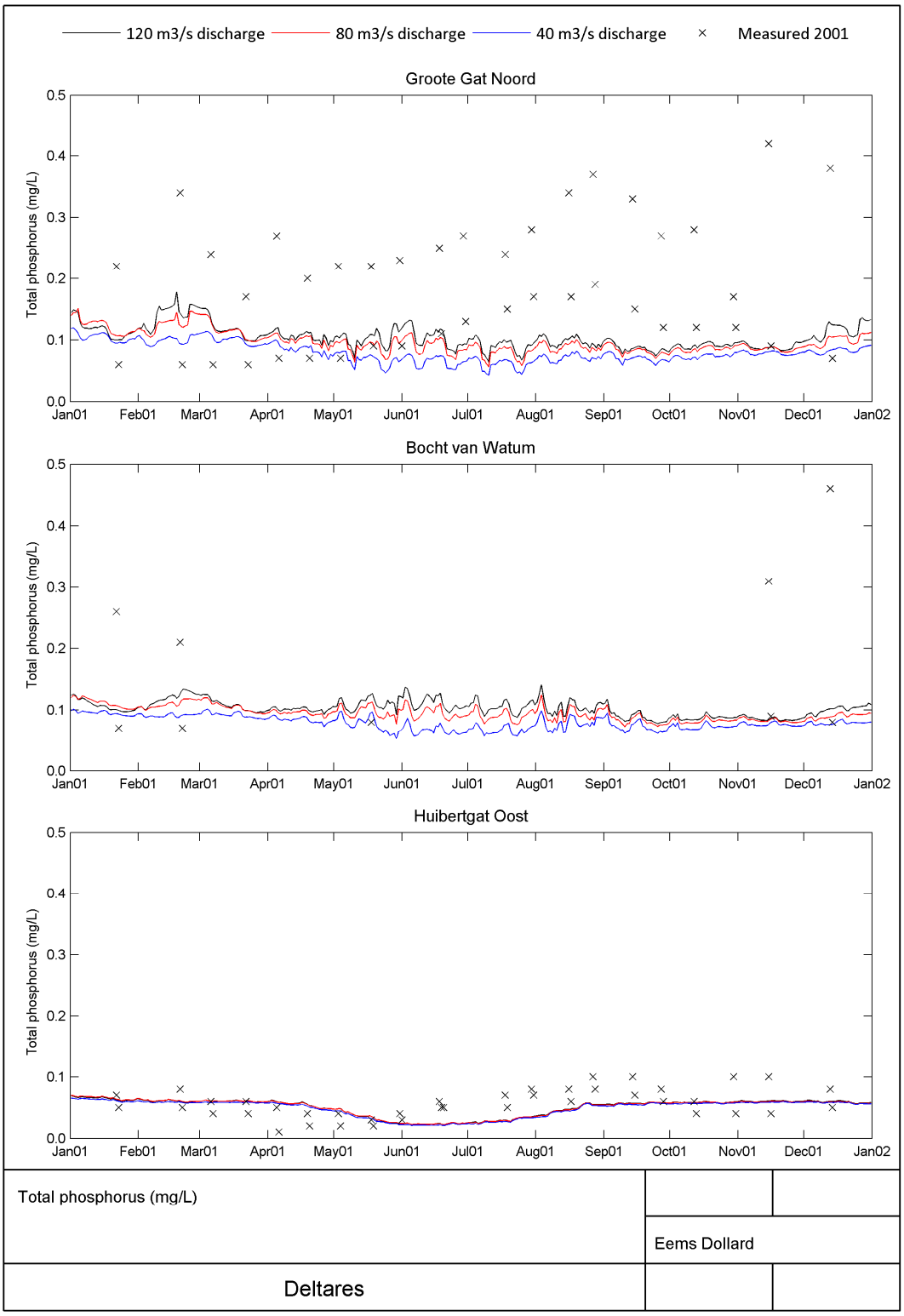

Figure 3.24 Measured and modelled dissolved total phosphorus at the reference stations

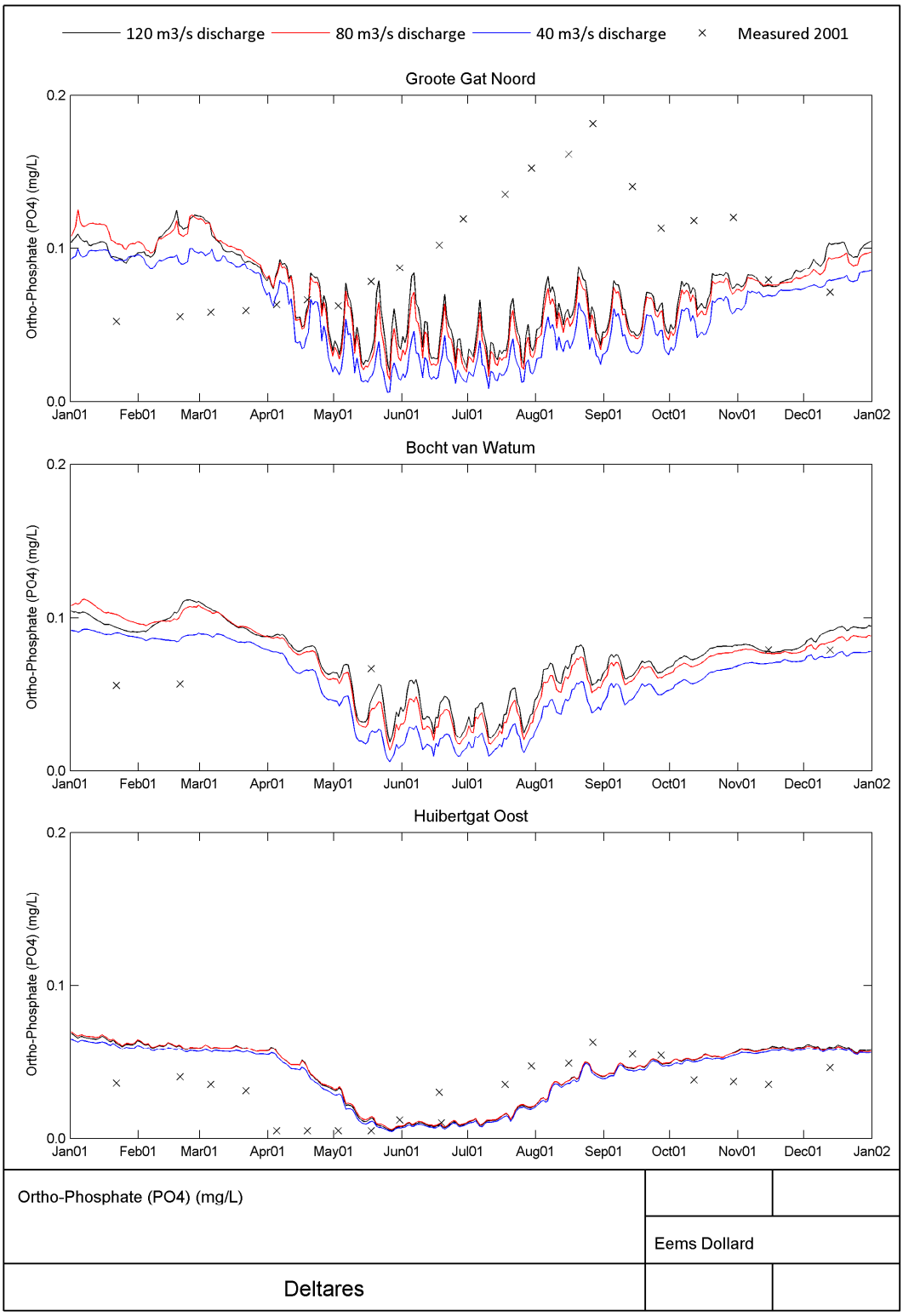

Figure 3.25 Measured and modelled dissolved inorganic phosphate concentration at the reference stations

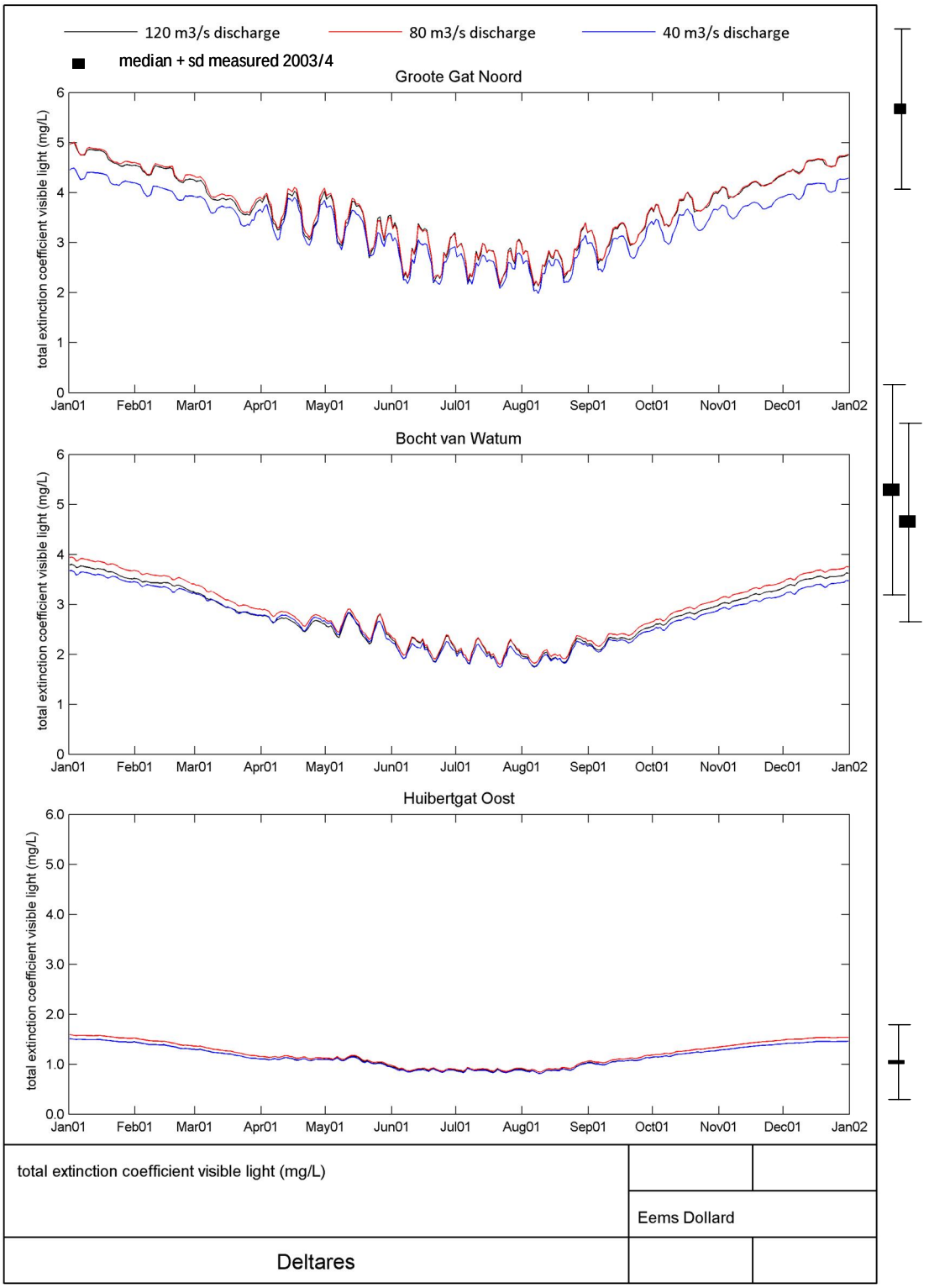

Figure 3.26 Measured (average and standard deviation over 2003 and 2004 at the right hand side) and modelled total extinction coefficient at the reference stations

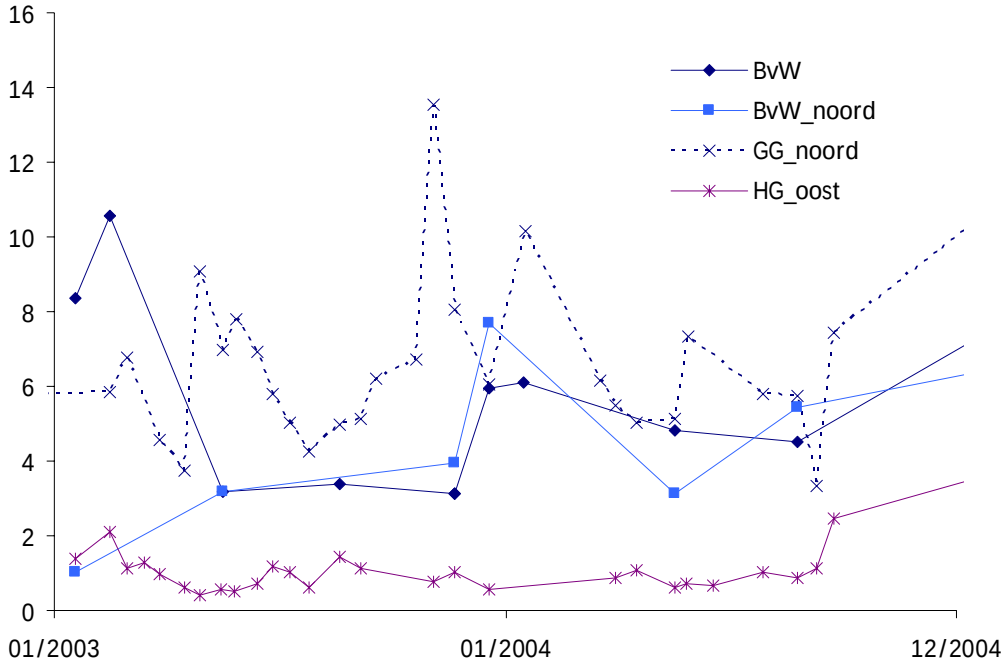

Figure 3.27 Total extinction coefficient for the reference stations for the years 2003 and 2004. Data for 2001 were not available.

3.5 Discussion of the results

Considering that these results are a first shot from a model set-up, with a number of imperfections (see previous sections) they are encouraging. Salinity, dissolved oxygen, total nitrogen, NO3, NH4 and to a lesser extent chlorophyll-a are in the right order of magnitude and show a seasonality which resembles the observations. Results for phosphorus, in the form of total phosphorus and PO4 are still unsatisfactory.

Salinity

Salinity, computed in Delft3D-WAQ using VarSAL process accounting for variable intra-annual changes in the riverine discharge, generally follows the trend observed in the salinity measurements (Figure 3.18). In the landward monitoring locations (Groote Gat Noord and Bocht van Watum), the results with high discharge (scenario 1) fit closer to the observations in the winter months characterized by high discharge rates, whereas the results with low discharge (scenario 2) match better the summer measurements. At the seaward location Huibertgat Oost, there is minimal difference in salinity between the three different runs since the influence of the freshwater river is not significant.

Oxygen

The gradual decline in oxygen between May and August was correctly simulated (**Error! Reference source not found.**). At Bocht van Watum station summer peaks in O_2 correspond to peaks in chlorophyll-a which appear to be high, but given the frequency of the measurements we cannot conclude that the model results are too high.

Chlorophyll-a

Primary production and therefore chlorophyll-a calculation in an estuarine environment can be expected to be more tide-dependent than for example salinity or nutrients. This variation can be explained by the strong light gradients due to suspended sediments in combination with the non-linear response of phytoplankton to light availability. In combination with the variation due to tidal transport, leading to variation in nutrient concentrations and salinity. Due to the frequency of chlorophyll measurements the short term variation in chlorophyll-a could neither be validated nor falsified. Nevertheless, the minimum modelled chlorophyll-a values coincide with the measured concentrations in the summer period, in both Groote Gat Noord and Bocht van Watum (Figure 3.20). At the seaward station Huibertgat Oost, the modelled chlorophyll-a started to increase rather late in spring, as compared to measurements. Also, the measured summer peak was not reproduced by the model. This could be related to the fact that the sediment function not yet matches the sediment measurements in this area, resulting in an underestimation of the light regime.

Nutrients

The yearly trends in both Total nitrogen (Figure 3.21) and NO3 (Figure 3.22) are well captured by the model in all three locations. Although nitrogen loading from the Ems river present the major source, the contribution of atmospheric deposition contributed to roughly 15 % increase in dissolve inorganic nitrogen concentrations (data not shown) at Huibertgat oost, the most seaward station. Analogous to the salinity results, the fit during spring was best for the high discharge scenario, while during summer, the low discharge scenario gave a better fit. A good fit is obtained for NH4 (Figure 3.23) although the model overestimates the measured concentrations between June and October at Groote Gat noord.

The general trend in Total Phosphorus (Figure 3.24) is reproduced except for the increase in the summer concentrations (July to October). This increase is most pronounced in the most inland station Groote Gat noord, and is most likely caused by the remobilization of sediment-bound phosphate under reducing conditions. Since this process is not yet included in the model, it can not be expected to be reproduced by the model. The model does not yet reproduce the trends and magnitude of PO4 concentrations (Figure 3.25) in particular in the landward of location Groote Gat Noord. Part of this is explained by redelivery from the sediment (see above). Also, the initial concentrations in the model run are ~ 0.05 mg/L higher than measured in the field.

Since no light extinction measurements were available for 2001, model results are compared with measurements from the years 2003 and 2004 (Figure 3.26 and Figure 3.27). On average, modelled light extinction was in the same range as the measurements. Short peaks of extremely high extinction that occur in the measurements were not abundant in the model results. Possibly, they are caused by short term processes not included by the model (storm events, passing ships, etc.). The tidal dynamics visible in the modelled results could not be validated, due to the relatively low frequency of measurements.

3.6 Conclusions and recommendations

The model results for water quality have clearly improved as compared to last year. In particular, salinity, dissolved oxygen and nitrogen compounds are described well by the current model. However, improvements have to be made in order to also describe chlorophyll-a and phosphorus dynamics more realistically. The proposed improvements for the next period (2011) will be structured according to a general validation procedure (Los et al. 2008) and will include the following steps.

The first important step in the improvement of the model performance is to improve the physical processes and forcings. For 2011, it is planned to develop an improved hydrodynamical model that simulates one complete year of simulation with a variable Ems discharge, forced by the measured discharge. This is required to describe the mixing processes and hence salinity correctly. Also, the boundary conditions facing the North Sea concerning nutrient concentrations need to be checked and where necessary improved. Improvements can be based on better interpolation of the measured values, by assimilation of values from the North Sea model, or a combination of these. The effect of additional station measurements in the calculation of the forcing concentrations also needs to be checked.

After the improvements of the physical processes, the performance of the model concerning important output parameters needs to be evaluated again. Primary production and thus chlorophyll-a is one of the most important output parameters. Light, which is the most important limiting factor for primary production in this estuary, is highly influenced by suspended sediments and to a lesser extent by nutrient concentrations and salinity. The next logical step for a better model performance is therefore to improve the sediment function for a better description of the suspended sediment concentration. Nutrient concentrations and salinity, which should benefit of the better hydrodynamical descriptions and boundary conditions mentioned above, need to be validated once more at this point.

Additionally, some processes that are not yet included in the model, should be added. The bottom sediment to water transport of phosphate due to anoxic sediment conditions should be added to better describe the summer phosphate increase observed at the inner estuary. Moreover, benthic primary production needs to be added, since this is considered to form an important part of the primary production in intertidal areas. The modelling process of benthic primary production is currently tested in another model set-up, the Scheldt estuary, and will, after testing, be implemented in the Ems-Dollard model set-up later during 2011.

Finally, in order to improve the overall model performance of primary production, it may be necessary to adjust some of the phytoplankton and/or phytobenthos physiological parameters. Most prominent, biomass ratios to chlorophyll-a may be adjusted to better match the values found in estuarine phytoplankton. However, it should be noted that this step needs to be carried out only if this is indicated by available biological data for algal physiological parameters in this specific area.

4 Ecology

4.1 Introduction

The report of last year regarding ecology (Dijkstra, 2010) in the Ems-Dollard estuary primarily provided a system description and an inventory of biota present in the area. Also, the choice for the use of 'Habitat', a GIS-based modelling tool that uses response curves to assess habitat suitability was discussed.

This year's report continues with the set-up of the modelling tool and identification of the key species in the Ems-Dollard, as well as the characteristics of their habitats. Subsequently, the sensitivity of the model for the grid size and for the input values –which are the output values of the preceding sediment and water quality models- is studied. This report concludes with recommendations for refinements in next year's Ems-Dollard study and continued model development.

The choice for the type of ecological model has already been discussed in Dijkstra (2010). For clarity, it is briefly summarized here again. The Ems-Dollard has four areas with distinct properties, which are treated in Section 4.2.1. Subsequently, the selection of representative conditions from the morphological and water quality models is described, paying attention to continuity and connectivity issues.

4.2 Modelling method: Habitat

When choosing a modelling approach, we should keep in mind that the aim of this project is to improve understanding of the effect-relationships between physics, water quality, biota and biota themselves in the Ems-Dollard area. Regarding ecology, one can create an ecotope map, determine habitat suitability or make a dynamic population model for individual species. The definition of an ecotope is a spatially limited, relatively homogeneous combination of physical and chemical conditions and characteristic flora and fauna, for example a salt marsh or sand bank. Since this definition is not species-specific and therefore not very transparent in showing the chain of effects, an ecotope map is not always the best output. Such a map is useful however to present aggregated information, and to say something about possibilities for species from which little information exists. Moreover, the ecotope-classification corresponds to the Natura2000 legislation. Population models require a lot of knowledge and data and are only suitable for a limited number of species and relatively short timescales. A habitat, a type of environment in which an organism or population occurs, is species-specific and changes in the environment will be reflected in the suitability index: this index does not say how many specimen will be present at a certain time, but it does say how suitable the environment will be for a certain species and why. Moreover, habitat loss or gain is easy to quantify. Therefore, habitat modelling is a suitable method to clarify the effect-chain in the Ems-Dollard.

Habitat modelling needs data at a high spatial resolution, which is difficult to measure in the field but easily obtained from numerical models. Temporal resolution however, important for e.g. drying/flooding times, the abundance of food and the passage of fish through temporally anoxic zones can be more complicated to incorporate.

To asses the present potential for habitats and the possible future changes, we use the GIS-based model 'Habitat'. Based on a number of user-specified relations, this model calculates a

habitat suitability index (HSI; 0-1) for each grid cell. One can specify a response curve for suitability based on parameters like depth, sediment composition or turbidity, but also the presence or absence of other vegetation or animals.

4.2.1 Regions and areas of special interest

The entire Ems-Dollard area is too extensive and too diverse to model it efficiently as a whole with sufficient attention for all relevant species. A division into smaller regions with similar characteristics therefore seems logical. The proposed regions are (Figure 4.1): the Outer area (O), the Ems estuary (E), the Dollard (D) and the Ems River (ER). The borders of these regions practically coincide with the water body classification according to the WFD (Schans, 2005).

The outer area is characterized by saline water, deep channels and considerable waves. Most of the borders are formed by dikes and man-made salt marshes. The Ems estuary has less saline water, a single moderately deep channel, some waves, a large sandy intertidal area (Hond-Paap) and steep shores, practically without salt marshes. The area labelled as Dollard also comprises the narrow and deep shipping channel to Emden harbour, but the actual Dollard is predominantly shallow with several meandering tidal channels. The water is brackish, with fresh water influences from pumping stations and the Ems River. The area is relatively sheltered and bordered by salt marshes. Fresh to brackish water, low oxygen concentrations and the absence of waves characterise the Ems River.

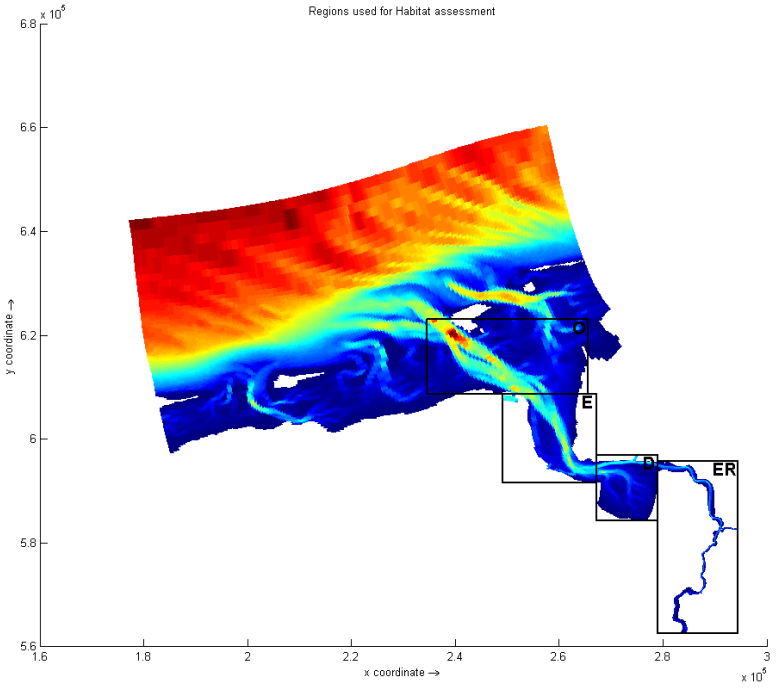

Figure 4.1 The four regions used for Habitat-modelling: the Outer area (O), the Ems estuary (E), the Dollard (D) and the Ems River (ER).

4.2.2 Determination of conditions

The conditions in Ems-Dollard change throughout the year, as does the presence of organisms. In order to cope with this, the suitability for a certain species will be assessed using conditions that are representative of the four seasons, or of the season in which the species –e.g. a breeding bird- occurs. Normally, the averaged conditions over one month, i.e. two spring-neap cycles, will be representative for a season. In some cases, however, it might be necessary to use extreme conditions that occur during such a period.

Likewise, some parameters can be averaged over the depth, whereas in other situations it is more realistic to use values from the bottom layer or the surface layer. Therefore, the input maps for the Habitat model have been given names that display where the map is from, over which period it is averaged, which layer is sampled and which water quality simulation it is derived from (see Figure 4.2). A similar naming convention is used for the output maps.

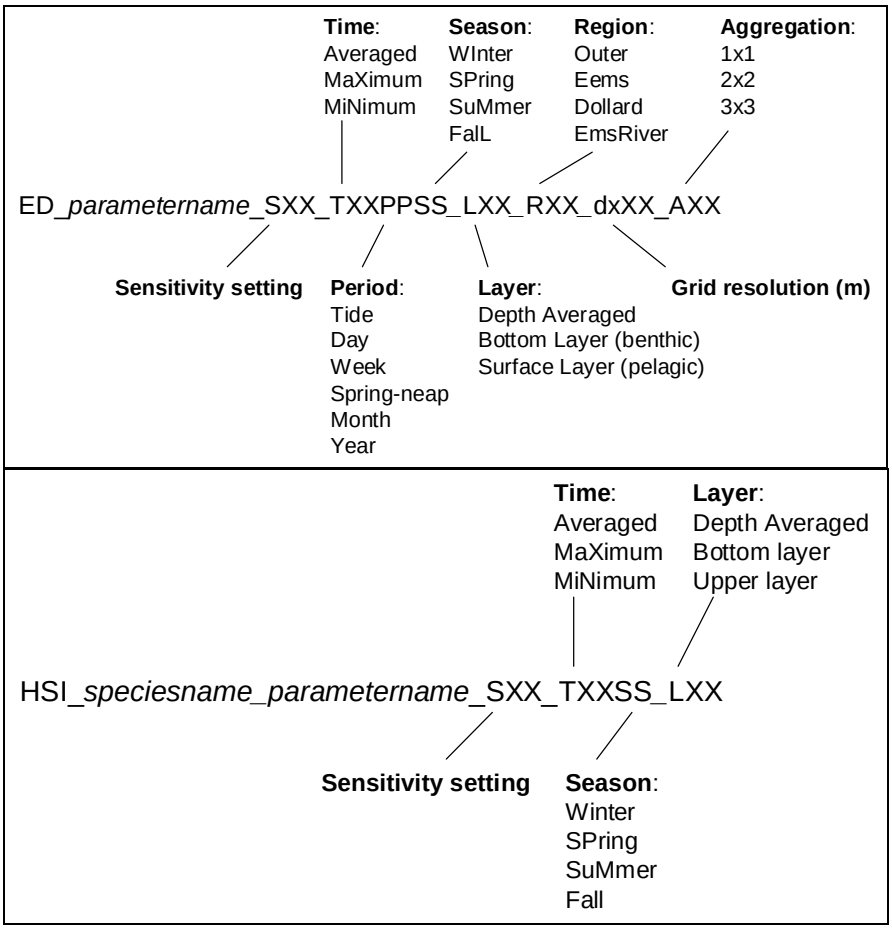

Figure 4.2 Naming conventions of Habitat in- and outputnames.

4.3 Identification and characterisation of key species

This chapter discusses the selection and characteristics of several key species that should be representative for the majority of the habitats in the Ems-Dollard. A selection needs to be made because the total number of plant- and animal species in the area is too large to study

all. Moreover, the available information about occurrence and behaviour only concerns a limited number of species.

Therefore, in this chapter species are grouped according to factors that are indicative of a species' environment, i.e. to parameters that characterise its habitat. These groups are chosen such that all aspects are covered: both pelagic and benthic, both piscivores and herbivores, both salt water and fresh water, both aerobic and anaerobic, etc. Besides these groups, several individual species will be treated as well, either because they are very well known and suitable for comparison to monitoring data or because they are of special interest.

4.3.1 Plants and habitat types

Because the water quality part already describes the state of the phytoplankton, this part will only consider the vascular plants or macrophytes in the Ems-Dollard. Most macrophyte species in this area are terrestrial: they grow above mean sea level on salt marshes. The occurrence of species mainly depends on the age or the level (a consequence of the age) of the salt marsh: the older the higher and the less affected by water and salt. In lower regions, where plants have to deal with salty water and very dynamic conditions, fewer but more specialised species like Spartina and Salicornia occur. In even lower (low-intertidal to subtidal) areas, seagrasses are the only macrophytes present. Also because of their value for other marine life, these seagrasses will be treated specifically, whereas the plants in higher areas are grouped into the habitattypes H1310 Salty pioneers, H1320 Spartina swards and H1330 Atlantic salt marshes.

In some areas the salt marshes are natural, but in most of the Dollard they are the result of former land reclamation works. These works are called 'kwelderwerken' and consist of small retention levees and drainage ditches. Nowadays, the maintenance of most of these 'kwelderwerken' has seized, but the traces are still present in the landscape. Traces of grazing are also present. This grazing and maintenance can affect these habitats and their value for other animals locally very strongly. At the moment, these management factors are not taken into account because this would require a considerable amount of information for a relatively small area. However, as the value of these salt marshes is directly affected by how they are managed, a more specific study is probably worthwhile later.

Key species:	*Eelgrass*
Key groups:	*H1310 Salty pioneers, H1320 Spartina swards and H1330 Atlantic salt marshes*
Main indicators:	*bed level, dynamics*

4.3.2 Invertebrates

The diversity of invertebrates in the Ems-Dollard is huge; therefore a division is made into three main groups of bivalves (molluscs), crustaceans and worms (polychaetes) and four species selected either because of their (possible) commercial interest, their importance as a prey for other animals or their role as an eco-engineer. The reef-building Blue mussel (Mytilus edulis) is an epi-benthic filter-feeding bivalve thriving in moderately dynamic areas, whereas the Cockle (Cerastoderma edule) is an endo-benthic filter-feeder that prefers calmer conditions. Lugworms (Arenicola marina) are polychaetes feeding in the bed on organic matter attached to sediment grains. The Mudshrimp (Corophium volutator) is a small crustacean that feeds on epibenthic diatoms from a burrow.

Suggested key species: Blue mussel, Cockle, Lugworm, Mudshrimp
Suggested key groups: Bivalves, Crustaceans, Worms

4.3.3 Fish

The Ems-Dollard area harbours more than fifty fish species, which is too much to be modelled individually. Moreover, these species have a lot in common: the majority either feeds on plankton or on invertebrates and fish and most of them tolerate a range of salinities. Therefore, they are subdivided in groups based on their distinctive position in the water column: pelagic, demersal 'deep' (deeper than 5 m) and demersal 'shallow' (intertidal to 30 m). An overlap between these areas exists, but the demersal 'deep' fish do no occur in water less than 5 m deep and the demersal 'shallow' fish do not occur below 30 m. For the demersal fish, sub-groups could be made with respect to the substrate they prefer.

A division into the frequency of occurrence in the estuary -i.e. groups of estuarine residents, diadromous species, marine juveniles, marine seasonal and accidental guests and fresh water species- was also considered, but not preferred as it is not necessarily representative of the preferences of fish in Ems-Dollard. Also, the suitability for species that have disappeared (e.g. salmon, sturgeon, sharks and rays) is not assessed for the moment, as the presence of these species probably depends more on the presence and health of populations in nearby estuaries.

Diadromous fish do get special attention though, as the salt water / fresh water transition that the estuary provides is essential for these species and their numbers decreased more than many other species in the past century. For diadromous fish, the connectivity between spawning area and living area is important, as is the oxygen level due to their substantial swimming effort. The suitability of their spawning areas will not be assessed, as these areas are situated outside the study area. The availability of food outside the study area will be considered neither.

Sparling (also called Smelt; Osmerus eperlanus) is chosen as one of the key species because it is a rather well known anadromic species and it is a food source for many birds and larger fish. Adult sparling is a pelagic piscivore that lives in open, preferably turbid water with plenty of oxygen. Its habitat is similar to that of other species such as salmon, sea trout and twaite shad

Key species:	*Sparling*
Key groups:	*Demersal deep, Demersal shallow, Pelagic*
Main parameters:	*Oxygen, depth, salinity, temperature, turbidity, food, connectivity*

4.3.4 Birds

The over fifty species of birds are grouped along characteristics like feeding preferences and nesting location. As these groups have similar characteristics, they share the same habitat. Bird species that are especially relevant to the area are modelled with more detailed, species-specific rules. Birds of prey are not incorporated in this study because they do not have a direct link with the marine system.

For a bird watcher, a division of estuarine bird species into stilts, geese and ducks, birds of prey and other species would be logical. Based on feeding characteristics however, a division

into piscivores, benthivores and herbivores is a better match to the habitat-approach used here: Piscivores require clear water and fish, benthivores shallow water or intertidal areas with macrofauna and herbivores require the presence of either water- or terrestrial plants. Note that the abiotic variables are easier and more reliably predicted than the presence of suitable food. The latter depends on abiotic circumstances itself, but also on population dynamics and on the amount that is consumed by predators. In this phase of this study, we assume that food sources are not depleted, hence the suitability for birds is determined by abiotic circumstances only. Some birds may feed outside the study area, i.e. on the North Sea or on nearby meadows. In some cases, the use of only grain size and emersion duration as suitability indicators has been applied successfully (Brinkman and Ens 1998), in other cases the actual abundance of food turned out to be the decisive factor and the approach failed (Ens, Brinkman et al. 2005).

For the moment, three key species are selected out of the three key groups: The benthivoric Avocet is selected because it is typical to the area, it is present all year and it breeds in the area. The herbivourous Eurasian widgeon is also typical to the area, but only occurs in fall/winter, and does not breed in the area. Two piscivorous species seem suitable: the Common tern and the Red-breasted merganser. Both are on the 'red list' of the Ministry of LNV (now EL&I) and are visual hunters, but they differ in occurrence and breeding habits: the Common tern lives in Ems-Dollard in spring and summer and also breeds there, whereas the Merganser is only present in winter.

Key species:	*Avocet, Eurasian Widgeon, Common Tern/Red-breasted Merganser*
Key groups:	*piscivores, benthivores and herbivores*
Main parameters:	*breeding ground, food (fish, benthos, plants), visibility*

4.3.5 Mammals

Only three species of large, marine mammals are indigenous to the Ems-Dollard. Of the two seal species in Ems-Dollard, the harbour seal is the more common one whereas the grey seal seems the least shy. Being large and of interest to the general public, these animals are quite well studied. However, their small numbers in combination with the large distances they can travel mean that they will not always occur in seemingly suitable habitats. Both the grey and common seal and porpoise feed on fish and large crustaceans, though not necessarily in the estuary itself. Hunting predominantly occurs using sounds and nostrils; visibility is not very important.

All these mammals are sensitive to noise and disturbance, which is difficult to quantify, but for seals especially relevant with respect to the sandy areas where they rest and give birth. Mammals can get stuck in nets, but since they –unfortunately- do not know these nets are there, the presence of nets probably does not affect their habitat. Pollution and diseases are other threats. None of the mammals has a natural predator in the Wadden Sea and all three species are protected.

Key species:	*Grey seal, Common seal, Porpoise*
Key groups:	*n/a*
Main parameters:	*food (fish), disturbance, presence of resting areas*

4.4 Determination of response curves for Habitat Suitability Indices

For several species in the Ems-Dollard estuary, knowledge about their habitat requirements is readily available in the Habitat-database (http://public.deltares.nl/display/HBTDB). When response curves were not available or not sufficient, information from multiple sources was used to construct these curves: scientific papers, reports from institutes such as Imares and the former RIKZ and online resources (e.g. soortenbank.nl, fishbase.org). The report of Meesters et al. (2008) on an 'indicator system for biodiversity in Dutch marine waters' was especially useful.

4.4.1 Macrophytes and habitattypes – response curves

Eelgrass –Zostera marina

Eelgrass grows from the intertidal to a few metres lower, depending on the turbidity of the water. The water should be brackish to salt (10-32 ppt). High nutrient concentrations are not problematic, as long as the amount of algae that could limit the light available to the eelgrass plants remains small. High flow velocities (to nearly 1 ms-1) are fine too, provided the substrate remains stable. The bed itself should not contain too much lutum (<35%), and not be dry for more than 5% of the time.

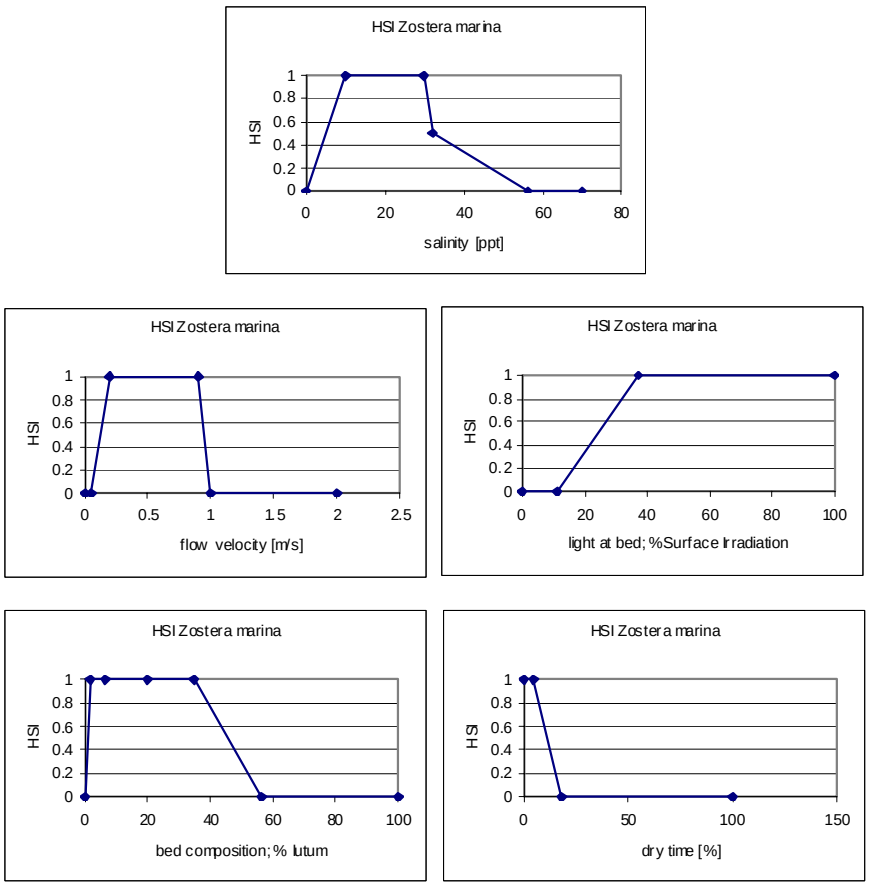

Figure 4.3 Response curves of Eelgrass Zostera marina.

These relationships have been validated in the Venice Lagoon (Erftemeijer & van de Wolfshaar, 2006), where the situation differs from that in Ems-Dollard: the study of Ochieng & Erftemeijer (subm.) showed that the turbidity near the Hond-Paap does not affect eelgrass growth, as the plants receive enough light during the time the area is dry.

Salty pioneers – H1310

These plants occupy the zone around the mean water line, preferably a little higher. They should be flooded every tide. Below MSL the vegetation becomes more open and patchy. If the area is too dynamic, plants will disappear and leave a bare intertidal flat. Though these relations are specified in the Habitat-database, the 'dynamics' -i.e. wave action- are not quantified. Purely fresh water is not tolerated; the minimum salinity is 0.55 ppt.

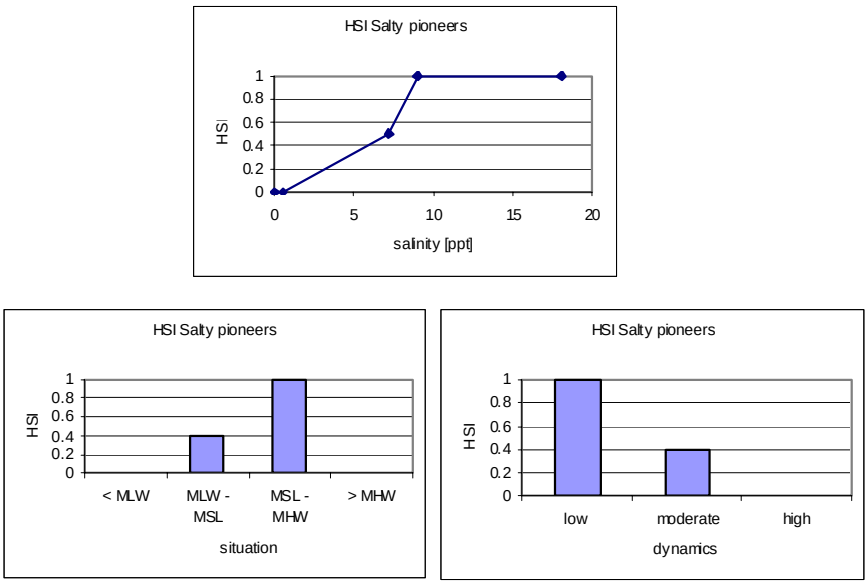

Figure 4.4 Response curves of Salty pioneers (H1310).

Spartina swards – H1320

The area that is suitable for salty pioneers is also suitable for Spartina swards, provided that the substrate is sufficiently soft and muddy. Once Spartina has established, it is more resistant to wave action than H1310.

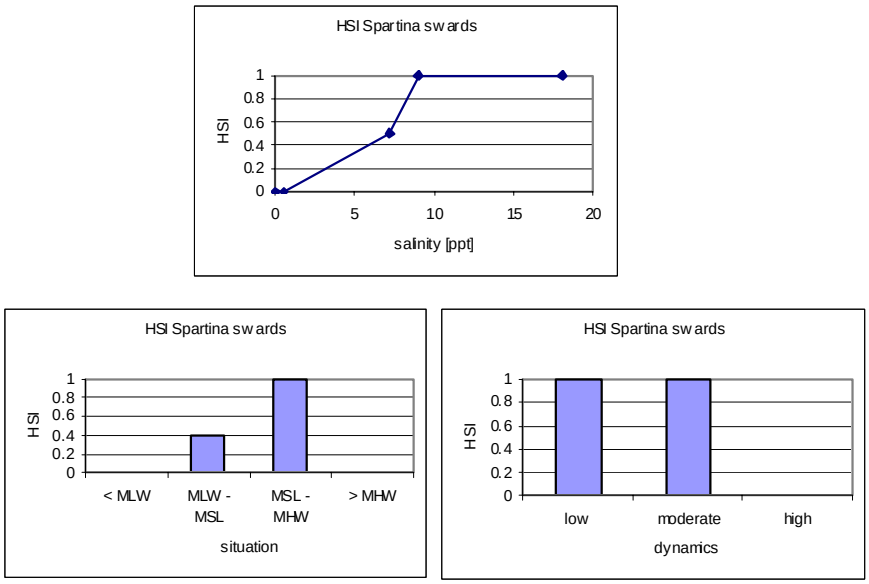

Figure 4.5 Response curves of Spartina swards (H1320).

Salt marshes and salty meadows – H1330

With respect to dynamics and salinity, the response curves of this habitattype are the same as for H1310 and H1320. The inundation frequency differs however: H1330 only occurs above mean sea level (MSL) and preferably above mean high water (MHW), corresponding to inundation during high tides only.

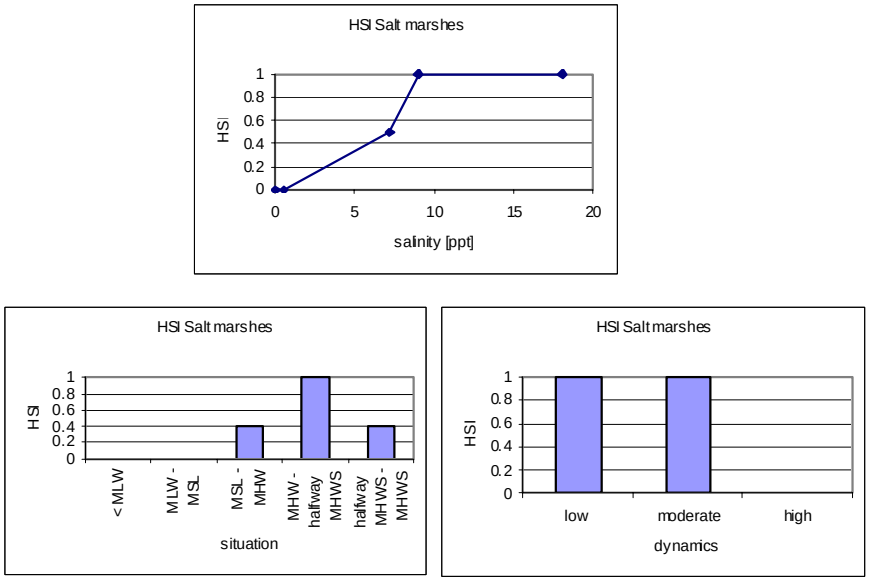

Figure 4.6 Response curves of Salt marshes (H1330).

4.4.2 Invertebrates – response curves

Cockle – Cerastoderma edule

The cockle lives in mud, sand, muddy sand or muddy gravel with a median grain diameter (D50) over 100 µm, about 20 cm deep. It has the ability to move a little using its 'foot', but is sensitive to rapid erosion or sedimentation.

As a filter feeder, the cockle does not survive long dry periods. Its occurrence is therefore limited to areas that are dry for 6 hours or less, which corresponds to depths slightly above MSL and lower, down to 15 m. The concentration of fines in the water column should not exceed 50 g/l to enable efficient feeding. Cockles prefer temperatures between 5 and 33 °C. Low salinities are tolerated briefly; values above 21ppt are preferred. Likewise, oxygen concentrations below 5 mg/l (estimate) are unfavourable but not immediately lethal.

Blue mussel – Mytilus edulis

Mussels occur in the inter- to subtidal, not lower than 20 metres and not higher than where they are emergent for more than 45% of the time. Initially, a solid substrate –rocks, piers, shells or seaweed- is required, later they grow on each other building a reef. Reefs are sensitive to very dynamic conditions: they can be damaged by waves or filled in with sediment. Some dynamics are required however to ensure a sufficient supply of food for this filter feeder.

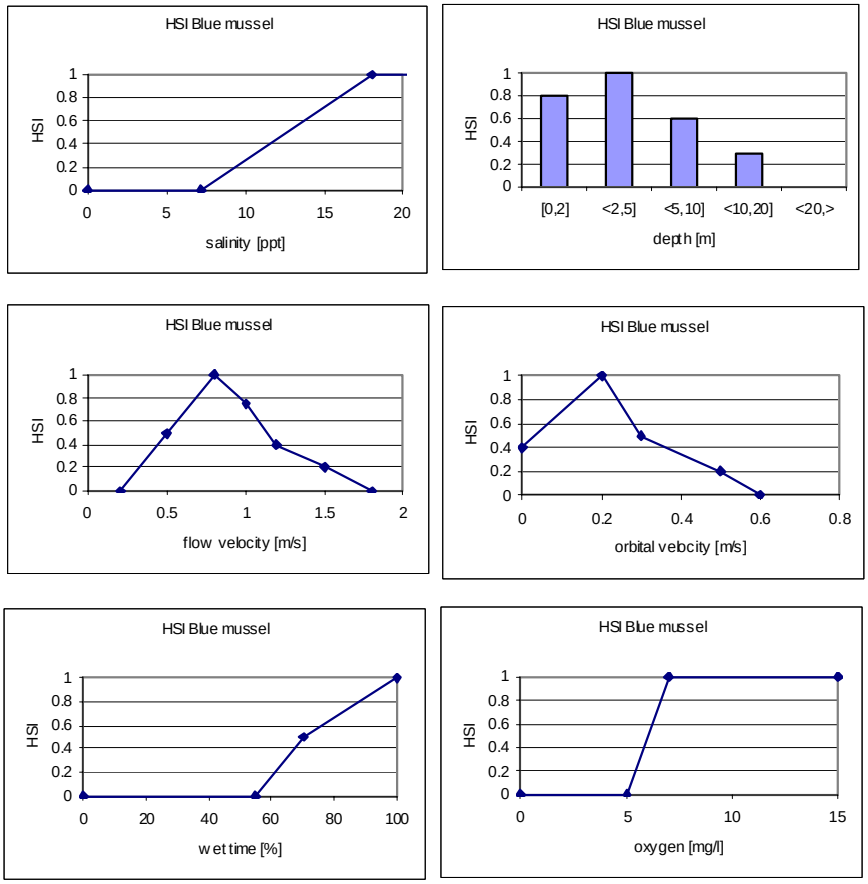

Figure 4.7 Response curves of the Blue mussel Mytilus edulis.

Mussels can deal with adverse conditions rather well, often simply by closing their shells filled with water. Periods with temperatures below 0°C or up to 40°C are not lethal, though temperatures between 2 and 23 °C are preferred. The optimal salinity for growth is above 18 ppt. High silt concentrations may hamper feeding. Silt and other inorganic matter are excreted as faecal pellets.

Lugworm – Arenicola marina

The lugworm lives in sand and silty sands (D50 > 60 µm; 1-15% silt), from the high intertidal to several meters deep. Juveniles occur higher and in more silty beds. The area may be dry

for 0-90% of the time. The salinity should be over 10 ppt, with maximum daily changes of 6 ppt. Low oxygen levels and anoxia are tolerated up to 5 days (2 days for juveniles). The tolerated yearly average water temperature lies between 0 and 18 °C, with a maximum for the average in the warmest month of 21 °C.

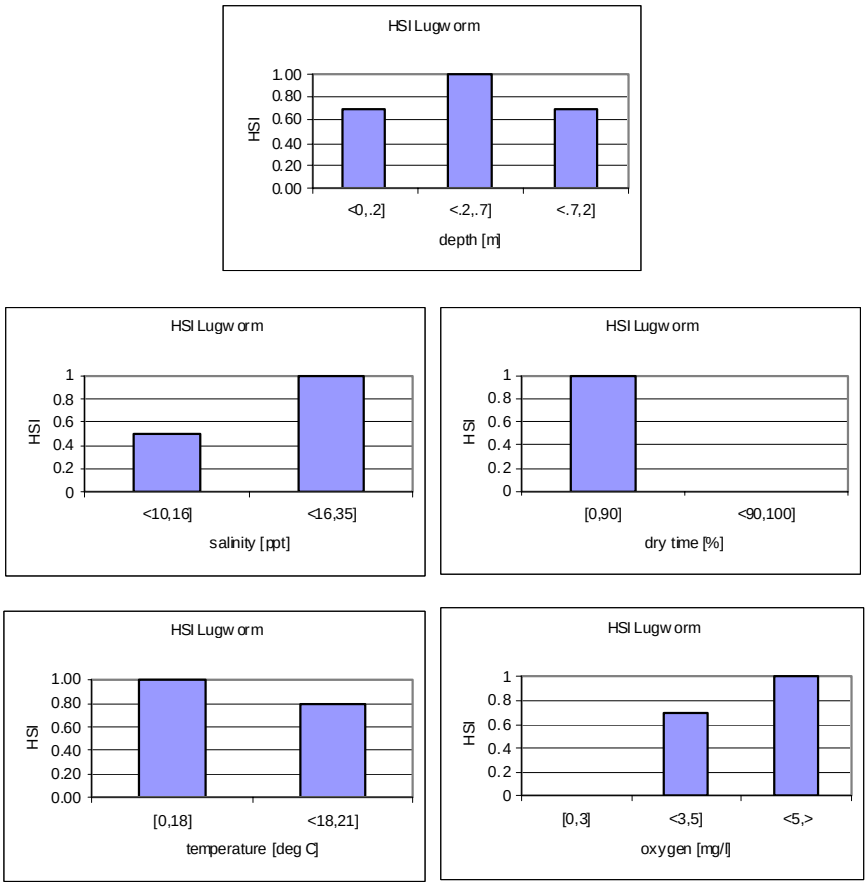

Figure 4.8 Response curves of the Lugworm Arenicola marina.

Lugworms feed on organic matter inside U-shaped tubes in the sediment, excreting used sediment to the surface. They do not have a preference for calm or dynamic areas; they live 15-40 cm inside the sediment, are fairly mobile and can recolonise small plots within one month.

Mudshrimp – Corophium volutator

As the name indicates, this amphipod prefers muddy areas, though there is no relation between median grain size or silt content and its occurrence. The high water level during neap tides forms the upper limit of its habitat, the low water line the lower limit. Near this lower limit, the competition with other macrofauna leads to lower densities than at higher areas where competition is less. Corophium tolerates a wide range of salinities (2-35 ppt), but prefers values around 20 ppt. No information on limiting oxygen levels or temperature could be found. Moving ice however can damage the burrows, as can storms. Recolonisation occurs quickly.

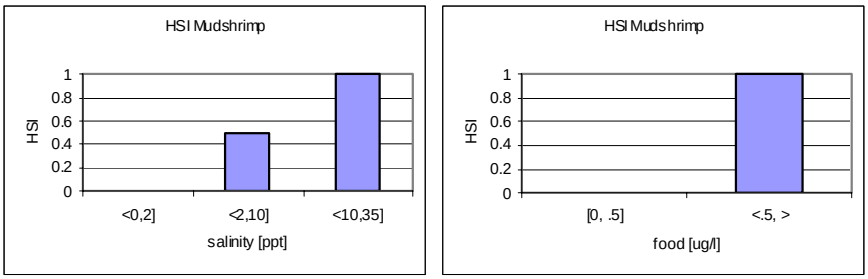

Figure 4.9 Response curves of the Mudshrimp Corophium volutator.

Hidden in a 5 cm deep burrow, it feeds on bacteria and diatoms either by pumping water through the burrow or by scraping deposits near one of the entrances. Hence, high levels of organic matter are preferred. The presence of macroalgae (especially Ulva) has a negative effect however, as Corophium are hindered during feeding by the weeds that physically obstruct the burrows and possible feeding area of the animals.

4.4.3 Fish – response curves

Sparling – Osmerus eperlanus

Apart from the availability of food, four factors determine the habitat suitability for Sparling: turbidity, temperature, oxygen concentration and access to fresh water for spawning (source: Habitat-database). Sparling prefers large, open and turbid waters to be able to hide from their predators. The Secchi-depth should not be more than 2 m, preferably less than 0.7 m. Temperatures below 20°C are ideal; up to 25°C are tolerated. The active swimming of these fish requires sufficient oxygen. As an absolute minimum, 2 mgl-1 is required, above 8 mgl-1 is optimal. More response curves are available with respect to their spawning areas but these areas are outside the study area.

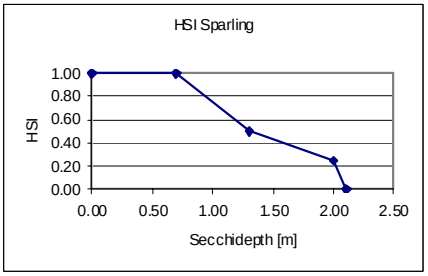

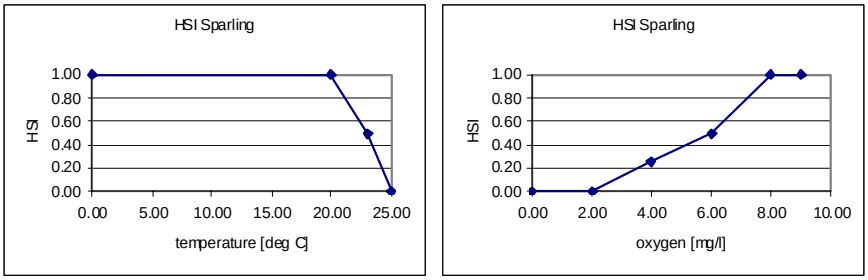

Figure 4.10 Response curves of Sparling Osmerus eperlanus.

Pelagic

Most pelagic fish that occur in the Ems-Dollard have somewhat similar characteristics to Sparling: they are active swimmers and prefer water temperatures below 20-22°C, though

some move to deeper and warmer waters in winter. None of these species minds brackish water. Turbidity is not used as a criterion because some of species that are visual hunters (Garfish, Perch) prefer clear water and others do not. For many species the optimum turbidity could not be found in literature.

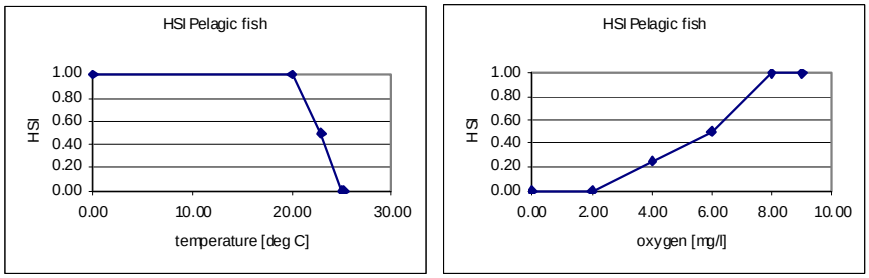

Figure 4.11 Response curves of the group Pelagic fish.

Demersal shallow

This group of typically estuarine fish contains all fish that live on or near the seabed at depths that range from the intertidal to roughly 30 m. Some of these fish are even able to survive periods out of the water during low tide. Because most of these fish are less active than pelagic fish their need for oxygen might also be lower, though this is not sure. The preference for substrate in this group is very diverse: sandy, muddy, rocky or a combination of any of these. Most of these animals are very well adapted to life near the seabed: they can hunt in conditions with very limited visibility and use camouflage or other means of hiding above fleeing for predators. Hence, this group is likely to prefer turbid conditions, though the preferred turbidity is difficult to quantify.

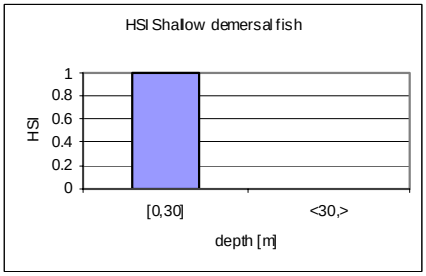

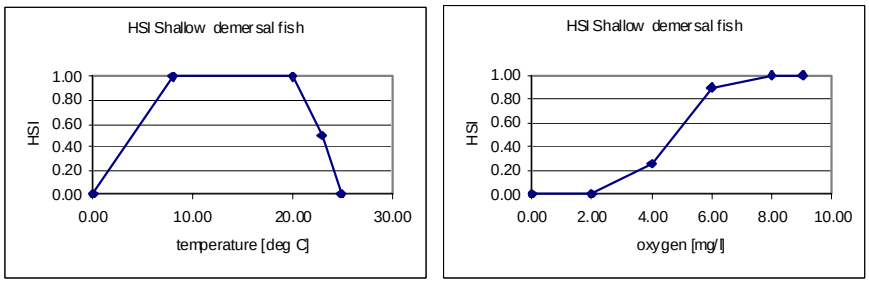

Figure 4.12 Response curves of the group Shallow demersal fish.

Demersal deep

This group contains all fish that live on or near the seabed, typically in waters of several metres to several hundreds of metres deep. Many of these fish are marine juveniles and most prefer sandy beds over muddy ones. Their tolerance for low salinities is less than that of the pelagic or shallow demersal species. Like other demersal fish, they are likely to cope well with somewhat lower oxygen levels and turbid water.

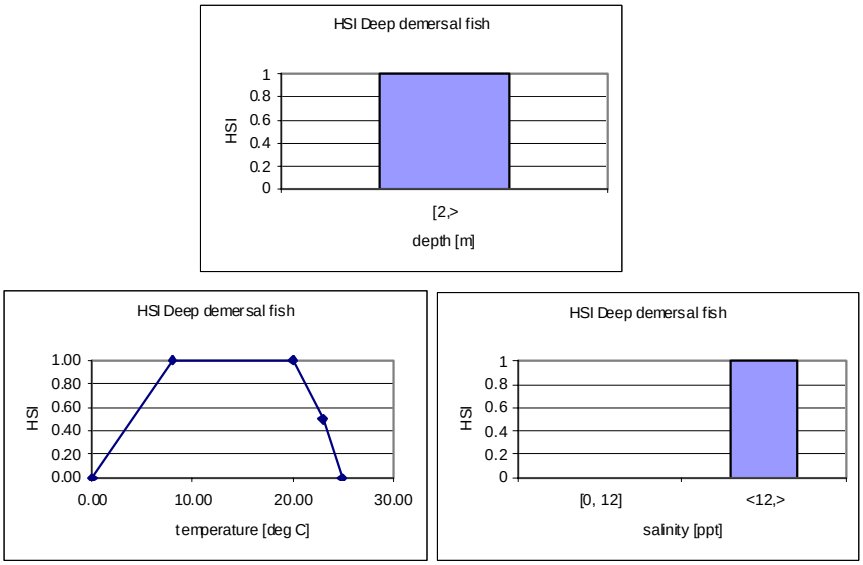

Figure 4.13 Response curves of the group Deep demersal fish.

4.4.4 Birds – response curves

Common Tern – Sterna hirundo

The common tern feeds by aerial diving for pelagic fish near the coast. Water clarity is important for spotting prey. They prefer either shallow water or water 10-20 metres deep with higher flow velocities where turbulence enhances prey availability near the surface (Schwemmer et al., 2009; Bugoni et al. 2005). Foraging activity is negatively correlated with the distance to their colony, with a maximum foraging distance of 8 to 10 kilometres (ibid). No significant relation between foraging preference and distance to productive estuaries was found. The common tern prefers sheltered, inshore areas over exposed seas.

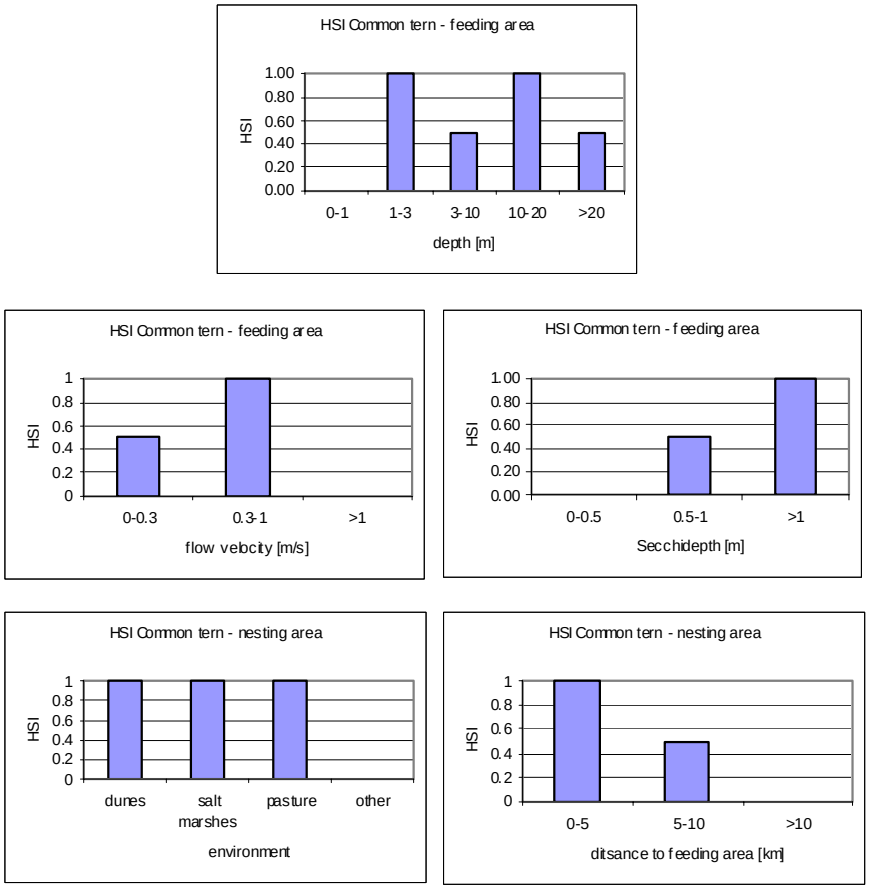

Figure 4.14 Response curves of the Common tern Sterna hirundo.

Breeding occurs in colonies located on open areas with some shelter from vegetation or boulders: pasture, salt marshes, dunes, but also flat roofs or abandoned piers. When breeding, terns are quite susceptible to disturbance by predators like gulls and rats.

No response curve was readily available; hence it was developed from the sources above. It is not validated.

Red-breasted merganser – Mergus serrator

The red-breasted merganser prefers salt water more than the larger Mergus merganser, though it should not be too exposed. Water depths to 3.5 m are preferred (soortenbank.nl). It catches prey by surface diving, hence the water needs to be clear. When foraging on benthic invertebrates it prefers calm conditions with little turbulence, when feeding on fish it prefers more dynamic conditions that help bring fish to the surface (Holm & Burger, 2002).

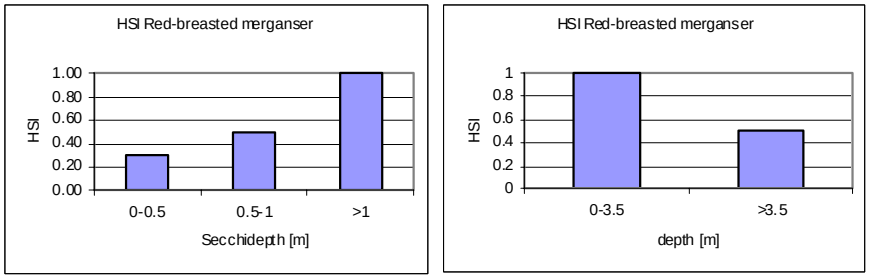

Figure 4.15 Response curves of the Red-breasted merganser Mergus serrator.

The curves are a combination of that from Mergus merganser (Habitat-database) and sources mentioned above. Not validated.

Eurasian widgeon – Anas penelope

In fall and winter, this bird lives at sea along muddy, not too dynamic coasts. It feeds on grass in pastures and on salt marshes, other plants, roots and seeds. It does not feed on Salicornia spp. because these plants do not provide sufficient energy (Durant et al. 2006). Except from edible plants, the Eurasion widgeon does not seem to have strict habitat demands.

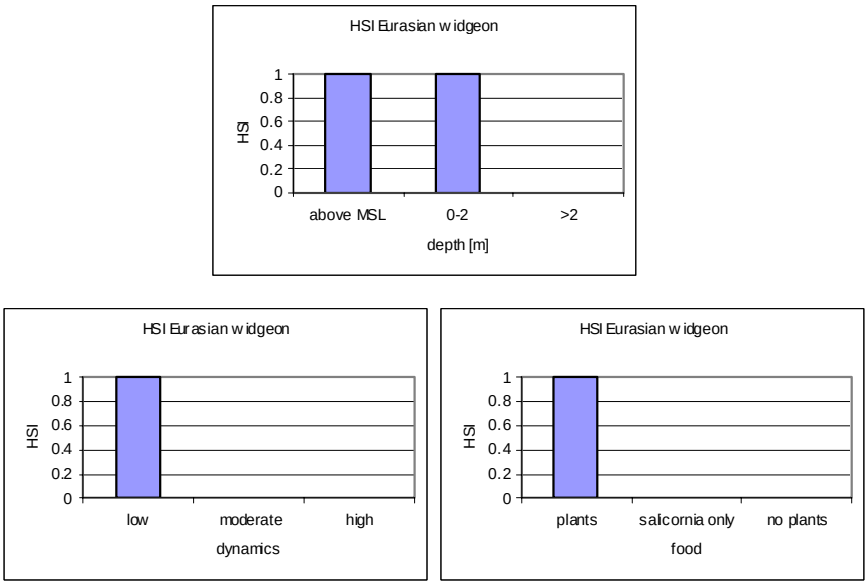

Figure 4.16 Response curves of the Eurasian widgeon Anas penelope.

Avocet – Recurvirostra avocetta

This is a wading bird that feeds on invertebrates in intertidal areas, from MHW down to MLW -0.2 m. The sediment needs to be soft (muddy) to be able to filter its prey out of the sediment. This 'softness' is difficult to quantify but a minimum of 20% fines might be a sufficient indicator. The avocet breeds in open areas and needs salt marshes or similar terrain to rest between feeding periods.

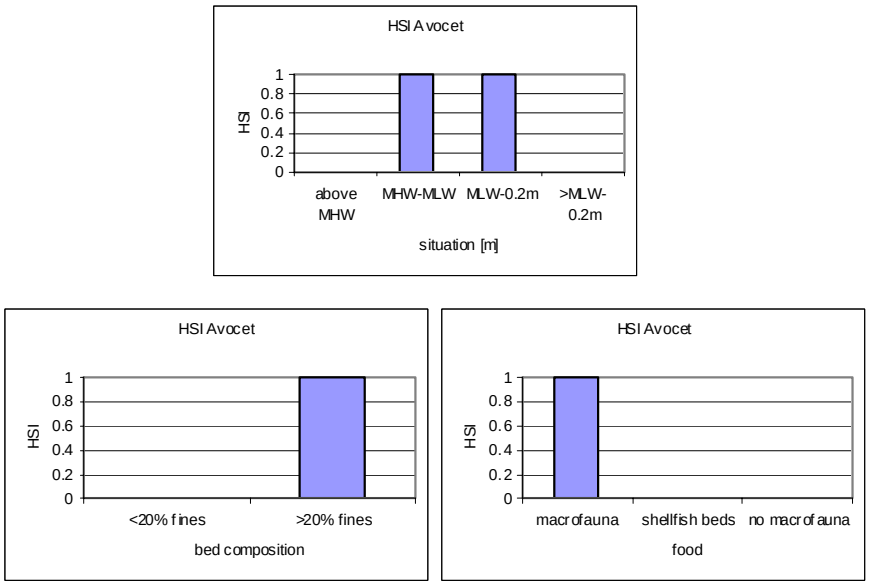

Figure 4.17 Response curves of the Avocet Recurvirostra avocetta.

The curves are estimated based on information of a.o. soortenbank.nl. Not validated.

4.4.5 Mammals – response curves

All three mammal species in the Ems-Dollard are to some degree susceptible to noise, either quasi-permanent like the sound of ship engines or temporarily from construction works. Exact values are lacking and require more research, but swimming mammals do not tend to avoid shipping lanes. Drilling activities, which produce very high noise levels (>200 dB) are a disturbance with a large spatial extent (over 21 km) but animals return to the area quickly after the activities are halted (Carstensen et al. 2006; Madsen et al. 2006; Tougaard et al. 2009). Long-term effects of noise are not known.

The presence of food is crucial, though mammals can cover considerable distances to feed. Especially fatty fish such as herring and sandeel is a popular prey, but mammals switch to other species when these are not available. Estuaries are often rich in food, as are areas where upwelling occurs; quantitative relations are missing however.

The presence of nets, mainly that of ‘staand want’ and fykes, can cause animals to get stuck and die, but this does not affect the suitability of their habitat.

Grey seal – Halichoerus grypus

The Habitat-database only provides dose-effect relationships on nursing areas. These need to be above mean high water, preferably higher as pups cannot swim the first 2-3 weeks after birth. Suitable areas also need to be sandy or rocky, without disturbance and easily accessible from a tidal channel.

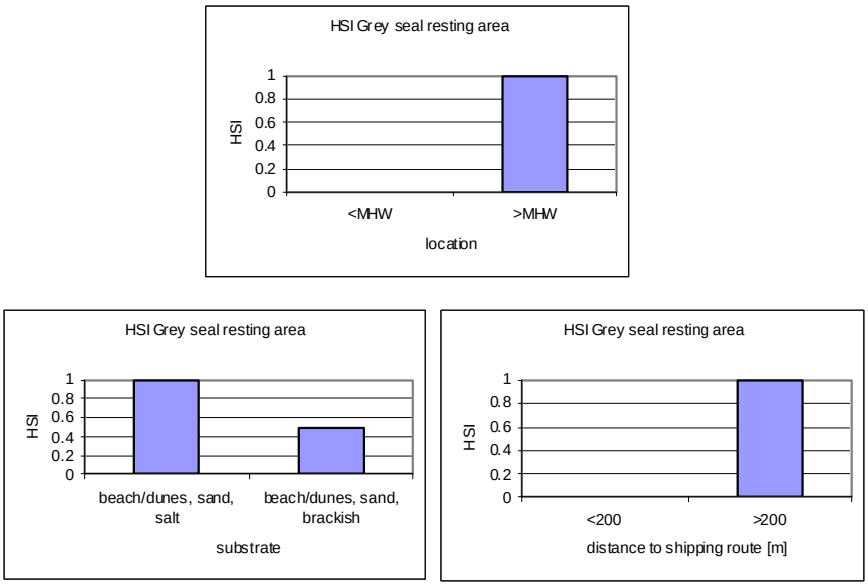

Figure 4.18 Response curves of the resting area of the Grey seal Halichoerus grypus.

For feeding, grey seals can dive to 100 metres depth. Their usual diving depth is up to 10-15 metres, requiring less energy. Feeding trips can be up to several tens of kilometres from their haul out stations. Seals do occur in brackish water but prefer salt water. Turbid water is not a problem, as seals use sounds and their nostrils to locate prey.
Only response curves for nursing areas available in the Habitat-database.

Common seal – Phoca vitulina
Similar to the grey seal in habitat demands, except for the fact that pups can swim almost directly after birth. Consequently, nursing areas can be lower. High nursing areas are still considered more favourable, as repeated swimming interrupts the feeding of the pups, thus decreasing their fitness.

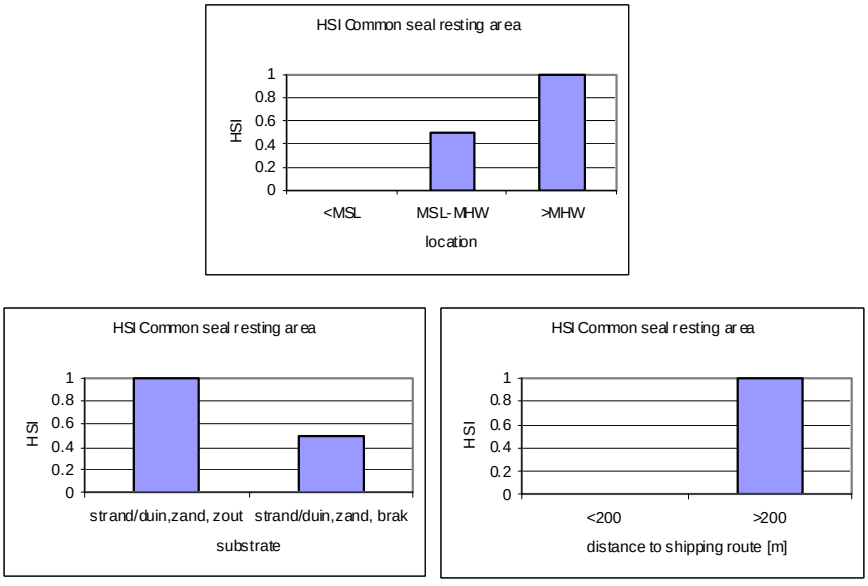

Figure 4.19 Response curves of the resting area of the Common seal Phoca vitulina.

No curves present in Habitat-database, therefore copied from grey seal.

Harbour porpoise – Phocoena phocoena

In the database, the only existing response curve concerns depth: all waters with a depth less than 200 metres are considered suitable. Indeed, salinity and turbidity do not matter to these animals, but Westgate et al. (2000) report that they do not usually occur in water with a temperature over 15°C. This is a remote-sensing study, so it cannot be ascertained that temperature itself is a negative factor or that it correlates with another –unmeasured- negative factor. A minimum depth of 3 metres also seems logical as porpoises need to avoid shallow areas where they might get stranded.

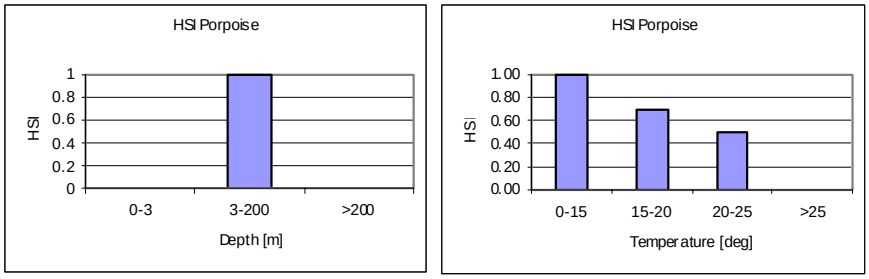

Figure 4.20 Response curves of the harbour porpoise Phocoena phocoena.

Curve for depth extended with a minimum depth, curve for temperature added.

4.5 Model sensitivity

In this section, the sensitivity of the habitat model for the grid size as well as for several environmental parameters is studied. Because the water quality simulation still required some improvements during this study, not all relevant parameters have been assessed. This will be done when satisfactory water quality results are available. For this study, the results of calculation waq10_1b (26-10-2010) have been used.

4.5.1 Sensitivity to grid size

All three submodels (sediment transport, water quality and ecology) use their own grid. The grid from the water quality model is an aggregation of the sediment transport grid. Both these grids are curvilinear. The rectangular grid used by the ecology model is created by resampling the results from the sediment transport or water quality models; the grid cell size needs to be smaller than that of the other models in order to follow the contours of the curvilinear grids well. A larger number of grid cells requires more computation time however.
Because good spatially explicit validation data is lacking, the similarity between the results at the tested grid size (dx=50, 100, 200 and 500 m) and at the lowest feasible grid size (dx=25 m) is used as a quality criterion. The more similar the results, the better is the quality. It is assumed that at dx=25 m, the terrain features are captured sufficiently well. A higher resolution is not feasible because of file sizes and computation times. A subdivision into smaller areas where a very high resolution is required, for example around the steep edges of salt marshes in the back of the Dollard, is possible but hampers the view on the entire estuary.

The sensitivity of the resulting suitable area to the Habitat grid size was determined using the response curves of the Red-breasted merganser (Mergus serrator; a diving bird) as an example. The Merganser was chosen because it is sensitive to depth, which has strong spatial gradients, and sensitive to turbidity, which is generally more spatially uniform. This

analysis was performed for both the Dollard area and the middle reaches of the Ems estuary (see Figure 4.1); the two most interesting areas with a distinct topography. Similar to the other suitability assessments, the total suitability is classified along four classes: unsuitable (HSI=0), moderately suitable (0-0.5), reasonably suitable (0.5-0.8) and very suitable (0.8-1).

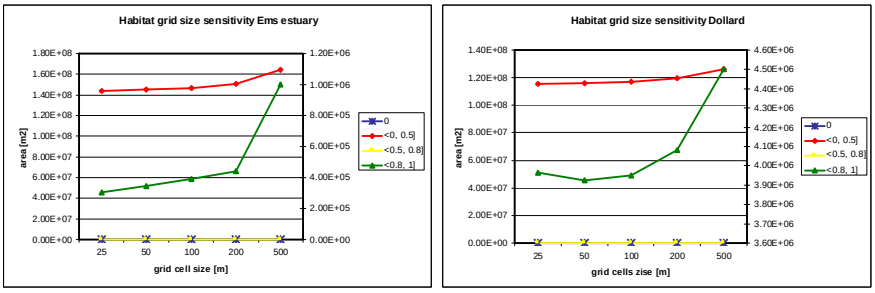

Figure 4.21 Area classified as suitable for Mergus serrator for different grid cell sizes. Note: the moderately suitable area (red line) is plotted on the left axis, the very suitable area (green line) on the right axis.

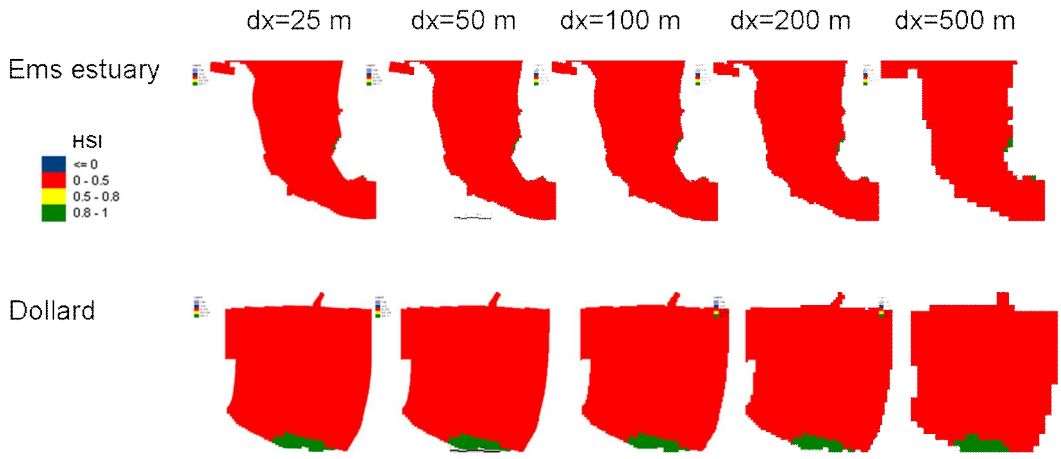

Figure 4.22 Area classified as suitable for Mergus serrator for increasing grid cell sizes.

At grid sizes of 25 m, 50 m and 100 m, the difference in very suitable area –which is only a very small part of the total area; see Figure 4.22 - is less than 10% in the Ems estuary and even less in the Dollard (Figure 4.21). At dx=200 m the difference is larger but still of similar order, whereas at dx=500 m the results deviate substantially. These trends are the same for the area classified as moderately suitable, though the relative differences are smaller due to the much larger area. Moreover, the outline of the estuary is visibly distorted at the largest grid sizes (dx=200 and 500 m). Based on these findings, a grid size of 50 m is considered suitable. The file sizes and computation time at this resolution are also manageable, as came forward during this sensitivity study.

4.5.2 Sensitivity to input conditions

Since the input for the Habitat model consist of the output of the sediment transport and water quality models, it is important to get an idea of how sensitive the habitat suitability is to variations in the output of these preceding models: Not only does this indicate uncertainties in the current results, it also indicates where modelling improvements in subsequent studies are the most useful and which changes in the physical system will have the strongest effects.

This sensitivity study is performed by imposing changes on a single input parameter while all other input parameters remain constant. These changes cover a range of extremes, which

might indicate variations on the long term, and smaller values that are representative for modelling inaccuracies. E.g. the water depth is varied in a range of -1, -0.5, -0.1, +0.1, +0.5 and + 1 meter around the original value of the morphological model. Together, this range indicates whether the response is linear or not. For some parameters absolute values are used, for others relative values make more sense: The water depth is nowhere likely to be off more than 1 m, regardless of the actual water depth, whereas for example turbidity (i.e. Secchidepth) no absolute limits exist. Table 4.1 lists which parameters are varied in which range.

Table 4.1 Variations in parameter ranges used for the input sensitivity study

		Water-depth	Temper-ature	Oxygen concentration	Turbidity
upper extreme	+	1 m	5°	100%	100%
medium increase	+	0.5 m	2.5°	50%	50%
small increase	+	0.1 m	1°	10%	10%
base	0				
small decrease	-	0.1 m	1°	10%	10%
medium decrease	-	0.5 m	2.5°	50%	50%
lower extreme	-	1 m	5°	100%	100%

Example 1: Sparling

Sparling (Osmerus eperlanus) is a fish that requires substantial oxygen and a high turbidity that limits its visibility to prey. Sparling prefers low to moderate temperatures (0-20°C). For this sensitivity study, the average conditions during one month in spring have been used. In the current water quality model, the temperature is spatially uniform: about 12°C in spring. This is implies a very good habitat suitability (HSI=1) for Sparling everywhere, which remains the same if the temperature would be raised or lowered 12°C. Hence, with the current results temperature is never a limiting factor and therefore not taken into account in this sensitivity study.

In normal conditions, both the Ems and the Dollard are very suitable for Sparling (Figure 4.23). Only in small areas of the Dollard, oxygen can be a limiting factor. Too clear water is the main factor that limits habitat suitability (Figure 4.24).

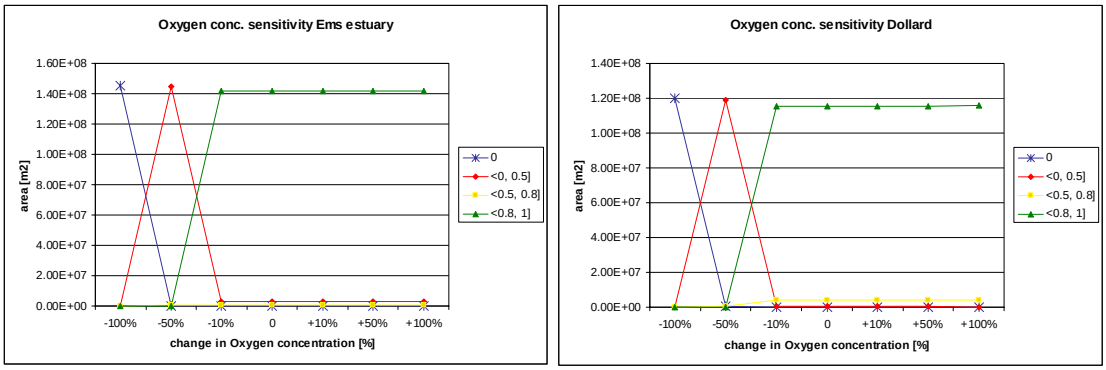

Figure 4.23 Area suitable for Sparling in the Ems and Dollard regions, at a range of oxygen concentrations.

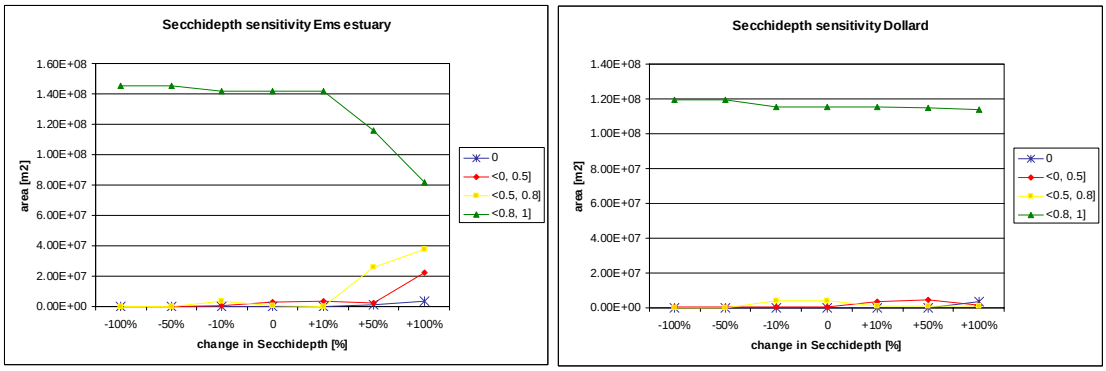

Figure 4.24 Area suitable for Sparling in the Ems and Dollard regions, at a range of Secchi depths.

Example 2: Red-breasted merganser

Only small parts of both the Ems and the Dollard are very suitable for the Red-breasted merganser. The majority of the study area is moderately suitable, which is a result of most parts having a depth exceeding 3.5 m. Decreasing the depth causes the loss of some shallow areas with suitable clear water. A small change (+/- 10%) in Secchi depth barely affects the suitable area, but a decrease of 50% (i.e. increase in turbidity) eliminates the very suitable area.

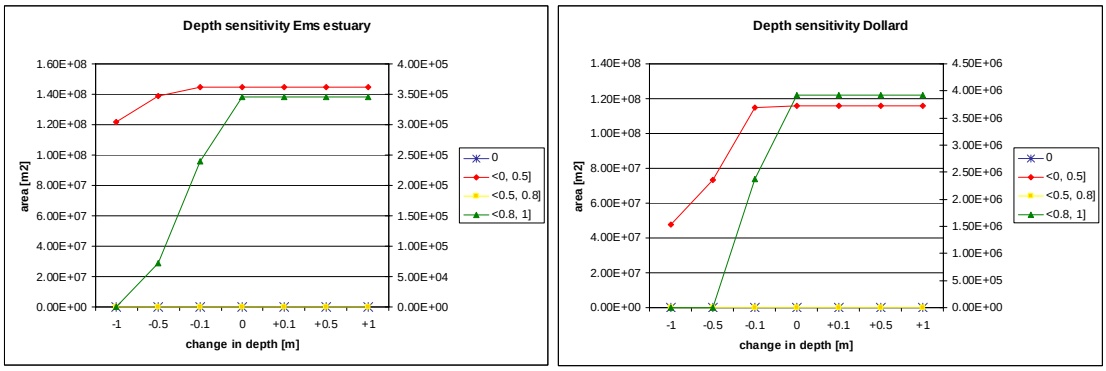

Figure 4.25 Area suitable for the Red-breasted merganser in the Ems and Dollard regions, at a range of water depths. Note: the moderately suitable area (red line) is plotted on the left axis, the very suitable area (green line) on the right axis.

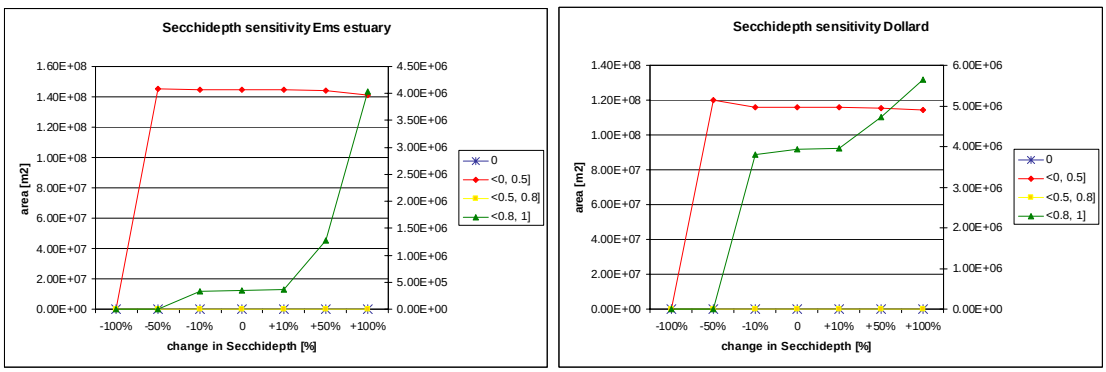

Figure 4.26 Area suitable for the Red-breasted merganser in the Ems and Dollard regions, at a range of Secchi depths. Note: the moderately suitable area (red line) is plotted on the left axis, the very suitable area (green line) on the right axis.

4.5.3 Further work

When satisfactory water quality data become available, other parameters will be assessed. Therefore, other species or habitattypes are necessary. The sensitivity to temperature, salinity, flow velocity and inundation/dry time are to be studied. The Blue mussel is a suitable species to assess these parameters. Furthermore, the analysis will be extended to the four seasons instead of spring only, thus incorporating a wider range in temperature, salinity and nutrients in particular.

4.6 Discussion and recommendations

4.6.1 Discussion

The model has improved substantially since last year, when mainly the system to be modelled and the information required to do so were identified. Now, the information –results from the sediment and water quality models, as well as the parameters that define habitat suitability- is much more complete, though still some improvements are necessary.

Model set-up

The chosen model set-up with sub-areas and the use of input files that contain only representative conditions makes makes the study more transparent and therefore less prone to errors.

Species selection

Though the species taken into account in this study are only a small number of the actual occurring species in the Ems-Dollard, the amount is still considerable. As a consequence, the eventual picture is a broad one rather than a very detailed one. Also, it should be realised that most information that is available considers the habitat requirements of ‘higher’ organisms: birds, fish and mammals. Organisms at lower trophic levels, such as invertebrates, are just as important, but less well known.

Response curves

The response curves have been made with the most care, using various sources. Most of them have not been validated however.

Sensitivity study

The sensitivity study is not complete yet and will require more attention in 2011. A grid size of 50 m seems sufficient for most purposes.

4.6.2 Recommendations

- Perform a more elaborate sensitivity study that incorporates all relevant parameters, using improved water quality results.
- Analyse the habitat suitability for all species throughout the year. This contributes to the understanding of what parameters are important in what time of year, but also to how variable the occurrence of organisms can be.
- Gather spatially explicit validation data for a number of species. This will not only contribute to the validity of the model, but might also contribute to a quantitative understanding of how habitat suitability is linked to actual occurrence.

- Improve the response curves of the most interesting (groups of) organisms, advised by the outcomes of the sensitivity study and validation phase. Especially pay attention to species that determine the habitat suitability for other species higher in the food chain.
- Define various scenarios of development of the Ems-Dollard region that are of interest to managers or NGO's; this will provide more focus in the choices and simulations to be made.
- Modelling of habitat suitability in and around the salt marshes in the Dollard might require a substantial locally dedicated effort.

5 Synthesis

The overall aim of the model setup is to quantify the effect of human interventions in the physical system to changes in hydrodynamics, sediment transport, water quality and ecosystem functioning. Two sediment transport models currently exist: the sediment-online version developed in 2009 (Van Maren, 2010), and the WAQ sediment model developed in 2010 (this year). The most important advantage of the WAQ model is that the sedimentation rate on the mudflats and the sediment concentration is more accurately simulated. Even more, the presently applied WAQ model computes the mud fraction of the sediment, which is an important parameter for the habitat suitability of certain species. Additionally, in the WAQ model waves are already implemented (in contrast with the currently available sediment online model), longer time periods can be computed (because the WAQ model is much faster), and the coupling with the water quality model is easier. The most important advantage of the sediment-online model is that it better represents sediment transport into the Ems River. One of the reasons for the large sediment import into the Ems was concluded to be the damping of turbulent mixing by sediment-induced density gradients (Van Maren, 2010). This cannot be combined with the WAQ model, because flow computations are decoupled from the sediment computations. Comparing both model advantages with the model requirements, it seems that the WAQ model is more suitable for the effect chain model than the sediment-online model. It should, however, be kept in mind that the sediment import into the Ems river is underestimated; parameterization of this sediment flux may be part of future work. Additional future work is to run the model with realistic forcing for a longer period, and compare results with observations. This may be done with the 1990-1991 observations in the Ems Estuary and the Dollard Estuary.

Modeling of dissolved oxygen and nitrogen has improved considerably, while chlorophyll and phosphorus need further improvement. Further analyses are needed to determine the reasons for the errors in chlorophyll computations. It may be related to the sediment transport model, but may also result from other sources. It is expected that model results will improve once a full year of hydrodynamics with realistic forcing is available.

The most hydrodynamic properties determining habitat suitability are the water depth and flow velocity, which can be readily derived from the model. Temperature is not modeled, but prescribed as an external function. The most important water quality parameters are the secchi depth (i.e. visibility) and oxygen (note that oxygen is only important in extreme environments as the Ems River, in natural systems the oxygen levels are sufficiently high not to influence habitat suitability), and food availability. The secchi depth is determined by the sediment concentration and the chlorophyll concentration, which both need further improvement: this is one of the main challenges for 2011. The base of the food chain is phytoplankton (chlorophyll), which provides food for invertebrates, fish, and zooplankton (which are in turn an important source of food). The relation between chlorophyll and the lower and higher trophic levels are poorly known in general, while the modeled chlorophyll levels are still not correctly simulated. This is therefore also an important improvement required in 2011. The main challenge for 2011 is the production of maps with habitat suitability based on the Habitat suitability curves presented in Chapter 4, based on more accurate chlorophyll and sediment transport simulations.

6 References

Blauw AN, Los FJ, Bokhorst M, Erftemeijer PLA (2008) GEM: a generic ecological model for estuaries and coastal waters. Hydrobiologia 618(1): 175-198

Brinkman, A. G., and Ens, B. J. (1998). "Effecten van bodemdaling in de Waddenzee op wadvogels." 371, Instituut voor Bos- en Natuuronderzoek, Wageningen.

Bugoni, L., Cormons, T. D., Boyne, A. W., and Hays, H. (2005). "Feeding grounds, daily foraging activities, and movements of common terns in southern Brazil, determined by radio-telemetry." Waterbirds, 28(4), 468-477.

Carstensen, J., Hendriksen, O. D., and Teilmann, J. (2006). "Impacts on harbour porpoises from offshore wind farm construction: Acoustic monitoring of echolocation activity using porpoise detectors (T-PODs). ." Marine Ecology-Progress Series, 321, 295-308.

De Jonge VN (2000), Importance of temporal and spatial scales in applying biological and physical process knowledge in coastal management, an example for the Ems estuary, Continental Shelf Research 20 (12-13) 1655-1686

Dijkstra, J. (2010). Eems-Dollard model setup: Habitats. Deltares report 1200739-000, 33 p.

Durant, D., Kersten, M., and Fritz, H. (2006). "Constraints of feeding on Salicornia ramosissima by wigeon Anas penelope: an experimental approach " Journal of Ornithology, 147, 1-12.

Ens, B. J., Brinkman, A. G., Dijkman, E. M., Meesters, H. W. G., Kersten, M., Brenninkmeijer, A., and Twisk, F. (2005). "Modelling the distribution of waders in the Westerschelde." 1193, Alterra, Wageningen.

Erftemeijer, P. L. A., and van de Wolfshaar, K. E. (2006). "Ecological model of het Lagoon of Venice. Part III: Seagrass Habitat Model." Z3733, WL|Delft Hydraulics, Delft.

Holm, H. J., and Burger, A. E. (2002). "Foraging behavior and resource partitioning by diving birds during winter in areas of strong tidal currents." Waterbirds, 25(3), 312-325.

Jager, Van Maren, de Kok, Van Wesenbeeck, Los en Nauta (2009). Required modelling tools to support the future management plan for the Ems-Dollard Deltares report Z4573, 75 p.

Kater, B. J., van Kessel, A., and Baars, J. (2006). "Distribution of cockles Cerastoderma edule in the Eastern Scheldt: habitat mapping with abiotic variables." Marine Ecology-Progress Series, 318, 221-227.

Los FJ, Villars MT, van der Tol MWM (2008) A 3-dimensional primary production model (BLOOM/GEM) and its applications to the (southern) North Sea. Journal of Marine Systems 74(1-2): 259-294

Madsen, P. T., Wahlberg, M., Tougaard, J., Lucke, K., and Tyack, P. L. (2006). "Wind turbine underwater noise and marine mammals: Implications of current knowledge and data needs." Marine Ecology-Progress Series, 309, 279-295.

Meesters, H. W. G., ter Hofstede, R., Deerenburg, C. M., Craeijmeersch, J. A. M., de Mesel, I. G., Brasseur, S. M. J. M., Reijnders, P. J. H., and Witbaard, R. (2008). "Indicator system for biodiversity in Dutch marine waters, II. Ecoprofiles of indicator species for Wadden Sea, North Sea and Delta Area." Imares, Wageningen.

Ochieng, C. A., and Erftemeijer, P. L. A. (submitted). "The effect of turbidity on light availability to intertidal eelgrass in the Ems estuary." Estuaries and Coasts.

Schans, H. (2005). "Kenmerken stroomgebied Deelstroomgebied Eems-Dollard estuarium."

Spiteri, C. (2010). Eems-Dollard model setup: Water quality module. Deltares report 1200739-000, 36 p.

Schwemmer, P., Adler, S., Guse, N., Markones, N., and Garthe, S. (2009). "Influence of water flow velocity, water depth and colony distance on distribution and foraging patterns of terns in the Wadden Sea." Fisheries Oceanography, 18(3), 161-172.

Tougaard, J., Hendriksen, O. D., and Miller, L. A. (2009). "Underwater noise from three offshore wind turbines: estimation of impact zones for harbor porpoises and harbor seals. ." Journal of the Acoustic Societey of America, 125(6), 3766-3773.

Van Kessel, T., J.C. Winterwerp, B. van Prooijen, M. van Ledden, and W. Borst (2010). Modelling the seasonal dynamics of SPM with a simple algorithm for the buffering of fines in a Sandy seabed. Cont. Shelf Res.

Van Maren, D.S., 2010. Eems-Dollard model setup: Sediment transport module. Deltares report 1200739, 165 p.

Westgate, A. J., Read, A. J., and Cox, T. C. "Watching puffing pigs from space: defining critical habitat using satellite telemetry." European Research on Cetaceans – 14, Cork, Ireland.

A List of processes and parameters used in the water quality Delft3D-WAQ model

Technical identification	Description
BLOOM_P	BLOOM II algae module
WM_DetC	Mineralisation detritus carbon
SedDetC	Sedimentation detritus carbon
Res_DetC	Resuspension detritus carbon
Secchi	Extinction of visible-light (370-680nm)
BMS1_DetC	Mineralisation detritus carbon in sediment S1
SedPhBlo_P	Sum sedimentation of algae - Bloom
BurS1_DetC	Burial detritus carbon from sediment S1
WM_DetN	Mineralisation detritus nitrogen
SedN_Det	Sedim. nutrients in detritus
ResN_Det	Resuspension nutrients in detritus
BMS1_DetN	Mineralisation detritus nitrogen in sediment S1
BurS1N_Det	Burial nutrients in detritus from sediment S1
WM_DetP	Mineralisation detritus phosphorus
BMS1_DetP	Mineralisation detritus phosphorus in sediment S1
WM_DetSi	Mineralisation detritus silicium
BMS1_DetSi	Mineralisation detritus silica in sediment S1
Nitrif_NH4	Nitrification of ammonium
DenSed_NO3	Denitrification in sediment
DenWat_NO3	Denitrification in water column
AdsPO4AAP	Ad(De)Sorption ortho phosphorus to inorg. matter
SEDALG	Sedimentation of algae species
RearOXY	Reaeration of oxygen
BODCOD	Mineralisation BOD and COD
PosOXY	Positive oxygen concentration
Chloride	calculation of chloride from salinity
Extinc_VL	Extinction of visible-light (370-680nm)
EXTINABVLP	Extinction of light by algae (Bloom)
CalcRad	Radiation at segment upper and lower boundaries
DynDepth	dynamic calculation of the depth
DepAve	Average depth for Bloom step
Daylength	Daylength calculation
vtrans	vertical mixing distribution over a period
VertDisp	vertical dispersion
Res_DM	Resuspension total bottom material (dry mass)
S1_Comp	Composition sediment layer S1
Bur_DM	Burial total bottom mass (dry matter)
Veloc	horizontal flow velocity
SaturOXY	Saturation concentration oxygen
TotDepth	depth water column
POC_Dyn	Composition of POC (Dynamo & Bloom)
ExtPODVL	Extinction of light by POC (Dynamo & Bloom)
Sum_Sedim	Total of all sedimenting substances
Sed_IM1	Sedimentation IM1
SedPODyn	Sum sedimentation of POC (Dynamo & Bloom)
CalVS_IM1	Sedimentation velocity IM1 = f (Temp SS Sal)
Compos	Composition
CalVS_DetC	CalVS_DetC
CalVSAlg	generic for all algae
SedAlg	sedimentation of all algae

AtmDep NH4	Atmospheric deposition of NH4
AtmDep NO3	Atmospheric deposition of NO3
Grd_Rho	Calculation of gradient in space of density
Grd_Vel	Calculation of gradient in space of horizontal velocity
CalVSDIN_E	CalVSDIN_E
CalVSDIN_N	CalVSDIN_N
CalVSDIN_P	CalVSDIN_P
CalVSMDI_E	CalVSMDI_E
CalVSMDI_N	CalVSMDI_N
CalVSMDI_P	CalVSMDI_P
CalVSMFL_E	CalVSMFL_E
CalVSMFL_N	CalVSMFL_N
CalVSMFL_P	CalVSMFL_P
CalVSPHA_E	CalVSPHA_E
CalVSPHA_N	CalVSPHA_N
CalVSPHA_P	CalVSPHA_P
EXTINABVL	EXTINABVL
SEDDIN_E	SEDDIN_E
SEDDIN_N	SEDDIN_N
SEDDIN_P	SEDDIN_P
SEDMDI_E	SEDMDI_E
SEDMDI_N	SEDMDI_N
SEDMDI_P	SEDMDI_P
SEDMFL_E	SEDMFL_E
SEDMFL_N	SEDMFL_N
SEDMFL_P	SEDMFL_P
SEDPHA_E	SEDPHA_E
SEDPHA_N	SEDPHA_N
SEDPHA_P	SEDPHA_P

Parameter	Description	Unit	Value
TimMultBl	ratio bloom/delwaq time step	(-)	144
Temp	ambient water temperature	(oC)	forcing function
SWBloomOut	switch on BLOOM output (0=no,1=yes)	(-)	0
FrAutMDI_E	frac. mort. algae dissolved as nutrients MDIATOMS_E	(-)	0.3
FrAutMDI_N	frac. mort. algae dissolved as nutrients MDIATOMS_N	(-)	0.3
FrAutMDI_P	frac. mort. algae dissolved as nutrients MDIATOMS_P	(-)	0.3
FrAutMFL_E	frac. mort. algae dissolved as nutrients MFLAGELA_E	(-)	0.3
FrAutMFL_N	frac. mort. algae dissolved as nutrients MFLAGELA_N	(-)	0.3
FrAutMFL_P	frac. mort. algae dissolved as nutrients MFLAGELA_P	(-)	0.3
FrAutDIN_E	frac. mort. algae dissolved as nutrients DINOFLAG_E	(-)	0.3
FrAutDIN_N	frac. mort. algae dissolved as nutrients DINOFLAG_N	(-)	0.3
FrAutDIN_P	frac. mort. algae dissolved as nutrients DINOFLAG_P	(-)	0.3
FrAutPHA_E	frac. mort. algae dissolved as nutrients PHAEOCYS_E	(-)	0.3
FrAutPHA_N	frac. mort. algae dissolved as nutrients PHAEOCYS_N	(-)	0.3
FrAutPHA_P	frac. mort. algae dissolved as nutrients PHAEOCYS_P	(-)	0.3
FrDetMDI_E	frac. mort. algae detritus production MDIATOMS_E	(-)	0.7
FrDetMDI_N	frac. mort. algae detritus production MDIATOMS_N	(-)	0.7
FrDetMDI_P	frac. mort. algae detritus production MDIATOMS_P	(-)	0.7
FrDetMFL_E	frac. mort. algae detritus production MFLAGELA_E	(-)	0.7
FrDetMFL_N	frac. mort. algae detritus production MFLAGELA_N	(-)	0.7
FrDetMFL_P	frac. mort. algae detritus production MFLAGELA_P	(-)	0.7
FrDetDIN_E	frac. mort. algae detritus production DINOFLAG_E	(-)	0.7
FrDetDIN_N	frac. mort. algae detritus production DINOFLAG_N	(-)	0.7
FrDetDIN_P	frac. mort. algae detritus production DINOFLAG_P	(-)	0.7
FrDetPHA_E	frac. mort. algae detritus production PHAEOCYS_E	(-)	0.7
FrDetPHA_N	frac. mort. algae detritus production PHAEOCYS_N	(-)	0.7
FrDetPHA_P	frac. mort. algae detritus production PHAEOCYS_P	(-)	0.7
ExtVlMDI_E	extinction coeff. visible light by algae MDIATOMS_E	(m2/gC)	0.24
ExtVlMDI_N	extinction coeff. visible light by algae MDIATOMS_N	(m2/gC)	0.21
ExtVlMDI_P	extinction coeff. visible light by algae MDIATOMS_P	(m2/gC)	0.21
ExtVlMFL_E	extinction coeff. visible light by algae MFLAGELA_E	(m2/gC)	0.25
ExtVlMFL_N	extinction coeff. visible light by algae MFLAGELA_N	(m2/gC)	0.225
ExtVlMFL_P	extinction coeff. visible light by algae MFLAGELA_P	(m2/gC)	0.225
ExtVlDIN_E	extinction coeff. visible light by algae DINOFLAG_E	(m2/gC)	0.2
ExtVlDIN_N	extinction coeff. visible light by algae DINOFLAG_N	(m2/gC)	0.175
ExtVlDIN_P	extinction coeff. visible light by algae DINOFLAG_P	(m2/gC)	0.175
ExtVlPHA_E	extinction coeff. visible light by algae PHAEOCYS_E	(m2/gC)	0.45
ExtVlPHA_N	extinction coeff. visible light by algae PHAEOCYS_N	(m2/gC)	0.413
ExtVlPHA_P	extinction coeff. visible light by algae PHAEOCYS_P	(m2/gC)	0.413
DMCFMDI_E	DM:C ratio algae MDIATOMS_E	(gDM/gC)	3
DMCFMDI_N	DM:C ratio algae MDIATOMS_N	(gDM/gC)	3
DMCFMDI_P	DM:C ratio algae MDIATOMS_P	(gDM/gC)	3
DMCFMFL_E	DM:C ratio algae MFLAGELA_E	(gDM/gC)	2.5
DMCFMFL_N	DM:C ratio algae MFLAGELA_N	(gDM/gC)	2.5
DMCFMFL_P	DM:C ratio algae MFLAGELA_P	(gDM/gC)	2.5
DMCFDIN_E	DM:C ratio algae DINOFLAG_E	(gDM/gC)	2.5
DMCFDIN_N	DM:C ratio algae DINOFLAG_N	(gDM/gC)	2.5
DMCFDIN_P	DM:C ratio algae DINOFLAG_P	(gDM/gC)	2.5
DMCFPHA_E	DM:C ratio algae PHAEOCYS_E	(gDM/gC)	2.5
DMCFPHA_N	DM:C ratio algae PHAEOCYS_N	(gDM/gC)	2.5
DMCFPHA_P	DM:C ratio algae PHAEOCYS_P	(gDM/gC)	2.5
NCRMDI_E	N:C ratio per algae type MDIATOMS_E	(gN/gC)	0.255
NCRMDI_N	N:C ratio per algae type MDIATOMS_N	(gN/gC)	0.07
NCRMDI_P	N:C ratio per algae type MDIATOMS_P	(gN/gC)	0.15
NCRMFL_E	N:C ratio per algae type MFLAGELA_E	(gN/gC)	0.2

NCRMFL_N	N:C ratio per algae type MFLAGELA_N	(gN/gC)	0.078
NCRMFL_P	N:C ratio per algae type MFLAGELA_P	(gN/gC)	0.113
NCRDIN_E	N:C ratio per algae type DINOFLAG_E	(gN/gC)	0.163
NCRDIN_N	N:C ratio per algae type DINOFLAG_N	(gN/gC)	0.064
NCRDIN_P	N:C ratio per algae type DINOFLAG_P	(gN/gC)	0.071
NCRPHA_E	N:C ratio per algae type PHAEOCYS_E	(gN/gC)	0.188
NCRPHA_N	N:C ratio per algae type PHAEOCYS_N	(gN/gC)	0.075
NCRPHA_P	N:C ratio per algae type PHAEOCYS_P	(gN/gC)	0.104
PCRMDI_E	P:C ratio per algae type MDIATOMS_E	(gP/gC)	0.032
PCRMDI_N	P:C ratio per algae type MDIATOMS_N	(gP/gC)	0.012
PCRMDI_P	P:C ratio per algae type MDIATOMS_P	(gP/gC)	0.01
PCRMFL_E	P:C ratio per algae type MFLAGELA_E	(gP/gC)	0.02
PCRMFL_N	P:C ratio per algae type MFLAGELA_N	(gP/gC)	0.01
PCRMFL_P	P:C ratio per algae type MFLAGELA_P	(gP/gC)	0.007
PCRDIN_E	P:C ratio per algae type DINOFLAG_E	(gP/gC)	0.017
PCRDIN_N	P:C ratio per algae type DINOFLAG_N	(gP/gC)	0.01
PCRDIN_P	P:C ratio per algae type DINOFLAG_P	(gP/gC)	0.015
PCRPHA_E	P:C ratio per algae type PHAEOCYS_E	(gP/gC)	0.023
PCRPHA_N	P:C ratio per algae type PHAEOCYS_N	(gP/gC)	0.014
PCRPHA_P	P:C ratio per algae type PHAEOCYS_P	(gP/gC)	0.011
SCRMDI_E	Si:C ratio per algae type MDIATOMS_E	(gSi/gC)	0.447
SCRMDI_N	Si:C ratio per algae type MDIATOMS_N	(gSi/gC)	0.283
SCRMDI_P	Si:C ratio per algae type MDIATOMS_P	(gSi/gC)	0.152
SCRMFL_E	Si:C ratio per algae type MFLAGELA_E	(gSi/gC)	0
SCRMFL_N	Si:C ratio per algae type MFLAGELA_N	(gSi/gC)	0
SCRMFL_P	Si:C ratio per algae type MFLAGELA_P	(gSi/gC)	0
SCRDIN_E	Si:C ratio per algae type DINOFLAG_E	(gSi/gC)	0
SCRDIN_N	Si:C ratio per algae type DINOFLAG_N	(gSi/gC)	0
SCRDIN_P	Si:C ratio per algae type DINOFLAG_P	(gSi/gC)	0
SCRPHA_E	Si:C ratio per algae type PHAEOCYS_E	(gSi/gC)	0
SCRPHA_N	Si:C ratio per algae type PHAEOCYS_N	(gSi/gC)	0
SCRPHA_P	Si:C ratio per algae type PHAEOCYS_P	(gSi/gC)	0
ChlaCMDI_E	Chlorophyll-a:C ratio per algae type MDIATOMS_E	(gChla/gC)	0.053
ChlaCMDI_N	Chlorophyll-a:C ratio per algae type MDIATOMS_N	(gChla/gC)	0.01
ChlaCMDI_P	Chlorophyll-a:C ratio per algae type MDIATOMS_P	(gChla/gC)	0.01
ChlaCMFL_E	Chlorophyll-a:C ratio per algae type MFLAGELA_E	(gChla/gC)	0.023
ChlaCMFL_N	Chlorophyll-a:C ratio per algae type MFLAGELA_N	(gChla/gC)	0.007
ChlaCMFL_P	Chlorophyll-a:C ratio per algae type MFLAGELA_P	(gChla/gC)	0.007
ChlaCDIN_E	Chlorophyll-a:C ratio per algae type DINOFLAG_E	(gChla/gC)	0.022
ChlaCDIN_N	Chlorophyll-a:C ratio per algae type DINOFLAG_N	(gChla/gC)	0.007
ChlaCDIN_P	Chlorophyll-a:C ratio per algae type DINOFLAG_P	(gChla/gC)	0.007
ChlaCPHA_E	Chlorophyll-a:C ratio per algae type PHAEOCYS_E	(gChla/gC)	0.023
ChlaCPHA_N	Chlorophyll-a:C ratio per algae type PHAEOCYS_N	(gChla/gC)	0.007
ChlaCPHA_P	Chlorophyll-a:C ratio per algae type PHAEOCYS_P	(gChla/gC)	0.007
PPMaxMDI_E	pot. maximum growth rate at 0 dg C MDIATOMS_E	(1/d)	0.083
PPMaxMDI_N	pot. maximum growth rate at 0 dg C MDIATOMS_N	(1/d)	0.066
PPMaxMDI_P	pot. maximum growth rate at 0 dg C MDIATOMS_P	(1/d)	0.066
PPMaxMFL_E	pot. maximum growth rate at 0 dg C MFLAGELA_E	(1/d)	0.09
PPMaxMFL_N	pot. maximum growth rate at 0 dg C MFLAGELA_N	(1/d)	0.075
PPMaxMFL_P	pot. maximum growth rate at 0 dg C MFLAGELA_P	(1/d)	0.075
PPMaxDIN_E	pot. maximum growth rate at 0 dg C DINOFLAG_E	(1/d)	0.132
PPMaxDIN_N	pot. maximum growth rate at 0 dg C DINOFLAG_N	(1/d)	0.113
PPMaxDIN_P	pot. maximum growth rate at 0 dg C DINOFLAG_P	(1/d)	0.112
PPMaxPHA_E	pot. maximum growth rate at 0 dg C PHAEOCYS_E	(1/d)	0.084
PPMaxPHA_N	pot. maximum growth rate at 0 dg C PHAEOCYS_N	(1/d)	0.078
PPMaxPHA_P	pot. maximum growth rate at 0 dg C PHAEOCYS_P	(1/d)	0.078
TcPMxMDI_E	temperature coefficient for growth MDIATOMS_E	(-)	-1.75
TcPMxMDI_N	temperature coefficient for growth MDIATOMS_N	(-)	-2.0

TcPMxMDI_P	temperature coefficient for growth MDIATOMS_P	(-)	-2.0
TcPMxMFL_E	temperature coefficient for growth MFLAGELA_E	(-)	-1.0
TcPMxMFL_N	temperature coefficient for growth MFLAGELA_N	(-)	-1.0
TcPMxMFL_P	temperature coefficient for growth MFLAGELA_P	(-)	-1.0
TcPMxDIN_E	temperature coefficient for growth DINOFLAG_E	(-)	5.5
TcPMxDIN_N	temperature coefficient for growth DINOFLAG_N	(-)	4.75
TcPMxDIN_P	temperature coefficient for growth DINOFLAG_P	(-)	4.75
TcPMxPHA_E	temperature coefficient for growth PHAEOCYS_E	(-)	-3.25
TcPMxPHA_N	temperature coefficient for growth PHAEOCYS_N	(-)	-3.0
TcPMxPHA_P	temperature coefficient for growth PHAEOCYS_P	(-)	-3.0
TFPMxMDI_E	growth response temp. (0-lin,<>0-expon) MDIATOMS_E	(-)	0
TFPMxMDI_N	growth response temp. (0-lin,<>0-expon) MDIATOMS_N	(-)	0
TFPMxMDI_P	growth response temp. (0-lin,<>0-expon) MDIATOMS_P	(-)	0
TFPMxMFL_E	growth response temp. (0-lin,<>0-expon) MFLAGELA_E	(-)	0
TFPMxMFL_N	growth response temp. (0-lin,<>0-expon) MFLAGELA_N	(-)	0
TFPMxMFL_P	growth response temp. (0-lin,<>0-expon) MFLAGELA_P	(-)	0
TFPMxDIN_E	growth response temp. (0-lin,<>0-expon) DINOFLAG_E	(-)	0
TFPMxDIN_N	growth response temp. (0-lin,<>0-expon) DINOFLAG_N	(-)	0
TFPMxDIN_P	growth response temp. (0-lin,<>0-expon) DINOFLAG_P	(-)	0
TFPMxPHA_E	growth response temp. (0-lin,<>0-expon) PHAEOCYS_E	(-)	0
TFPMxPHA_N	growth response temp. (0-lin,<>0-expon) PHAEOCYS_N	(-)	0
TFPMxPHA_P	growth response temp. (0-lin,<>0-expon) PHAEOCYS_P	(-)	0
Mort0MDI_E	mortality rate at 0 dg C MDIATOMS_E	(1/d)	0.07
Mort0MDI_N	mortality rate at 0 dg C MDIATOMS_N	(1/d)	0.08
Mort0MDI_P	mortality rate at 0 dg C MDIATOMS_P	(1/d)	0.08
Mort0MFL_E	mortality rate at 0 dg C MFLAGELA_E	(1/d)	0.07
Mort0MFL_N	mortality rate at 0 dg C MFLAGELA_N	(1/d)	0.08
Mort0MFL_P	mortality rate at 0 dg C MFLAGELA_P	(1/d)	0.08
Mort0DIN_E	mortality rate at 0 dg C DINOFLAG_E	(1/d)	0.075
Mort0DIN_N	mortality rate at 0 dg C DINOFLAG_N	(1/d)	0.08
Mort0DIN_P	mortality rate at 0 dg C DINOFLAG_P	(1/d)	0.08
Mort0PHA_E	mortality rate at 0 dg C PHAEOCYS_E	(1/d)	0.07
Mort0PHA_N	mortality rate at 0 dg C PHAEOCYS_N	(1/d)	0.08
Mort0PHA_P	mortality rate at 0 dg C PHAEOCYS_P	(1/d)	0.08
TcMrtMDI_E	temperature coefficient for mortality MDIATOMS_E	(-)	1.072
TcMrtMDI_N	temperature coefficient for mortality MDIATOMS_N	(-)	1.085
TcMrtMDI_P	temperature coefficient for mortality MDIATOMS_P	(-)	1.085
TcMrtMFL_E	temperature coefficient for mortality MFLAGELA_E	(-)	1.072
TcMrtMFL_N	temperature coefficient for mortality MFLAGELA_N	(-)	1.085
TcMrtMFL_P	temperature coefficient for mortality MFLAGELA_P	(-)	1.085
TcMrtDIN_E	temperature coefficient for mortality DINOFLAG_E	(-)	1.072
TcMrtDIN_N	temperature coefficient for mortality DINOFLAG_N	(-)	1.085
TcMrtDIN_P	temperature coefficient for mortality DINOFLAG_P	(-)	1.085
TcMrtPHA_E	temperature coefficient for mortality PHAEOCYS_E	(-)	1.072
TcMrtPHA_N	temperature coefficient for mortality PHAEOCYS_N	(-)	1.085
TcMrtPHA_P	temperature coefficient for mortality PHAEOCYS_P	(-)	1.085
MRespMDI_E	maintenance respiration rate at 0 dg C MDIATOMS_E	(1/d)	0.06
MRespMDI_N	maintenance respiration rate at 0 dg C MDIATOMS_N	(1/d)	0.06
MRespMDI_P	maintenance respiration rate at 0 dg C MDIATOMS_P	(1/d)	0.06
MRespMFL_E	maintenance respiration rate at 0 dg C MFLAGELA_E	(1/d)	0.06
MRespMFL_N	maintenance respiration rate at 0 dg C MFLAGELA_N	(1/d)	0.06
MRespMFL_P	maintenance respiration rate at 0 dg C MFLAGELA_P	(1/d)	0.06
MRespDIN_E	maintenance respiration rate at 0 dg C DINOFLAG_E	(1/d)	0.06
MRespDIN_N	maintenance respiration rate at 0 dg C DINOFLAG_N	(1/d)	0.06
MRespDIN_P	maintenance respiration rate at 0 dg C DINOFLAG_P	(1/d)	0.06
MRespPHA_E	maintenance respiration rate at 0 dg C PHAEOCYS_E	(1/d)	0.06
MRespPHA_N	maintenance respiration rate at 0 dg C PHAEOCYS_N	(1/d)	0.06
MRespPHA_P	maintenance respiration rate at 0 dg C PHAEOCYS_P	(1/d)	0.06

TcRspMDI_E	temperature coefficient for respiration MDIATOMS_E	(-)	1.066
TcRspMDI_N	temperature coefficient for respiration MDIATOMS_N	(-)	1.066
TcRspMDI_P	temperature coefficient for respiration MDIATOMS_P	(-)	1.066
TcRspMFL_E	temperature coefficient for respiration MFLAGELA_E	(-)	1.066
TcRspMFL_N	temperature coefficient for respiration MFLAGELA_N	(-)	1.066
TcRspMFL_P	temperature coefficient for respiration MFLAGELA_P	(-)	1.066
TcRspDIN_E	temperature coefficient for respiration DINOFLAG_E	(-)	1.066
TcRspDIN_N	temperature coefficient for respiration DINOFLAG_N	(-)	1.066
TcRspDIN_P	temperature coefficient for respiration DINOFLAG_P	(-)	1.066
TcRspPHA_E	temperature coefficient for respiration PHAEOCYS_E	(-)	1.066
TcRspPHA_N	temperature coefficient for respiration PHAEOCYS_N	(-)	1.066
TcRspPHA_P	temperature coefficient for respiration PHAEOCYS_P	(-)	1.066
MrtExMDI_E	extra rapid mortality rate MDIATOMS_E	(1/d/C)	0
MrtExMDI_N	extra rapid mortality rate MDIATOMS_N	(1/d/C)	0
MrtExMDI_P	extra rapid mortality rate MDIATOMS_P	(1/d/C)	0
MrtExMFL_E	extra rapid mortality rate MFLAGELA_E	(1/d/C)	0
MrtExMFL_N	extra rapid mortality rate MFLAGELA_N	(1/d/C)	0
MrtExMFL_P	extra rapid mortality rate MFLAGELA_P	(1/d/C)	0
MrtExDIN_E	extra rapid mortality rate DINOFLAG_E	(1/d/C)	0
MrtExDIN_N	extra rapid mortality rate DINOFLAG_N	(1/d/C)	0
MrtExDIN_P	extra rapid mortality rate DINOFLAG_P	(1/d/C)	0
MrtExPHA_E	extra rapid mortality rate PHAEOCYS_E	(1/d/C)	0
MrtExPHA_N	extra rapid mortality rate PHAEOCYS_N	(1/d/C)	0
MrtExPHA_P	extra rapid mortality rate PHAEOCYS_P	(1/d/C)	0
Mort2MDI_E	salinity dependent mortality rate at 0 dg C MDIATOMS_E	(1/d)	0
Mort2MDI_N	salinity dependent mortality rate at 0 dg C MDIATOMS_N	(1/d)	0
Mort2MDI_P	salinity dependent mortality rate at 0 dg C MDIATOMS_P	(1/d)	0
Mort2MFL_E	salinity dependent mortality rate at 0 dg C MFLAGELA_E	(1/d)	0
Mort2MFL_N	salinity dependent mortality rate at 0 dg C MFLAGELA_N	(1/d)	0
Mort2MFL_P	salinity dependent mortality rate at 0 dg C MFLAGELA_P	(1/d)	0
Mort2DIN_E	salinity dependent mortality rate at 0 dg C DINOFLAG_E	(1/d)	0
Mort2DIN_N	salinity dependent mortality rate at 0 dg C DINOFLAG_N	(1/d)	0
Mort2DIN_P	salinity dependent mortality rate at 0 dg C DINOFLAG_P	(1/d)	0
Mort2PHA_E	salinity dependent mortality rate at 0 dg C PHAEOCYS_E	(1/d)	0
Mort2PHA_N	salinity dependent mortality rate at 0 dg C PHAEOCYS_N	(1/d)	0
Mort2PHA_P	salinity dependent mortality rate at 0 dg C PHAEOCYS_P	(1/d)	0
MrtB1MDI_E	coeff. b1 salinity dependent mort.func. MDIATOMS_E	(gCl/m3)	0.002
MrtB1MDI_N	coeff. b1 salinity dependent mort.func. MDIATOMS_N	(gCl/m3)	0.002
MrtB1MDI_P	coeff. b1 salinity dependent mort.func. MDIATOMS_P	(gCl/m3)	0.002
MrtB1MFL_E	coeff. b1 salinity dependent mort.func. MFLAGELA_E	(gCl/m3)	0.002
MrtB1MFL_N	coeff. b1 salinity dependent mort.func. MFLAGELA_N	(gCl/m3)	0.002
MrtB1MFL_P	coeff. b1 salinity dependent mort.func. MFLAGELA_P	(gCl/m3)	0.002
MrtB1DIN_E	coeff. b1 salinity dependent mort.func. DINOFLAG_E	(gCl/m3)	0.002
MrtB1DIN_N	coeff. b1 salinity dependent mort.func. DINOFLAG_N	(gCl/m3)	0.002
MrtB1DIN_P	coeff. b1 salinity dependent mort.func. DINOFLAG_P	(gCl/m3)	0.002
MrtB1PHA_E	coeff. b1 salinity dependent mort.func. PHAEOCYS_E	(gCl/m3)	0.002
MrtB1PHA_N	coeff. b1 salinity dependent mort.func. PHAEOCYS_N	(gCl/m3)	0.002
MrtB1PHA_P	coeff. b1 salinity dependent mort.func. PHAEOCYS_P	(gCl/m3)	0.002
MrtB2MDI_E	coeff. b2 salinity dependent mort.func. MDIATOMS_E	(gCl/m3)	8000
MrtB2MDI_N	coeff. b2 salinity dependent mort.func. MDIATOMS_N	(gCl/m3)	8000
MrtB2MDI_P	coeff. b2 salinity dependent mort.func. MDIATOMS_P	(gCl/m3)	8000
MrtB2MFL_E	coeff. b2 salinity dependent mort.func. MFLAGELA_E	(gCl/m3)	8000
MrtB2MFL_N	coeff. b2 salinity dependent mort.func. MFLAGELA_N	(gCl/m3)	8000
MrtB2MFL_P	coeff. b2 salinity dependent mort.func. MFLAGELA_P	(gCl/m3)	8000
MrtB2DIN_E	coeff. b2 salinity dependent mort.func. DINOFLAG_E	(gCl/m3)	8000
MrtB2DIN_N	coeff. b2 salinity dependent mort.func. DINOFLAG_N	(gCl/m3)	8000
MrtB2DIN_P	coeff. b2 salinity dependent mort.func. DINOFLAG_P	(gCl/m3)	8000
MrtB2PHA_E	coeff. b2 salinity dependent mort.func. PHAEOCYS_E	(gCl/m3)	8000

MrtB2PHA_N	coeff. b2 salinity dependent mort.func. PHAEOCYS_N	(gCl/m3)	8000
MrtB2PHA_P	coeff. b2 salinity dependent mort.func. PHAEOCYS_P	(gCl/m3)	8000
RcDetC	first-order mineralisation rate DetC	(1/d)	0.12
TcDetC	temperature coefficient for mineralisation DetC	(-)	1.11
TauCSDetC	critical shear stress for sedimentation DetC	(N/m2)	0.1
MinDepth	minimum waterdepth for sedimentation	(m)	0.1
SecchiExt1	Secchi depth if extinction = 1 (Poole-Atkins)	(m)	1.35
RcDetCS1	first-order mineralisation rate DetC in layer S1	(1/d)	0.015
TcBMDetC	temperature coeff. mineralisation DetC in sediment	(-)	1.11
RcDetN	first-order mineralisation rate DetN	(1/d)	0.08
TcDetN	temperature coefficient for mineralisation DetN	(-)	1.11
RcDetNS1	first-order mineralisation rate DetN in layer S1	(1/d)	0.015
TcBMDetN	temperature coeff. mineralisation DetN in sediment	(-)	1.11
RcDetP	first-order mineralisation rate DetP	(1/d)	0.08
TcDetP	temperature coefficient for mineralisation DetP	(-)	1.11
RcDetPS1	first-order mineralisation rate DetP in layer S1	(1/d)	0.025
TcBMDetP	temperature coeff. mineralisation DetP in sediment	(-)	1.11
RcDetSi	first-order mineralisation rate DetSi	(1/d)	0.04
TcDetSi	temperature coefficient for mineralisation DetSi	(-)	1.047
RcDetSiS1	first-order mineralisation rate DetSi in layer S1	(1/d)	0.008
TcBMDetSi	temp. coeff. mineralisation DetSi in sediment	(-)	1.11
TcNit	temperature coefficient for nitrification	(-)	1.06
RcNit	first-order nitrification rate	(1/d)	0.07
pH	pH	(-)	8.1
RcDenSed	first-order denitrification rate in the sediment	(m/d)	0
TcDenWat	temperature coefficient for denitrification	(-)	1.11
COXDEN	critical oxygen concentration for denitrification	(g/m3)	101
RcDenWat	first-order denitrification rate in water column	(1/d)	0.003
OOXDEN	optimum oxygen concentration for denitrification	(gO2/m3)	100
IM1	inorganic matter fraction 1 (IM1)	(gDM/m3)	segment function
IM2	inorganic matter fraction 2 (IM2)	(gDM/m3)	segment function
SWAdsP	switch PO4 adsorption <0=Kd|1=Langmuir|2=pHdep>	(-)	1
KdPO4AAP	distrib. coeff. (-) or ads. eq. const.	(m3/gP)	0.1
MaxPO4AAP	adsorption capacity TIM for PO4	(gP/gFe)	0.005
RcAdPO4AAP	adsorption rate PO4 --> AAP	(1/d)	0
TaucS	critical shear stress for sedimentation algae	(N/m2)	0.1
VWind	wind speed	(m/s)	Time series
SWRear	switch for oxygen reaeration formulation (1-12)	(-)	9
KLRear	reaeration transfer coefficient	(m/d)	4
RcBOD	decay rate BOD (first pool) at 20 oC	(1/d)	0.3
AlgFrBOD	fraction algae contributing to BOD-inf	(-)	0.5
fSODaut	autonomous SOD (no effect SOD stat.var)	(gO2/m2/d)	0
RcSOD	decay rate SOD at 20 oC	(1/d)	0.1
TcSOD	temperature coefficient decay SOD	(-)	1.04
ExtVlIM1	VL specific extinction coefficient M1	(m2/gDM)	0.025
ExtVlBak	background extinction visible light	(1/m)	0.08
RadSurf	irradiation at the water surface	(W/m2)	Time series
SWDepAve	switch for module DepAve (0=off, 1=on)	(-)	1
Latitude	latitude of study area	(degrees)	52.1
RefDay	daynumber of reference day simulation	(d)	244
SWTau	switch <1=Tamminga|2=Swart|3=Soulsby>	(-)	1
ZResDM	zeroth-order resuspension flux	(gDM/m2/d)	25000
TaucRS1DM	critical shear stress for resuspension DM layer S1	(N/m2)	0.2
PeriodVTRA	period for calculating vertical distribution	(h)	24
VBurDMS1	first order burial rate for layer S1	(1/d)	0.003
MaxVeloc	maximum horizontal flow velocity	(m/s)	0
OON	Other Organic Nitrogen (OON)	(gN/m3)	0
ExtVlDetC	VL specific extinction coefficient DetC	(m2/gC)	0.1

FETCH	fetch length for wind	(m)	1000
InitDepth	depth where wave is created <-1: actual depth>	(m)	-1
SwChezy	switch (1=White/Coolbrook, 2=Manning)	(-)	1
TaucSIM1	critical shear stress for sedimentation IM1	(N/m2)	0.1
V0SedIM1	sedimentation velocity IM1	(m/d)	0
COXNit	critical oxygen concentration for nitrification	(g/m3)	-1
CTMin	critical temperature for mineralisation	(oC)	-1
CTNit	critical temperature for nitrification	(oC)	-1
ExtVLSal0	extra VL extinction at Salinity = 0	(1/m)	0.97
IM1S1	IM1 in layer S1	(gDM)	1.16E+14
MaxThS1	maximum thickness layer S1	(m)	1000000
NCMinLimH	upper limit N:C ratio detritus	(gN/gC)	0.15
NCMinLimL	lower limit N:C ratio detritus	(gN/gC)	0.1
nDetC	coefficient in flocculation function DetC	(-)	0
OOXNit	optimum oxygen concentration for nitrification	(g/m3)	0
PCMinLimH	upper limit P:C ratio detritus	(gP/gC)	0.015
PCMinLimL	lower limit P:C ratio detritus	(gP/gC)	0.01
PorS1	porosity of sediment layer S1	(-)	0.3
RcDetCHigh	maximum first-order mineralisation rate DetC	(1/d)	0.18
RcDetNHigh	maximum first-order mineralisation rate DetN	(1/d)	0.18
RcDetPHigh	maximum first-order mineralisation rate DetP	(1/d)	0.18
RcDetSHigh	maximum first-order mineralisation rate DetSi	(1/d)	0.01
SiCMinLimH	upper limit Si:C ratio detritus	(gSi/gC)	0.01
SiCMinLimL	lower limit Si:C ratio detritus	(gSi/gC)	0.005
SWSediment	switch for sediment (0=fixed, 1=variable)	(-)	1
tau	total bottom shear stress	(N/m2)	-1
TCSed	temperature coefficient for sedimentation	(-)	1
V0SedDetC	sedimentation velocity	(m/d)	1.5
V0SedDIN_E	sedimentation velocity	(m/d)	0
V0SedDIN_N	sedimentation velocity	(m/d)	0
V0SedDIN_P	sedimentation velocity	(m/d)	0
V0SedMDI_E	sedimentation velocity	(m/d)	0.5
V0SedMDI_N	sedimentation velocity	(m/d)	1
V0SedMDI_P	sedimentation velocity	(m/d)	1
V0SedMFL_E	sedimentation velocity	(m/d)	0
V0SedMFL_N	sedimentation velocity	(m/d)	0.5
V0SedMFL_P	sedimentation velocity	(m/d)	0.5
V0SedPHA_E	sedimentation velocity	(m/d)	0
V0SedPHA_N	sedimentation velocity	(m/d)	0.5
V0SedPHA_P	sedimentation velocity	(m/d)	0.5
AAP	Adsorbed Inorganic Phosphate	(gP/m3)	0
ScaleVDisp	scaling factor for vertical diffusion	(-)	1.4
Salinity	Salinity	(ppt)	VARSAL
sw1DfwaPO4	load option 0=all, 1=top, 2=bottom segments	(-)	2
sw2DfwaPO4	maximise withdrawel to mass 0=no, 1=yes	(-)	1
MaxIter	Max. number of iterations	(-)	100
Tolerance	acceptable error	(-)	1.0E+7